UNIVERSITÀ
DEGLI STUDI
DI PADOVA

UNIVERSITA' DEGLI STUDI DI PADOVA

Dipartimento di Biologia

SCUOLA DI DOTTORATO DI RICERCA
IN BIOCHIMICA E BIOTECNOLOGIE

INDIRIZZO BIOTECNOLOGIE

XIII CICLO

Molecular Characterization of Mitochondria Interactions with other Organelles

Direttore della Scuola: Ch.mo Prof. Giuseppe Zanotti

Coordinatore dell'Indirizzo: Ch.mo Prof. Giorgio Valle

Supervisore: Ch.mo Prof. Fiorella Lo Schiavo

Dottoranda: Cristina Ruberti

INDICE

ABSTRACT

The topic of this PhD thesis was to study organelles in plant cells, analysing in particular the mitochondrial morphology. Recent papers have, in fact, reported that regulation of mitochondrial morphology is important not only for maintaining mitochondrial number during cell division, and mitochondrial distribution within each cell (Westermann, 2010; Logan, 2003), but also for executing many biological functions. In animals, a shift in mitochondrial morphology towards the organelle fragmentation is an early event during apoptosis (Suen *et al.*, 2008). In plants, a link between mitochondrial morphology and senescence-associated cell death (i.e. a genetically controlled programme of self destruction) has been reported in *Medicago truncatula* cultured cells (Zottini *et al.*, 2006).

The understanding of molecular mechanisms, used by plants to regulate senescence, might allow biotechnological applications through genetic manipulations of key elements affecting senescence and provide interesting applicative outputs, especially in agronomically relevant species.

In light of these findings, I focused on the study of mitochondrial morphology during senescence in grapevine (*Vitis* spp.) plants, one of the most important crops in Mediterranean area that has also the potentiality of becoming a model organism for fruit trees due to the knowledge of its genome sequence (Jaillon *et al.*, 2007; Velasco et *al.*, 2007).

Suspension cell cultures of *Vitis* spp. were chosen as an initial model system to study mitochondrial morphology during senescence/PCD, because they are an accessible and not complex experimental system, sharing some of fundamental regulatory mechanisms with PCD processes in plant. Then, in order to study changes in mitochondrial morphology during different stages of leaf development and senescence, transgenic grapevine plants, expressing GFP (green fluorescent protein) fluorescent marker targeted to mitochondria, were generated. In the grapevine leaves the senescence/PCD process was characterized by analyzing the chlorophyll degradation and the expression of several *VvSAGs* genes (i.e. *Vitis* homologues of *Arabidopsis* senescence associated genes). Analyses performed in grapevine senescent leaves showed mitochondria prefunding altered in their morphology. Then, we moved to investigate to the molecular aspects of these

morphological changes. Indeed, it is known that in eukaryotic cells, the number, size and distribution of mitochondria are regulated by continuous cycles of mitochondrial fusions and fission events (Logan, 2003) but so far in plants, no genes involved in mitochondrial fusion machinery have been identified, while several genes involved in mitochondrial fission have been recently described in *Arabidopsis thaliana*, a plant model organism. Hence, I moved to *Arabidopsis* plant and I focused on the study of the subcellular localization, expression and interaction of two proteins (ELM1 and BIGYIN), known to be involved in mitochondrial fission. ELM1 and BIGYIN subcellular localization was carefully analyzed, by using several organelle fluorescent markers and adopting different methods of transient expression in leaf cells, combined with confocal microscope analyses. Yet, I investigated whether *in vivo* interactions between ELM1 and BIGYIN occurred in plant cells. Then, I analyzed ELM1 and BIGYIN expression pattern in plant to verify if their presence in the same tissues was indeed detected. The analysis was carried out through histochemical GUS assay in transgenic plants, stable expressing the *ELM1* and *BIGYIN* promoter region fused to the *β-glucuronidase* (GUS) reporter.

In order to define the physiological role of BIGYIN, a detailed subcellular localization of BIGYIN was performed in the whole plant, stably expressing BIGYIN under control of its own promoter, in order to mimic physiological conditions. These analyses allowed us to establish an association between BIGYIN and chloroplasts/plastids and, in particular, to identify protrusions, marked by YFP::BIGYIN, extruding from chloroplast, mitochondria and peroxisomes. Such kind of tubular protrusions has already been observed and termed matrixules, peroxules stromules respectively, and it has been proposed to play a role in physical inter-organellar interactions, by increasing the transfer efficiency of metabolites/molecules among organelles (Scott *et al.*, 2007). The presence of BIGYIN on these protrusions is indeed an unexpected finding that led us to investigate more in detail this peculiar BIGYIN localization. I focused in detail on the dynamics and behaviour of these YFP::BIGYIN marked tubules, and investigated, in different tissues and different developmental stages, whether a protein trafficking through these organelles indeed occurred.

The understanding of physical inter-organellar interactions is connected with the importance of elucidating relationships and cross-talks among organelles, key events to understand the mechanisms of interactions between plant and its environment that can be of particular importance for the coordination of the senescent program.

RIASSUNTO

In questa tesi di dottorato, è stata condotta un'analisi degli organelli in cellule vegetali, studiando, in particolare, i mitocondri e la loro morfologia in diverse condizioni fisiologiche. La regolazione della morfologia mitocondriale è importante sotto molteplici aspetti, infatti controlla il numero dei mitocondri durante la divisione cellulare e la loro distribuzione all'interno di ogni cellula (Wastermann, 2010; Logan, 2003), controlla infine alcune funzioni biologiche. Nelle cellule animali, per esempio, la frammentazione dei mitocondri è un evento precoce che caratterizza il processo di apoptosi (Suen *et al.*, 2008). Un'associazione tra morfologia mitocondriale e senescenza/morte cellulare programmata (PCD) è stata riportata anche in colture cellulare vegetali (Zottini *et al.*, 2006).

La comprensione dei meccanismi molecolari, utilizzati dalla pianta per regolare il processo di senescenza/PCD, può essere importante da un punto di vista biotecnologico, in quanto potrebbe permettere una modulazione dei parametri di crescita e di sviluppo della pianta attraverso miglioramenti genetici e manipolazioni di fattori ambientali che regolano il processo di senescenza. I risvolti applicativi di tale approcio sono molto interessanti, soprattutto per le specie di rilevanza agronomica.

Alla luce di tali premesse, la morfologia mitocondriale è stata dettagliatamente analizzata durante il processo di senescenza/PCD in vite (*Vitis* spp). La vite rapprensenta una delle più importanti piante coltivate della zona del Mediterraneo, ed a seguito del sequenziamento del suo genoma (Jaillon *et al.*, 2007; Velasco et *al.*, 2007), è ritenuta un organismo modello negli studi sugli alberi da frutto. Inizialmente l'analisi della morfologia mitocondriale durante il processo di senescenza/morte cellulare programmata è stata condotta in colture cellulari di *Vitis* spp.. In seguito, lo studio è stato continuato in pianta, in particolare è stata portata avanti un'analisi dettagliata della morfologia mitocondriale durante i differenti stadi di sviluppo e di senescenza della foglia. A tal fine, sono state prodotte ed analizzate piante transgeniche, esprimenti un marcatore fluorescente mitocondriale. Le analisi condotte hanno dimostrato che in foglie senescenti i mitocondri presentano delle morfologie caratteristiche. Questi risultati ci hanno

indirizzato ad uno studio degli aspetti molecolari coinvolti nella regolazione della morfologia mitocondriale.

In numerose cellule eucariotiche, la morfologia mitocondriale è regolata dal continuo alternarsi di eventi di fusione e fissione mitocondriale (Logan, 2003). Nelle piante, i componenti molecolari coinvolti nel meccanismo di fusione mitocondriale non sono stati ancora individuati, mentre i componenti proteici implicati nella fissione sono stati recentemente descritti in *Arabidopsis*. A tuttoggi non è stato ancora compreso nè il preciso ruolo svolto da tali proteine, nè le loro precise interazioni fisiche, responsabili del processo di fissione mitocondriale. Durante il mio dottorato, ho quindi analizzato, nel sistema modello *Arabidopsis thaliana*, la localizzazione subcellulare, l'espressione e l'interazione di due proteine (ELM1 ed BIGYIN), coinvolte nel processo di divisione mitocondriale. La localizzazione subcellulare di ELM1 e BIGYIN è stata determinata in cellule vegetali, utilizzando differenti metodi di espressione transiente combinati con analisi di microscopia confocale. Sono state poi eseguite analisi per verificare l'interazione di queste due proteine *in vivo* in cellule vegetali. Successivamente è stata condotta in pianta un'analisi del pattern di espressione di *BIGYIN* ed *ELM1*, in modo tale da verificarne l'espressione di queste due proteine negli stessi tessuti, prerequisito fondamentale per una loro eventuale interazione. A tal fine, sono state prodotte ed analizzate mediante saggio istochimico-colorimetrico piante transgeniche di *Arabidopsis thaliana* stabilmente esprimenti il promotore di tali geni fuso al gene che codifica per l'enzima *β-glucuronidasi* (GUS).

Per definire il ruolo fisiologico di BIGYIN, una dettagliata localizzazione subcellulare di questa proteina è stata eseguita in piante di *Arabidopsis*, stabilmente esprimenti il costrutto *YFP::BIGYIN* sotto il controllo del proprio promotore. Queste analisi hanno messa in evidenza un'associazione tra BIGYIN e cloroplasti/plastidi ed ha portato ad individuare particolari protrusioni, marcate con la proteina di fusione YFP::BIGYIN, che si estondono dai cloroplasti, mitocondri e perossisomi. Protrusioni simili erano già state riportate in letteratura e prendono il nome di 'stromuli', 'matrixuli', 'peroxuli' a seconda che si estendano rispettivamente da cloroplasti, mitocondri o perossisomi. Recentemente, è stato ipotizzato che tali le protrusioni abbiano un ruolo nelle interazioni fisiche tra i differenti organelli, aumentando i contatti fisici tra gli

organuli e migliorando l'efficienza di scambio di metaboliti/molecule (Scott *et al.*, 2007). Tuttavia nessun dato è stato riportato a conferma di tale ipotesi. L'inattesa presenza di BIGYIN su tali protrusioni, ci ha permesso di studiare in dettaglio la loro dinamicità e di analizzare la presenza di interazioni fisiche tra gli organelli.

La comprensione delle interazioni fisiche tra gli organelli si colloca nel campo di indagine delle relazioni tra tali compartimenti subcellulari che viene ora considerato un campo fondamentale per la conoscenza dei meccanismi di base della biologia cellulare vegetale.

INTRODUCTION

Mitochondria, peroxisomes and plastids are essential and ubiquitous subcellular organelles in plants. Each of these organelles are specialized compartments playing specific functions. Extensive metabolic exchanges are well known (Schrader and Yoon, 2007; Bauwe *et al.*, 2010), instead, physical and functional signalling interactions among them are now emerging form recent data (Sweetlove *et al.*, 2007; Rhoads and Subbaiah, 2007).

Mitochondria

Mitochondria are essential bio-energetic subcellular organelles in most eukaryotic cells. Their major role is to synthesize ATP, by coupling substrate oxidation to electron transport and the generation of a proton electrochemical gradient. Mitochondria are also involved in a range of other processes, i.e. in controlling cellular redox state (Noctor *et al.*, 2006), in Ca^{2+} homeostasis (Vandecasteele *et al.*, 2001; Logan and Knight, 2003) and in programmed cell death (PCD) (Lam, 2004) both in animals and in plants. Moreover mitochondria are not independent and autonomous organelles, but they are involved in metabolic and functional connection with other subcellular compartments. For example, in higher plants, mitochondria, peroxisomes, chloroplasts and cytosol are involved together in photorespiration process (Bauwe *et al.*, 2010).

Each mitochondrion is composed of compartments that carry out specialized functions. These compartments include the outer membrane, the inner membrane, the intermembrane space (the space between the outer and inner membranes), the matrix (space within the inner membrane), the crystal membrane (infolding of the inner membranes) and the intercrystal space (Logan, 2006). The outer membranes act as a barrier to large molecules (>10 kDa), that can only enter into mitochondria through specific pores located within the lipid bilayer. The inner membrane is characterized by a highly complex structure. Components of the electron transport system and the ATP synthetase are an integral part of the inner membranes. The matrix contains enzymes responsible for the citric acid

cycle reaction and also several metabolites (i.e. NAD, NADP, ADP, and ATP) (Bowsher and Tobin, 2001).

It is widely accepted that mitochondria originate from a common ancestral free-living α-proteobacterium, that colonised pro-eukaryotic cell around two billion years ago (Gray *et al.*, 1999). During evolution, the engulfed proteobacterium transferred the majority of its genes to the nucleus. As result of this process, several mitochondrial processes (i.e. biochemistry pathways) are now under nuclear control. In addition, the mitochondria lost also components of their bacterial origin (i.e. genes originally involved in its division as prokaryotic cell); and it co-opted other components from the host (i.e. the main components involved in division machinery of the outer membrane, originated in consequence of incorporation into the host eukaryotic cell) (Schrader, 2006).

Mitochondria are not created *de novo*, but they arise by fission events of pre-exiting mitochondria in the cytosol. In various eukaryotic cells, mitochondria undergo continuous cycles of fission and fusion and these concerted activities control the maintenance of mitochondrial number during cell division, and the mitochondrial distribution and morphology within a single cell (Logan, 2003). As result of these fission-fusion events, mitochondrial shape and size are continually changing within the living cells. This great heterogeneity in the dynamics and morphology of mitochondria has been reported within a single cell, in different cell types of the same organism, and also in different organisms.

In yeasts and in most animal cell types, mitochondria are usually described as an ‘interconnected reticular network’, because the chondriome (i.e. all the mitochondria in a cell collectively) is organized into long tubules or reticula, characterized by dynamical shifting between a fragmentized state and a tubular ‘reticulum continuum’ (Logan, 2006). By contrast, in higher plants, the chondriome is described as a ‘discontinuous whole’, because it is a highly dynamic structure composed mainly of discrete organelles (Logan, 2006).

Yeasts, mammals and higher plants show a common molecular mechanism involved in mitochondrial fission events (Delille *et al.*, 2009). Concerning, instead, the molecular mechanisms involved in mitochondrial fusion event, in yeasts and mammals the molecular players have been described (Westermann,

2010), while in plants none molecular component has yet been identified (Logan, 2003).

Mitochondrial fission machinery

Molecular mechanisms involved in mitochondrial fission events have been studied extensively in yeast *Saccharomyces cerevisiae*. Mitochondrial fission machinery in yeast is composed by four proteins: Fission1 (Fis1), Dynamin1 (Dnm1), Mitochondrial division1 (Mdv1) and Caf4. Fis1 is an integral membrane protein, located to the mitochondrial outer membranes. Its N-terminal domain is exposed to the cytoplasmatic side and forms a tetratricopeptide (TRP)-like bundle helix, involved in protein-protein interaction (Suzuki *et al.*, 2003), while the C-terminal tail contains a single transmembrane domain. For this topology, Fis1 is considered a member of tail-anchored (TA) (N_{out}-C_{in}) family of membrane proteins (Borghese *et al.*, 2007). Dnm1 is a yeast dynamin-related protein (DRP), characterized by a N-terminal GTPase domain and a C-terminal GTPase effector. During mitochondrial fission, Fis1 recruits to mitochondrial fission sites the cytosolic molecular adapter Mdv1 (and its paralog Caf4) and Dnm1. Dnm1 and Mdv1 are thought to form higher-order multimer complexes, named fission complexes, that surround and pinch off mitochondria (Fig.1).

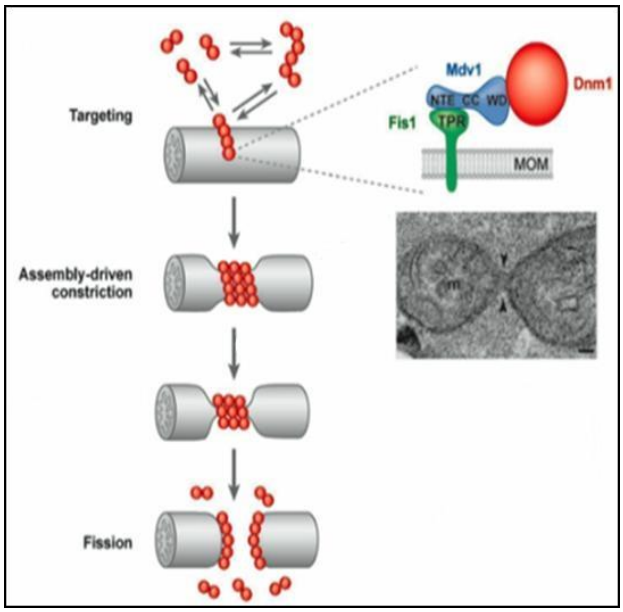

Fig.1. Molecular model of mitochondrial fission in Yeast: interaction between Dnm1, Mdv1 and Fis1. MOM stands for the mitochondrial outer membrane.

In higher plants, studies on molecular mechanism, involved in mitochondrial fission events, have just begun. Recently, in *Arabidopsis thaliana*, several genes involved in remodelling of mitochondria have been described: two dynamin-related proteins (DRPs), termed DRP3A (formerly, *Arabidopsis* dynamin-like protein 2A [ADL2a] and ADL2b, respectively; (Zhang and Hu, 2008a); two fission-like protein, homologue of yeasts Fis1, termed BIGYIN and FIS1B (Scott *et al.*, 2007); a plant specific protein, named ELM1, which does not present sequence similarity with the yeast Mdv1/Caf4 (Arimura *et al.*, 2008).

How these proteins specifically interact among them and what is the precise role of each of these proteins during mitochondrial fission events is yet unclear. So far, it is known that DRP3A and BIGYIN do not interact each other, while DRP3A, DRP3B and ELM1 interact among them (Arimura *et al.*, 2008; Zhang and Hu, 2008a) (Fig. 2). Moreover, ELM1 is required for the subcellular transfer of DRP3A from the cytosol to mitochondrial fission sites (Arimura *et al.*, 2008). Since ELM1 protein structure does not present transmembrane domain or other predicted membrane-anchoring domains, it has been supposed that its mitochondrial localization could depend on the interaction with protein(s) located to mitochondrial surfaces. BIGYIN is one of the proteins that have been proposed to interact with ELM1, but results showing this interaction have not yet reported.

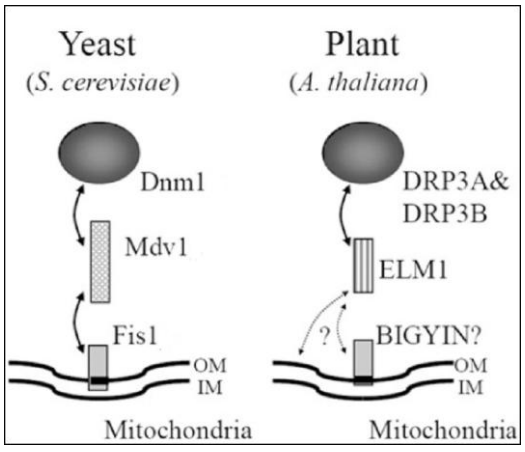

Fig.2 Comparison of Mitochondrial fission Factors in Yeas and in Plant. In Yeast, Dnm1, a dynamin-related protein, is recruited from the cytosol to mitochondria in a manner dependent on Fis1 and an adaptor protein (Mdv1). In the Plant Arabidopsis, dynamin related protein, DRP3A and DRP3B, interact with ELM1 for their localization to mitochondria. A black bar in Fis1 shows putative transmembrane domains. OM, outer membrane; IM, inner membrane (Arimura *et al.*, 2008)

Roles of mitochondrial fission

Mitochondrial fission is important not only for the maintenance of mitochondrial number during cell division, or for mitochondrial morphology within a single cell (Westermann, 2010; Logan, 2003), but mitochondrial architecture is also important for executing many biological functions. For example, mitochondrial fission and subsequent mitochondrial fragmentation are an early event during apoptosis in yeasts and mammals (Suen *et al.*, 2008). By contrast, a decrease in mitochondrial fission and the subsequent giant elongated mitochondria are protective features in old human endothelial cells cultivated *in vitro* (Mai *et al.*, 2010). Elongation of mitochondria allows both a decrease of the energy-consuming processes of mitochondrial dynamics, and a fast distribution and exchange of molecules into the mitochondrial matrix. As result, these elongation of mitochondria rendered cells more resistant against apoptotic stimuli (Mai *et al.*, 2010). In plants, similar giant mitochondria during senescence-associated cell death have been reported in *Medicago truncatula* cultured cells (Zottini *et al.*, 2006) and in *Arabidopsis* leaf and mesophyll protoplasts (Scott and Logan, 2008), suggesting a link between plant mitochondrial morphology and senescence-associated cell death.

Matrixules

Mitochondrial morphology could be characterized by particularly tubular structures, named 'matrixules' (i.e. 'matrix-filled tubules'), extending from the mitochondrial outer membranes. Matrixules were observed for the first time by Logan colleagues in an *Arabidopsis* T-DNA insertion line for *DRP3A* (an *Arabidopsis* dynamin-like protein involved in mitochondrial division) (Logan *et al.*, 2004). Initially, these structures were retained artefacts of defective mitochondrial division, in which DRP3A was involved. Recently, matrixules were observed, instead, also in wild type plants opening interesting discussions about the role/s of these structures. An intriguing possibility is that these protrusions have a function in metabolite transport by increasing mitochondrial surface area, in genetic material transfer or in physical interaction between mitochondria (Scott *et al.*, 2007).

Chloroplasts

Plant cell contains plastids, which represent one of the principal hallmarks that differentiate plant cell from other eukaryotic cells. 'Plastid' is a general term applied to an important and wide group of functionally distinct subcellular organelles. Plastids develop from small undifferentiated proplastids in dividing meristematic cells. These undifferentiated proplastids differentiate into a variety of specific plastid type, depending on the particular cell type in which they are located and the stage of cellular development. 'Leucoplasts', lacking of pigmentation, are specialized for bulk storage ('amyloplasts'), or lipids ('elaioplasts'), or protein ('proteinoplasts') (Bowsher and Tobin, 2001). 'Chloroplasts', instead, contain chlorophyll, they are involved in photosynthesis and presumably for this important role they are also the best studied among the different plastidial type.

Chloroplasts arose from an endosymbiotic event between a prokaryote and a photosynthetic prokaryote (Gray, 1999). During evolution numerous plastid genes have been lost or transferred to the nuclear genome. As result, the correct plastid development and function are now under nuclear control.

Chloroplasts are not created *de novo*, but arise by division of pre-existing organelles through binary fission, as do bacteria. The chloroplast fission process can be separated into four distinct stages (Fig.3): (1) chloroplast elongation; (2) chloroplast constriction, that provokes the formation of the typical 'dumbbell-shape'; (3) further chloroplast constriction, provoking a isthmus formation and thylakoid membrane separation; (4) and the final stage characterized by isthmus breakage, plastid separation and envelope releasing (Aldridge *et al.*, 2005).

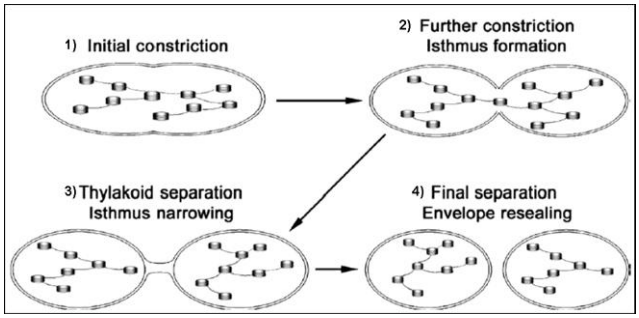

Fig. 3. Schematic overview of morphological changes occurring during chloroplast division in higher plants. (Aldridge *et al.*, 2005).

Chloroplast fission machinery

In most organisms, the chloroplast division apparatus consist of a double ring structure, with one ring on the cytosolic face of the outer membrane (outer ring), and one on the stromal face of the inner envelope (inner ring) (Maple and Møller, 2007). The plastid division is controlled by a combination of prokaryote-derived and host eukaryote-derived proteins, but the precise roles of these components in chloroplast division machinery and how these components are coordinated is still unclear.

In *Arabidopsis*, homologues of the bacterial cell division FtsZ have been identify in the nuclear genome (i.e. AtFtsZ1-1 and AtFtsZ2-1). These proteins are imported into chloroplasts and formed a ring (Z-ring) on the stromal side of the inner membrane. In detail, the Z-ring probably determines the site of division, where successively molecular components of eukaryotic origin are assembled to form the inner and outer ring (Aldridge *et al.*, 2005). The correct position of the Z-ring at the chloroplast centre could be, at least in part, mediated by the AtMinD1 and AtMinE1, homologues of the bacterial MinD and MinE. The Z-ring is probably stabilized and anchored to the inner membrane by the interaction between AtFtsZ2-1 and the transmembrane protein ARC6, protein of prokaryotic origin localized to the stromal side of the inner membrane (Maple and Møller, 2007).

Unlike the Z-ring, the inner and the outer rings have been probably recruited from the eukaryotic cells, and, so far, the composition of both rings is unknown. Several component of eukaryotic origin involved in plastid division have been recently identified in *Arabidopsis*: DRP5B (i.e. dynamin-related protein5B, named also ARC5), PDV1 and PDV2 (i.e. plastid division1 and plastid division2). PDV1 and PDV2 are transmembrane proteins integrated into the chloroplast outer membrane, with the N-terminal region exposed to the cytosol. PDV1 and PDV2 are required for the localization of DRP5B at the division site (Miyagishima *et al.*, 2006). DRP5B is a member of the dynamin-like superfamily of eukaryotic membrane-remodelling GTPases. Since members of the dynamin-like superfamily are involved in membrane pinching events in eukaryotes and also in mitochondrial membrane scissions in yeast, mammals and plants, it is

reasonable that DRP5B may play a role to pinch off the outer chloroplast membrane at late stages of the division process (Gao *et al.*, 2003).

Stromules

In higher plants, all plastid types are characterized by highly dynamic protrusions, named ‘stromules’ (i.e. ‘stroma-filled tubules), extending from plastidial surfaces (Köhler and Hanson, 2000). Stromules could protrude from a single plastid or connect two o more plastids among them. It has been reported that stromules are involved in exchange of endogenous stromal proteins (i.e. RubisCO and aspartate aminotransferase), between connected chloroplasts (Kwok and Hanson, 2004a). However, this is not the primary function of stromules, given that stromules can freely extend from a single chloroplast without necessarily to be linked to another chloroplast. Stromules could have a function in metabolite/molecules exchange also with cytosol, and, since a close apposition of stromules and nuclei has been frequently observed, it has also been suggested that stromules could play a role in interactions between plastids and nuclei, such as allowing the rapid transit of molecules and signals between these subcellular compartments (Kwok and Hanson, 2004b).

Peroxisomes

Peroxisomes are single-membrane organelles ubiquitously present in all eukaryotic cells. In plants, peroxisomes mediate several metabolic functions, i.e. fatty acid β-oxidation or hydrogen peroxide degradation.

During evolution, these organelles arose from cellular membrane system, probably the endoplasmic reticulum, as an invention of eukaryotic cells (Michels *et al.*, 2005).

Peroxisomes are highly dynamic organelles, capable of adapting to a variety of environmental and developmental cues by altering their abundance and morphology. Peroxisomes generated mainly from pre-existing peroxisomes through a constitutive division (named also ‘peroxisomal division’) or through an induced many-fold increment in their number (termed ‘peroxisomal

proliferation'). Peroxisomal division and peroxisomal proliferation are characterized by elongation, constriction and fission of peroxisomal (Fig. 4) (Kaur and Hu, 2009).

Peroxisomal fission machinery

Three evolutionarily conserved families of proteins are involved in peroxisomal division/proliferation: Peroxin11 (PEX11), Dynamin-related proteins (DRPs) and Fission1-like protein (FIS1).

In *Arabidopsis*, several molecular components involved in peroxisomal division have been identified (**Fig. 4**): five PEX11 isoforms, three dynamin-related proteins and two Fission1-like proteins. The five PEX11 isoforms are integral membrane proteins localized to peroxisomal membranes and play a rare-limiting role in initiating peroxisomal elongation **(Kaur and Hu, 2009).** DRP3A and DRP3B are instead dynamin-like protein involved in the organelle final fission, while another dynamin like protein (DRP5B) has presumably a distinct unknown role in peroxisomal division **(Zhang and Hu, 2010)**. The two Fis1-like proteins, BIGYIN (termed also FIS1A) and FIS1B are peroxisomal integral membrane proteins, involved in peroxisomal division, even if their role is yet unclear **(Zhang and Hu, 2008b)**.

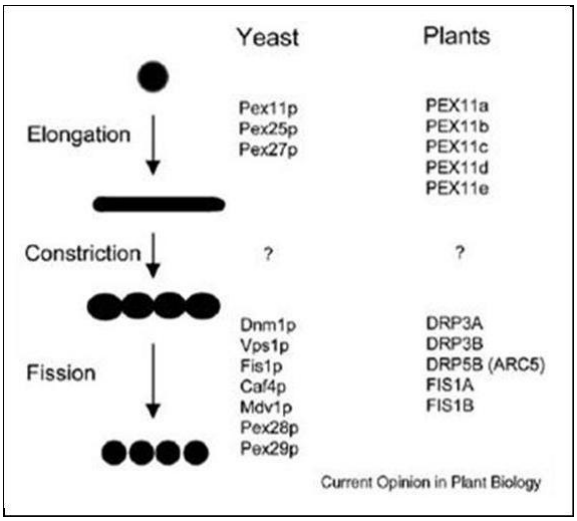

Fig. 4. Comparison of proteins involved in peroxisomal fission/proliferation in Yeast and Plants. Peroxisomes proliferation occurs through elongation, constriction and fission. In all cases, PEX11 proteins are involved in the initial elongation, while the factors involved in peroxisomal constriction are yet unknown. Peroxisomal fission is mediated by dynamin-like proteins (in yeast; Dnm1 and Vsp1; in Arabidopsis: DRP3A, DRP3B, DRP5B), which are recruited to the peroxisomal membranes by the tail-anchored protein FIS1 (in yeast: Fis1; in Arabidopsis: BIGYIN and FIS1B). In yeast Caf4 and Mdv1 are adaptors. (Kaur and Hu, 2009)

Peroxules

Peroxisomes morphology could be characterized by tubular protrusions, termed 'peroxules' (Scott *et al.*, 2007). These tubules were observed by Cutler *et al.* (2000) in *Arabidopsis* plants stable expressing random GFP::cDNA fusion proteins obtained to visualize subcellular structures. In detail, Cutler and colleagues described 'peroxules' as highly dynamic peroxisomal tubular extensions. They showed that peroxisomes can change from a spherical to an elongate morphology in a few seconds, and that this process begins with the production of a short tubular tail, which then rapidly expands to become longer than the original organelle.

However, peroxules are described as 'common and transient peroxisomal phenomenon in plant cells' (Sinclair *et al.*, 2009), and their role(s) is until now unknown. Although Cutler *et al.* (2000) described peroxules as intermediates in peroxisomal fission/proliferation, it has been also demonstrated that peroxule extensions occurred in response to low levels of hydroxyl radical reactive oxygen species (ROS), suggesting that peroxules may be a part of a responsive machinery, aimed at relief of subcellular stress created by toxic ROS (Sinclair *et al.*, 2009). Other possible functions of peroxules might be that they increase the peroxisomal surface-to-volume ratio enhancing the access of cytosolic metabolites (Jedd and Chua, 2002) or enhancing the exchange of molecules between peroxisomes (Mano *et al.*, 2002).

Mitochondria, peroxisomes and chloroplasts: metabolic, functional and physical inter-connections

Analyzing the molecular mechanism involved in fission events of mitochondria, peroxisomes and chloroplasts in *Arabidopsis*, a common fission pathway, that shares several proteins, emerges among these different organelles. Peroxisomes and mitochondria share the dynamin-related proteins (i.e. DRP3A and DRP3B) and the Fission1-like proteins (i.e. BIGYIN and FIS1B) (Kaur and Hu, 2009). Similarly, DRP5B (ARC5), a dynamin protein involved in peroxisomal division in *Arabidopsis*, plays a role also in plastid division (Zhang and Hu, 2010). The use

of shared components could be a mechanism to promote coordinated division among these organelles that are at least metabolically linked (Schrader, 2006). Photorespiration, fatty acid metabolism, and jasmonic biosynthesis are among some of the metabolite pathways that spanning peroxisomes, chloroplasts and/or mitochondria (Kaur and Hu, 2009). Moreover, inter-organellar interactions are fundamental also in several biological processes. For example, chloroplasts and mitochondria are both involved in generating intermediate signals involved in plant cell death (PCD) (Van Breusegem and Dat, 2006), suggesting that a signalling-exchange among these organelles is important for the regulation of PCD, a fundamental genetically regulated process of cell suicide, that accomplishes a central role in development, homeostasis and integrity of eukaryotic organisms.

In the light of the metabolite and signal exchanges among these organelles, it has been proposed the existence of structures that promote directional metabolite/molecules trafficking among these organelles. In detail, it has been suggested that matrixules, peroxules and stromules could be involved in physical interactions among organelles (Scott *et al.*, 3007; Foyer and Noctor, 2007)). So far, no data have been reported to confirm this hypothesis.

Leaf senescence: a physiological process where mitochondria and chloroplasts presumably co-operate

Leaf senescence is the final stage of leaf development and one type of programmed cell death (PCD; i.e. a genetically controlled system of self destruction), that occurs in plants (Quirino *et al.*, 2000). Leaf senescence is a slow physiological process, under the control of several factors both endogenous (hormones) and external (light, starvation, pathogens). In detail, senescence involves the ordered disassembly of cellular components that are redirected to other plant organs, meanwhile senescing tissues eventually die by programmed cell death (PCD) (Keeck *et al.*, 2007). At the cellular level, the senescence program unfolds in an orderly manner. Chloroplasts, that contain most of proteins in leaf cell, are one of the first organelles to be targeted for degradation

(Hörtensteiner and Kräutler, 2011). Other organelles, such as peroxisomes, undergo biochemical changes, while nucleus, necessary for gene transcription, and mitochondria, necessary for providing energy, remain intact until the last stages of the senescence (Keeck *et al.*, 2007).

Various cell death-signalling pathways are critically dependent on mitochondria, whose action is played not only through the release of pro-apoptotic factors, but also through the alteration of their dynamics and morphology, as stated before. Recently it has been also suggested that chloroplasts could regulate the onset of leaf senescence by increasing the reduction state of electron transporters and by generating reactive oxygen species (ROS) (Zapata *et al.*, 2005).

Thus, increasing evidences suggest that these organelles co-operate in signalling-pathway regulation and in the developing of the senescence process, but a detailed study on this topic has just at the beginning. There is, therefore, a need for further investigation into the respective roles of chloroplasts and mitochondria in the process of leaf senescence.

Topics of PhD project

During my PhD project, I focused on organelles in plant cells, analysing in detail the mitochondrial morphology during senescence/programmed cell death (PCD) in cell cultures and plants of grapevine (*Vitis spp.*), an agronomically relevant species (Chapter 1).

In order to define the molecular mechanisms responsible for mitochondrial morphology, I moved to *Arabidopsis* plant, a model organism in plant biology, and I analyzed in detail two proteins involved in mitochondrial fission machinery (Chapter 2).

Last, I investigated the molecular aspects of physical inter-organellar interactions, by imaging analyses of a protein localized to these organelles (Chapter 3).

REFERENCE

- **Aldridge C**, Maple J, Møller SG (2005).The molecular biology and plastid division in higher plant. Journal of Experimental Botany, 56 (414):1016-1077
- **Arimura SI**, Fujimoto M, Doniwa Y, Kadoya N, Nakazono M, Sakamoto W, Tsutsumi N (2008). *Arabidopsis* ELONGATED MITOCHONDRIA1 is required for the localization of DYNAMIN-RELATED PROTEIN3A to mitochondrial fission sites. The Plant Cell, 20(6):1555-66
- **Bauwe H**, Hagemann M, Ferine AR (2010). Photorespiration: players, partners and origin. Trends in Plant Science, 15 (6):330-336
- **Borghese N**, Brambilasca S, Colombo S (2007). How tails guide tail-anchored proteins to their destinations. Current Opinion in Cell Biology, 19:368–375
- **Bowsher CG**, Tobin AK (2001). Compartmentation of metabolism within mitochondria and plastids. Journal of Experimental Botany, 52 (356):513-518
- **Cutler SR**, Ehrhardt DW, Griffitts JS, Sommerville CR (2000). Random GFP::cDNA fusions enable visualization of subcellular structures in cells of *Arabidopsis* at high frequency. PNAS, 97 (7):3718-3723
- **Delille HK**, Alves R, Schrader M (2009). Biogenesis of peroxisomes and mitochondria: linked by division. Histochem Cell Biol, 131: 441-446
- **Foyer CH**, Noctor G (2007). Shape-shifters building bridges? Stromules, matrixules and metabolite channelling in photorespiration. TRENDS in Plant Science, 12 (9):381-382
- **Gao H**, Kadirjan-Kalbach D, Froehlich JE, Osteryoung W (2003). ARC5,a cytosolic dynamin-like protein from plants, is part of the chloroplast division machinery. PNAS, 100 (7): 4328-4333
- **Gray MV** (1999). Evolution of organellar genomes. Current Opinion in Genetics and Development, 9 (6):678-687
- **Gray MW**, Burger G, Lang BF (1999). Mitochondrial evolution. Science, 283 (5407):1476-1481

- **Hörtensteiner S** and Kräutler (2011). Chlorophyll breakdown in higher plants. Biochimica et Biophysica Acta, doi:10.1016/j.bbabio.2010.12.007
- **Kaur N**, Hu J (2009). Dynamic of peroxisomes abundance: a tale of division and proliferation. Current Opinion in Plant Biology, 12: 781-788
- **Keeck O**, Pesquet E, Ahad A, Askne A, Nordvall D, Vodnala SM, Tuominen H, Hurry V, Dizengremel P, Gardeström P (2007). The different fates of mitochondrial and chloroplasts during dark-induced senescence in Arabidopsis leaves. Plant, Cell and Environment, 30:1523-1534
- **Köhler RH**, Hanson MR (2000). Plastid tubules of higher plants are tissue-specific and developmentally regulated. Journal of Cell Science, 113 (1):81-89
- **Kwok EY**, Hanson MR (2004a). GFP-labelled Rubisco and aspartate aminotransferase are present in plastid stromules and traffic between plastids. Journal of Experimental Botany, 55(397):595-604
- **Kwok EY**, Hanson MR (2004b). Stromules and dynamic nature of plastid morphology. Journal of Microscopy, 214 (2):124-137
- **Jaillon O**, Aury JM, Noel B, Policriti A, Clepet C, Casagrande A, Choisne N, Aubourg S, Vitulo N, Jubin C, Vezzi A, Legeai F, Hugueney P, Dasilva C, Horner D, Mica E, Jublot D, Poulain J, Bruyère C, Billault A, Segurens B, Gouyvenoux M, Ugarte E, Cattonaro F, Anthouard V, Vico V, Del Fabbro C, Alaux M, Di Gaspero G, Dumas V, Felice N, Paillard S, Juman I, Moroldo M, Scalabrin S, Canaguier A, Le Clainche I, Malacrida G, Durand E, Pesole G, Laucou V, Chatelet P, Merdinoglu D, Delledonne M, Pezzotti M, Lecharny A, Scarpelli C, Artiguenave F, Pè ME, Valle G, Morgante M, Caboche M, Adam-Blondon AF, Weissenbach J, Quétier F, Wincker P; French-Italian Public Consortium for Grapevine Genome Characterization. (2007) The grapevine genome sequence suggests ancestral hexaploidization in major angiosperm phyla. Nature 449: 463-467

- **Jedd G**, Chua NH (2002). Visualization of peroxisomes in living plant cells reveals acto-myosin dependent cytoplasmic streaming and peroxisome budding. Plant Cell Physiology, 43 (4):384-392
- **Lam E** (2004). Controlled cell death, plant survival and development. Molecular Cell Biology, 4:305-315
- **Logan DC** (2006). The mitochondrial compartment. Journal of Experimental Botany, 57 (6): 1225-1243
- **Logan DC**, Scott I, Tobin AK (2004).AL2a, like ADL2b, is involved in the control of higher plant mitochondrial morphology. Journal of Experimental Botany, 55(397):783-785
- **Logan DC**, Knight MR (2003). Mitochondrial and cytosolic calcium dynamics are differentially regulated in plants. Plant Physiology, 133: 21-24
- **Logan DC** (2003). Mitochondrial dynamics. New Phytologist, 160 (3): 463–478
- **Michels PA**, Moyersoen J, Krazy H, Galland N, Herman M, Hannaert V (2005). Peroxisomes, glyoxysomes and glycosomes. Molecular membrane biology, 22(1-2):133-145
- **Mai S**, Klinkenberg M, Auburger G, Bereiter-Hahn J, Jendrach M (2010). Decreased expression of Drp1 and Fis1 mediates mitochondrial elongation in senescent cells and enhances resistance to oxidative stress through PINK1. Journal of Cell Science, 123: 917-926
- **Mano S**, Nakamori C, Hayashi M, Kato A, Kondo M, Nishimura M (2002). Distribution and characterization of peroxisomes in *Arabidopsis* by visualization with GFP: dynamic morphology and actin-dependent movement. Plant Cell Physiology, 43 (3):331-341
- **Maple J** and Møller SG (2007). Plastid division coordination across a double-membraned structure. FEBS Letter, 581 (11):2162-2167.
- **Miyagishima SY**, Froehlich JE, Osteryoung KW (2006). PDV1 and PDV2 mediate recruitment of the dynamin-related protein ARC5 to the plastid division site. The Plant Cell, 18 (10):2517-2530
- **Noctor G**, De Paepe R, Foyer CH (2007). Mitochondrial redox biology and homeostasis in plants. TRENDS in Plant Science, 12 (3):125-134

- **Quirino BF**, Noh YS, Himelblau E, Amasino RM (2000). Molecular aspects of leaf senescence. 5(7):278-82.
- **Rhoads DM**, Subbaiah C (2007). Mitochondrial retrograde regulation in plants. Mitochonrion, 7: 177-194
- **Schrader M**, Yoon Y (2007). Mitochondria and peroxisomes: are the 'Big Brother' and the 'Little Sister' closer than assumed? BioEssay, 29: 1105-1114
- **Schrader M** (2006). Shared components of mitochondrial and peroxisomal division. Biochimica et Biophysica Acta, 1763(5-6):531-541
- **Scott, I** and Logan, D.C. (2008) Mitochondrial morphology transition is an early indicator of subsequent cell death in Arabidopsis. New Phytologist 177, 90-101
- **Scott I**, Sparkes IA, Logan DC (2007). The missing link: inter-organellar connection in mitochondria and peroxisomes? TRENDS in Plant Science, 12 (9):380-381
- **Scott I**, Tobin AK, Logan DC (2006). BIGYIN, an orthologue of human and yeast FIS1 genes functions in the control of mitochondrial size and number in *Arabidopsis thaliana*. Journal of Experimental Botany, 57 (6):1275-1280
- **Sinclair AM**, Trobacher CP, Mathur N, Greenwood JS, Mathur J (2009). Peroxule extension over ER-defined paths constitutes a rapid subcellular response to hydroxyl stress. The Plant Journal, 59:231-247
- **Suen DF**, Norris KL, Youle RJ (2008). Mitochondrial dynamics and apoptosis, Genes and Development, 22: 1577-1590
- **Suzuki M**, Jeong SY, Karbowski M, Youle RJ, Tjandra N (2003). The solution structure of human mitochondria fission protein Fis1 reveals a novel TPR-like helix bundle. Journal of Molecular Biology, 334 (3):445-58.
- **Sweetlove L**, Fait A, Nunes-Nesi A, Williams T, Fernie AR (2007). The mitochondrion: an integration point of cellular metabolism and signalling. Critical Reviews in Plant Sciences, 26:17-43
- **Van Breusegem F**, Dat JF (2006). Reactive oxygen species in plant cell death. Plant Physiology, 141 (2):384-90

- **Vandecasteele G**, Szabadkai G, Rizzuto R (2001). Mitochondrial calcium homeostasis: mechanisms and molecules. IUBMB Life, 52: 213-219
- **Velasco R**, Zharkikh A, Troggio M, Cartwright DA, Cestaro A, Pruss D, Pindo M, FitzGerald LM, Vezzulli S, Reid ., Malacarne G, Iliev D, Coppola G, Wardell B, Micheletti D, Macalma TM, Facci M,. Mitchell JT, Perazzolli M, Eldredge G, Gatto P, Oyzerski R, Moretto M, Gutin N, Stefanini M, Chen Y, Segala C, Davenport C, Demattè L, Mraz A, Battilana J, Stormo K, Costa F, Tao Q, Si-Ammour A, Harkins T, Lackey A, Perbost C, Taillon B, Stella A, Solovyev V, Fawcett JA, Sterck L, Vandepoele K, Grando MS, Toppo S, Moser C, Lanchbury J, Bogden R, Skolnick M, Sgaramella V,. Bhatnagar SK, Fontana P, Gutin A, Van de Peer Y, Salamini F, Viola RA, (2007) High quality draft consensus sequence of the genome of a heterozygous grapevine variety, PLoS ONE , 2 (12), p. e1326
- **Westermann B**, (2010). Mitochondrial fusion and fission in cell life and death. Molecular Cell Biology, 11: 872-884
- **Zapata JM**, Guera A, Esteban-Charrasco A, Martin M, Sebater B (2005). Chloroplast regulate leaf senescence: delayed senescence in transgenic *ndh*F-defective tobacco
- **Zhang XC**, Hu JP (2010). The *Arabidopsis* chloroplast division protein DYNAMIN-RELATED PROTEIN5B also mediates peroxisomes division. The Plant Cell, 22 (2):431-42.
- **Zhang XC**, Hu JP (2008a).Two small protein families, DYNAMIN-RELATED PROTEIN3 and FISSION1, are required for peroxisome fission in *Arabidopsis*. The Plant Journal, 57(1):146-59
- **Zhang XC**, Hu JP (2008b). FISSION1A and FISSION1B proteins mediate the fission of peroxisomes and mitochondria in Arabidopsis. Molecular Plant, 1(6):1036-47
- **Zottini M**, Barizza E, Bastianelli F, Carimi F, Lo Schiavo F (2006). Growth and senescence of *Medicago truncatula* cultured cells are associated with characteristic mitochondrial morphology. New Phytologist, 172 :239-247

Chapter 1

Changes in mitochondrial morphology associated with cell aging during grapevine leaf spontaneous senescence

INTRODUCTION

Leaf senescence is the final stage of leaf development and it is a slow physiological process, under the control of several factors both endogenous (hormones) and external (light, starvation, pathogens). Senescence involves the ordered disassembly of cellular components that are redirected to other plant organs; meanwhile senescing tissues eventually die by programmed cell death (PCD) which presents some typical hallmarks of apoptosis (Yoshida, 2003).

Understanding the molecular mechanisms used by the plant to regulate senescence might provide applicative outputs, especially in agronomical relevant species, such as grapevine (*Vitis spp*). Moreover, after the sequencing of its genome (Jaillon *et al.*, 2007; Velasco *et al.*, 2007), grapevine has the potential to become a model organism for fruit trees. A decrease in the leaf photosynthetic efficiency during grapes maturation may, actually, result in an insufficient sugar level in berries. The knowledge of the regulative aspects of leaf senescence and berry ripening might lead to govern plant growth and development and possibly to control the environmental conditions affecting senescence and berry yield.

In eukaryotic cells, mitochondria play a central role in energy and carbon metabolism (Siedow and Day, 2000), but they also play a significant role in control of programmed cell death pathways, as a stress sensor and dispatcher. Various cell death-signalling pathways are indeed critically dependent on mitochondria, whose action is played not only through the release of pro-apoptotic factors such as cytochrome c, but also through the alteration of their dynamics and morphology. Although mitochondria are often portrayed as static, oval or rod-shaped organelles, recent studies have demonstrated that they are among the most plastic organelles of cells in terms of form and distribution. Yet, changes in their architecture and their ability to move rapidly throughout the cytoplasm appear to be of critical importance for executing their cellular functions. A link between senescence-associated cell death and plant mitochondrial dynamics and morphology has been reported in *Medicago truncatula* cell cultures (Zottini *et al.*, 2006) and confirmed in *Arabidopsis* leaf and mesophyll protoplasts (Scott and Logan, 2008). In particular, in *Medicago truncatula* cell cultures it has been observed that alterations in mitochondrial dynamics and morphology were

associated with cell ageing during senescence occurring spontaneously (Carimi *et al.* 2004).

In this report, analyses of mitochondrial morphology were performed first on grapevine cell cultures and then on grapevine leaf tissue. We produced suspension cell cultures starting from leaf tissue (Zottini *et al.*, 2008) to perform experiments in cultured cells, and embriogenic cell lines (Carimi *et al.*, 2005) to be used in transformation procedures. For analyses in leaf tissues, in fact, we produced plants transformed with the green fluorescent protein (*GFP*) targeted to the mitochondria. These transgenic plants allowed us to bypass the technical problem of poor staining of plant tissues with exogenous fluorescent dyes (Kohler *et al*., 1997). By using them, we were able to detect, in an accurate way, changes of mitochondrial morphology occurring at different stages of grapevine leaf senescence.

RESULTS

Analyses of mitochondrial morphology during spontaneous senescence in grapevine suspension cell cultures

To analyse in detail the mitochondrial morphology, suspension cell cultures has been chosen as initial model system. By using our standard protocol (Zottini *et al*., 2008), a grapevine cell culture line was produced starting from leaf tissue (cultivar Köber5bb) and its basic physiological parameters, such as growth curve and cell viability, were determined (Fig. 1).

Concerning mitochondrial morphology analysed via TMRM staining (Fig. 1A-B), we observed that, in the initial phase of the growth curve (4 days after culture initiation), mitochondria were numerous and spread throughout the cytoplasm. In 7-day-old proliferating cells (viability 95%), typical reticular arrangements of mitochondria were detected. At 18 days, when cells started to senesce and cell viability reduced to 70%, mitochondria network disintegrated. During spontaneous senesce, dotty giant mitochondria were observed. In this senescence phase, cell death rapidly increased, as indicated by the decrease of viability to about 80% in 28 day-old cells (Fig. 1D). These results were in agreement with those obtained in *Medicago truncatula* cultured cells confirming the characteristic morphology of mitochondria analysed at different growth and senescence phases (Zottini *et al.*, 2006).

Grapevine plants transformed with *β-GFP*-targeted to mitochondria

In order to analyse mitochondria morphology in plants, new tools had to be developed. In fact, the TMRM staining gave poor resolution when applied to leaf tissues. So, plants transformed with *β-GFP*-targeted to mitochondria were produced. To do that, we constructed a vector containing the mitochondrial leading sequence of the *β-ATPase* bound to the *GFP* gene under 35S promoter (for details see 'Material and Methods'). We applied a transformation procedure

using embryogenic cell cultures as starting material. Embryogenic cultures were the starting material for transformation experiments. *GFP*-transformed embryos were visualized by epi-fluorescence stereomicroscope: *GFP* expression was detectable with a patchy distribution in ten days embryogenic callus (Fig. 2A; t1). Three and four months later (Fig. 2A; t2 and t3), transformed globular and torpedo embryos were clearly observed, respectively. In order to avoid chimeras, secondary embryos were regenerated from primary transgenic plantlets (Fig. 2 B). Adult plants obtained from those selected transgenic secondary embryos maintained GFP fluorescence in leaf and root tissues (Fig. 2B) thus demonstrating the absence of silencing phenomena eventually developed during plant growth. Laser scanning confocal microscopy was employed to determine the distribution of GFP-fluorescent mitochondria at the cellular level. In Fig. 2C mitochondria were visualized at the embryo level, in the following paragraphs analyses at the level of leaf tissues will be presented.

Analyses of mitochondrial morphology during leaf senescence

In grapevine plants transformed with *β-GFP* targeted to mitochondria, we were able to detect changes in mitochondrial morphology during leaf senescence (Fig. 3). In fully expanded mature leaf (M) (Fig. 3A), the mitochondria were numerous as observed at the level of stomata cells, mesophyll cells and epidermal tissues. During different phases of leaf senescence, characterised by a different percentage of leaf yellowing (S1, S2, S3), the number of mitochondria was progressively reduced from S1 to S3 with a concomitant increase in their volume (Fig. 3B-D). In particular we observed that the number of typical giant mitochondria increases during senescence progression associated with the expected decrease of chloroplast number. Change of mitochondrial number and dimension during leaf senescence was evaluated by ImageJ analysis. Number reduction of mitochondria was quantitative demonstrated and a concomitant increase in their volume was detected (Fig. 3E).

Physiological and molecular characterization of grapevine leaf senescence

The characterization of leaf senescence in our experimental system was performed through the measurement of different physiological parameters and the expression level of specific molecular markers, at the different senescence stages.

Photosynthetic capacity

During the first phases of senescence, the maximum efficiency of photosystem II (PSII) (*F*v/*F*m) remained around 0.7 ± 0.03 in mature and S1 leaves (Fig. 4A). In S2 leaves, the *F*v/*F*m decreased only slightly and reached 0.61 ± 0.02, indicating that most of the PSII reaction centers remained functional. However, in S3, *F*v/*F*m declined rapidly to 0.16 ± 0.02. Associated with these measurements of photosynthetic capacity, photosynthetic pigments were quantified by HPLC analysis. In M the leaves show a pigment content of about 1 mg/gr off FW, in S1 the leaves maintained pigment contents similar to M with only a small decline (0.99 mg/gr). In leaves from S2 to S3 phase the total chlorophyll content strongly decreases from 0.56 mg/gr to 0.1 mg/gr chlorophylls (Fig. 4B).

Molecular markers

A molecular characterization of senescence was done by RT-PCR analyses of two senescence associated genes (*SAGs*), namely, *VvSAG13* (*Vitis vinifera SAG13*), and *VvNAM* (*Vitis vinifera NAM*) (Espinoza *et al.*, 2007) In Fig. 4C, it is reported their expression pattern. A comparison between fully expanded leaves and S3 senescent leaves confirmed, at the molecular level, the increased level of expression of these two SAG genes as markers of senescent tissues.

DISCUSSION

In this work we describe the mitochondria dynamics and morphology occurring in *Vitis vinifera* leaves during natural senescence. The molecular aspects of the various stages of senescence are not known in details; due to the slowness and heterogeneity of the process. Being simple and homogeneous, cell cultures represent an ideal system for studying some general aspects of senescence, allowing defining the relationships between senescence and PCD (Carimi *et al.* 2004).

In order to perform an accurate analysis of mitochondria, during senescence, at the cellular level, we used suspension cell cultures for our initial experiments. So, a grapevine cell culture from leaf tissues was produced and its growth curve established. The growth curve, as usual, identified different phases: initial, in which cells condition their medium; log, in which cell division takes place; and final, in which cells stop dividing, elongate and senesce. In fact, if cells were not sub-cultured at the end of the growth period, they started senescing and PCD ensued. The last phase of the curve is identified as spontaneous senescence phase. Growing cultured cells showed typical reticular arrangements of fast moving mitochondria; the networks disappear in ageing cells and giant, not mobile mitochondria characterised this type of cells. These results are matching the ones observed in *Medicago truncatula* cell cultures, where similar analyses were done (Zottini, *et al.* 2006).

Then, we developed new tools to observe alterations of mitochondrial morphology in plant. In fact, we produced grape plants transformed with β–GFP targeted to mitochondria and we were able to detect in an accurate way morphology and dynamics of mitochondria during leaf senescence. A significant progress in producing transgenic grapevines was made when embryogenic cell lines were used as target tissue (Vivier and Pretorius, 2002). Our transformation protocol based, in fact, on long lasting embryogenic cell lines, that we produced and maintained as such indefinitely. We were able to achieve that alternating cycles of cell de-differentiation with cycles of embryo differentiation (see 'Material and Methods' for detail). The use of PEM combined with *Agrobacterium* infection provided an efficient transformation procedure.

As reported in fig.4, we observed the evolution of mitochondrial morphology at different leaf stages. In fully expanded green leaf, the mitochondria visualised in different tissues (i.e. epidermis, stomata and mesophyll cells), were numerous and mobile. In senescent leaf, their number reduced, their volume increased and giant mitochondria are detected. The ageing cells of senescent leaf tissue is therefore characterized by these mitochondrial morphological alterations. These data are in agreement with the alterations of mitochondrial morphology and motility observed in *Arabidopsis* protoplast and leaf tissues during induced PCD (Yao *et al.*,2004; Scott and Logan, 2008).

It is important to underline the similarity of events observed in cell cultured and in leaf tissue. The correspondence between the evolution of dynamics and morphology of mitochondria from growth to ageing cells in cultures and from greening to yellowing cells in leaf tissue confirms that analyses performed in cell cultures may contribute positively in dissecting and understand cellular mechanisms of important physiological processes, such as cell ageing and senescence in plants. This is, in fact, a good example in which results from experiments performed in cultured cells can be used as guidelines to perform experiments in complex tissues.

Yet, the understanding of some of the cellular mechanisms occurring during grapevine senescent events might lead to a controlled regulation of this process with important potentials in improving quantity and quality of an important crop production and its post-harvest shelf life.

MATERIAL AND METHODS

Suspension cell cultures and TMRM treatment

Suspension cell cultures preparation was according to Zottini *et al.* (2008). Briefly, grapevine cultivar Köber5bb cell lines were obtained from leaf dish explants incubated on selective B5 (Gamborg B5 medium, Duchefa; Gamborg et al. 1968) solid (8 g l^{-1} agar) medium supplemented with 2.26 µM 2,4-dichlorophenoxy-acetic acid (SIGMA) (B5F). After several subculture cycles aliquots of callus were utilized for liquid cultures. For subculture cycles, 2 ml were transferred to Erlenmeyer flasks (250 ml) filled with 50 ml liquid B5 medium supplemented with 2.26 µM 2,4-dichlorophenoxy-acetic acid . The suspension cultures were subcultured in fresh medium every week and maintained in a climate growth chamber at 25 °C on an orbital shaker (80 rpm) under a 16 h day length. To determine dry weight, integer cells were separated from the culture medium and cell debris through a vacuum filtration unit (Sartorius, Florence, Italy).

A Nikon PCM2000 laser scanning confocal microscope (Nikon, Italy) was used for analysis of mitochondrial morphology. The tetramethylrhodamine methyl ester dye (TMRM) (Molecular Probes, Leiden, the Netherlands), a mitochondrial membrane potential sensor, was used for visualizing mitochondria in cell culture as described by Zottini *et al*. (2006). Cell suspensions (300 µl) were collected at different times during their growth cycle, and incubated in 700 µl B5F medium containing 1 µM TMRM for 15 min on a rotary shaker. Cells were centrifuged for 3 min at 10 000 x*g*, the supernatant was discarded and the pellet washed twice with 700 µl B5F. Cells were then resuspended in 500 µl B5F. For microscope analysis, 100 µl cell suspension was placed on a microscope slide and visualized under a confocal microscope (excitation 548 nm, emission 573 nm). Images were processed using Corel PHOTO -PAINT. For mitochondrial morphology experiments, a randomized complete block design was used with three replicates (individual Erlenmeyer flasks). Each experiment was repeated three times.

Cell viability assay

Cell viability was determined by fluorescein diacetate (FDA) assay according to Amano *et al.* (2003). Immediately before each assay, a stock solution of FDA (0.5% w/v in acetone) was diluted with distilled water to create a fresh 0.01% w/v FDA working solution which was kept in the dark at 4°C. Cell suspensions of grapevine was aliquot in 2 ml fractions on Poly-Prep Cromatography columns (BioRad) then diluited 1/10 with PBS (2.7mM KCl, 137mM NaCl, 1.8mM KH_2PO_4, 4.0mM Na_2HPO_4). 100 µl of this solution was then mixed by gentle stirring with 0.01% w/v FDA in a quartz cuvette. A spectrophotofluorimeter (Perkin Elmer, UK) equipped with a stirrer was employed. Excitation and emission wavelengths were selected at 493 and 510 nm, respectively. The increase in fluorescence was recorded over a 120-s time period. The slope of the fluorescence increase (between 60 to 90 s) was calculated for each cellular suspension to determine the correlation between cell viability and the velocity of FDA conversion. A standard cell viability curve was set up using several cellular suspensions containing different known amounts of viable cells. To achieve this, dead cells were prepared by boiling of viable cells. After, aliquots of these control dead cells were added to several different quantities of healthy viable cells to obtain suspensions whose cellular viabilities varied between 0 and 100% (in increments of 20%). Cell suspension set was then used to determine the correlation between FDA conversion and cell viability using a spectrofluorimetric assay.

Cell cultures and plant material

Plasmid construction and Agrobacterium tumefaciens used for transformation

For the expression of *GFP* targeted to the mitochondria, the *Agrobacterium tumefaciens* strain GV3101 harbouring the p BI121 binary vector, with a T-DNA incorporating the *Green Fluorescent Protein* (*GFP*) gene targeted to mitochondria (*β*::*GFP*) was obtained following the procedures as previously described by Zottini *et al.* (2008). Briefly, the cDNA coding sequences of *β::GFP* were subcloned from the *β*::GFP plasmid (Zhao *et al.*, 2000; Duby *et al.*, 2001) to the

pBI121 binary vector (Clontech Laboratories, USA) by replacing the β-glucuronidase cDNA sequence. For sub-cloning, the *β*-GFP fusion construct into the pBI121 binary vector the *BglII/SacI* restriction sites were used. The p BI121 binary vector contain the coding sequence for *neomycin phosphotransferase II* (*nptII*) that allowed for selection of transgenic cells based on kanamycin resistance.

Competent cells of *Agrobacterium tumefaciens* GV3101 strain were prepared according to Sambrook *et al.* (1989) and the binary vectors were introduced by electroporation as described by Zottini *et al.* (2008). The growth of bacteria was optimized by growing in YEP medium (Bacto-Trypton, 10 gL^{-1}; yeast extract, 10 gL^{-1}, NaCl, 5 gL^{-1}; pH 7.0) The media were supplemented with the antibiotics rifampicin 100 mgL^{-1}, gentamycin 50 mgL^{-1}, kanamycin 50 mgL^{-1}.

Regeneration of embryogenic cell lines

Embryogenic cell lines of grapevine (cv Moscato giallo) were produced from stigma/style cultures as described by Carimi *et al.* (2005). Briefly, explants were dissected from unopened flowers and placed on Nitsch and Nitsch (1969) salts and vitamins, 88 mM sucrose, 9 µM BA and 10 µM NOA. Medium pH was adjusted to 5.7 before the addition of 8 g l^{-1} Plant agar (Duchefa) and autoclaving at 121 °C for 20 min. Cultures were placed in an acclimatized cabinet at 25°C and 16 h light photoperiod, and subcultured at 30-day intervals. White embryogenic globules, around 1-3 mm in size, were separated from the callus grown from the original stigma/style explants and were cultured alternating, every 3 weeks, solid MS growth regulator free medium and solid B5 2.26 µM 2-4D medium. The alternation of such medium permitted us to maintain the embryogenic cell line for long time.

Liquid suspensions for transformation were initiated from habituated embryogenic cultures by transferring 1 g of PEM collected from solid MS growth regulator free medium (MS-) to Erlenmeyer flasks (250 ml) filled with 50 ml liquid MS- medium. The flasks were cultured for 3 days on an orbital shaker at 80 rpm and incubated at 25 °C in the dark.

Transformation of embryogenic cultures and selection of transgenic plants

Before transformation with *Agrobacterium tumefaciens*, 500 mg of PEM and embryos were transferred into a petri disc contained 1 ml of liquid induction medium (LIM = NN medium supplemented with 58 mM sucrose, 2.26 µM 2,4-D) and were incised with a sharp razor blade. Bacteria suspension preparation was according to Zottini *et al.* (2008). *Agrobacterium tumafaciens* suspension was diluted to OD_{550} 0.5 in LIM and added (5 mL) to the dissected embryos that were previously transferred in bacteria-free LIM (1 mL). Embryo were incubated (room temperature, dark) for 10 min after which the cultures were washed 5 times with induction medium (3 min washing). Infected embryos were blotted dry on sterile filter paper and plated on NN solid medium and incubated at 25 °C in the dark. Two days later the cultures were transferred to NN solid medium supplemented with 300 mgL^{-1}cefotaxime and maintained at 25°C in the dark. After 10 days the cultures were transferred on NN solid medium supplemented with 20 mgL^{-1} kanamycin and 300 mgL^{-1}cefotaxime. After 20 days the cultures were transferred on NN solid medium supplemented with 40 mgL^{-1}kanamycin and 300 mgL^{-1}cefotaxime and subcultured at 20 day-intervals.Embryo clusters differentiated at the callus surface maintained on 40 mgL^{-1} kanamycin were collected and transferred on NN hormone free solid medium for germination. Individual germinated somatic embryos were transferred to Microbox Containers (Duchefa, The Netherland) in half strength MS solid medium (0.8% plant agar Duchefa, The Netherland) supplemented with 44 mM sucrose and were multiplied by clonal propagation and maintained (30-day intervals). Plants were incubated in a growth chamber at 25+1 °C under a 16 h day length, and a photosynthetic photon flux of 35 µmol m^{-2} s^{-1} Osram cool-white 18 W fluorescent lamps.

Hydroponic cultivation

Transformed plants grown *in vitro* were transferred with roots, after elimination of agar by washing, to hydroponic conditions. The nutrient solution composition was designed, tested and optimized for *Vitis vinifera* : 0.5 mM KH_2PO_4; 0.5 mM K_2SO_4; 2 mM $Ca(NO_3)_2.4H_2O$; 0.65 mM $MgSO_4$; 0.5 µM H_3BO_3; 0.045 µM $CuSO_4X\ 5H_2O$; 0.05 µM $ZnSO_4\ X\ 7H_2O$; 0.02 µM $(NH_4)_6Mo_7O_{24}\ X\ 4H_2O$; 0.5 µM $MnSO_4$; 10 µM Fe-EDDHA. The hydroponic system consists in a Microbox

Containers containing a floating polystyrene circle with a sponge placed in the middle holding the plant.

Evaluation of gene expression trough fluorescent proteins

GFP-dependent fluorescence in leaves was analyzed using an epifluorescence stereo microscope. Suspension cells and transformed leaves were analyzed using a confocal microscopy Nikon PCM2000 (Bio-Rad, Germany) laser scanning confocal imaging system. For GFP detection, excitation was at 488 nm and emission between 515/530 nm. Image analysis was done with the ImageJ bundle software (http://rsb.info.nih.gov/ij/).

Semi-quantitative RT-PCR analysis in p*BIGYIN::GUS* plants

Total RNA was extracted from leaved characterized by different phases of leaf senescence (M, S1, S2, S4). RNA isolation was carried out using the 'Master Pure Plant RNA Purification' Kit (EPICENTRE® Biotechnologies), according to manufacturer's specification. After DNAse I treatment (Ambion Ltd, UK), first strand synthesis and PCR were carried out starting from 1 μg of total RNA, according to the manufacturer's instructions (ImProm Reverse Transcriptase, Promega). After first strand cDNA synthesis, samples were diluted 5 times and used as templates for semi-quantitative RT-PCR. RT-PCR analyses were performed using the follow specific primers: *VvActin-1* (housekeeping gene, For: 5' -GACAATGGAACTGGAATGGTGAAG-3'; Rev 5'-TACGCCCACTGGCATATAGAGAAA-3'), for *VvSAG13* (For: 5'-GCTTCCTGCTCCAGATGC-3'; Rev: 5'- TGCCACCGTACACACCTG-3'), for *VvNam* For: 5'-ATGCTCACAATCCGTAACCG-3'; Rev 5'-CAGCCACAACATCAAGCATC-3').

RT-PCR reactions were performed using GoTaq® DNA Polymerase (Promega), in a total reaction volume of 50μL according to manufacturer's recommendations containing 5μL of cDNA. PCR amplification cycle was performed with an initial denaturation step at 94°C for 2min, followed by 32 cycles for *avVvActin-1*, 31 cycle for *VvNam* and 28 cycles for *VvSAG13* (95°C for 20s; 61°C for 30s; 72°C for 30s), and finally with an elongation step at 72°C for 5min.

REFERENCES

- **Amano** T, Hirasawa K, O'Donohue MJ, Pernolle JC, Shioi Y (2003). A versatile assay for the accurate, time-resolved determination of cellular viability. Analytical Biochemistry, 314: 555-565
- **Carimi F**, Terzi M, De Michele R, Zottini M, Lo Schiavo F (2004). High levels of cytokinin BAP induce PCD by accelerating senescence. Plant Science, 166 : 963-969
- **Carimi F**, Barizza E, Gardiman M, Lo Schiavo F (2005). Somatic embryogenesis from stigmas and styles of grapevine. In vitro cellular development biology – plant, 41(3): 249-252
- **Duby G**, Oufattole M, Boutry M (2001) Hydrophobic residues within the predicted N-terminal amphiphilic alpha-helix of a plant mitochondrial targeting presequence play a major role in in vivo import. Plant Journal, 27:539–549
- **Espinoza C**, Medina C, Sommerville S, Arce-Johnson (2007). Senescence-associated genes induced during compatible viral interactions with grapevine and Arabidopsis. Journal of Experimental Botany, 58 (12):3197-3212
- **Gamborg OL**, Miller RA, Ojima K (1968). Nutrient requirements of suspension cultures of soybean root cells. Experimental Cell Research 50:151-158.
- **Jaillon O**, Aury JM, Noel B, Policriti A, Clepet C, Casagrande A, Choisne N, Aubourg S, Vitulo N, Jubin C, Vezzi A, Legeai F, Hugueney P, Dasilva C, Horner D, Mica E, Jublot D, Poulain J, Bruyère C, Billault A, Segurens B, Gouyvenoux M, Ugarte E, Cattonaro F, Anthouard V, Vico V, Del Fabbro C, Alaux M, Di Gaspero G, Dumas V, Felice N, Paillard S, Juman I, Moroldo M, Scalabrin S, Canaguier A, Le Clainche I, Malacrida G, Durand E, Pesole G, Laucou V, Chatelet P, Merdinoglu D, Delledonne M, Pezzotti M, Lecharny A, Scarpelli C, Artiguenave F, Pè ME, Valle G, Morgante M, Caboche M, Adam-Blondon AF, Weissenbach J, Quétier F, Wincker P; French-Italian Public Consortium for Grapevine Genome Characterization (2007). The grapevine genome sequence suggests

ancestral hexaploidization in major angiosperm phyla. Nature, 449: 463-467

- **Kohler RH**, Zipfel WR, Webb WW, Hanson MR (1997). The green fluorescent protein as a marker to visualize plant mitochondria *in vivo*. The Plant Journal, 11(3): 613-621
- **Main GD**, Reynolds S, Gartland JS (1995) Electroporation protocols in Agrobacterium. In: Gartland KMA, Davey MR (eds) Methods in molecular biology, vol 44: Agrobacterium protocols. Humana Press, Totowa, pp 405–412
- **Nitsch JP**; Nitsch C (1969). Haploid plants from pollen grains. Science, 163:85-87.
- **Sambrook J**, Fritsch EF, Maniatis T (1989). Molecular Cloning: A Laboratory Manual, 2nd edn. Cold Spring Harbor Laboratory Press, New York.
- **Siedow JN**, Day DA (2000). Respiration and photorespiration, in Biochemistry and Molecular Biology of Plants, edited by B. B. Buchanan, W. Gruissem and R. L. Jones, Eds., American Society of Plant Physiologists, pp. 676-728.
- **Scott I**, Logan DC (2008). Mitochondrial morphology transition is an early indicator of subsequent cell death in *Arabidopsis*. New Phytologist, 177, 90-101
- **Velasco R**, Zharkikh A, Troggio M, Cartwright DA, Cestaro A, Pruss D, Pindo M, FitzGerald LM, Vezzulli S, Reid ., Malacarne G, Iliev D, Coppola G, Wardell B, Micheletti D, Macalma TM, Facci M,. Mitchell JT, Perazzolli M, Eldredge G, Gatto P, Oyzerski R, Moretto M, Gutin N, Stefanini M, Chen Y, Segala C, Davenport C, Demattè L, Mraz A, Battilana J, Stormo K, Costa F, Tao Q, Si-Ammour A, Harkins T, Lackey A, Perbost C, Taillon B, Stella A, Solovyev V, Fawcett JA, Sterck L, Vandepoele K, Grando MS, Toppo S, Moser C, Lanchbury J, Bogden R, Skolnick M, Sgaramella V,. Bhatnagar SK, Fontana P, Gutin A, Van de Peer Y, Salamini F, Viola RA, (2007) High quality draft consensus sequence of the genome of a heterozygous grapevine variety, PLoS ONE , 2 (12), p. e1326

- **Vivier MA**, Pretorius IS (2002). Genetically tailored grapevines for the wine industry. Trends in Biotechnology, 20, 472-478
- **Yao N**, Eisfelder BJ, Marvin J, Greenberg, JT (2004). The mitochondrion-an organelle commonly involved in programmed cell death in *Arabidopsis thaliana*. Plant Journal, 40:596-610
- **Yoshida S** (2003). Molecular regulation of leaf senescence. Current Opinion of Plant Biology, 6: 79-84
- **Zhao** R, Dielen V, Kinet JM, Boutry M (2000) Cosuppression of a plasma membrane H+-ATPase isoform impairs sucrose translocation, stomatal opening, plant growth, and male fertility. Plant Cell, 12:535–546
- **Zottini M**, Barizza E, Bastianelli F, Carimi F, Lo Schiavo F (2006). Growth and senescence of *Medicago truncatula* cultured cells are associated with characteristic mitochondrial morphology. New Phytologist, 172: 239-247
- **Zottini M**, Barizza E, Costa A, Formentin E, Ruberti C, Carimi F and Lo Schiavo F (2008). Agroinfiltration of grapevine leaves for fast transient assays of gene expression and for long-term production of stable transformed cells. Plant Cell Report. 27 (5): 845-853

Chapter 2

BIGYIN, a tail anchored protein, recruits cytosolic ELM1 protein at mitochondria and chloroplast level

INTRODUCTION

Plant mitochondria, in addition to playing important roles in common with mitochondria of most eukaryotic cells, such as in respiration and in metabolism (Sweetlove *et al.*, 2007), reveal in photosynthetic cells also plant-specific roles, such as photorespiration and redox regulation (Bauwe *et al.*, 2010; Noctor *et al.*, 2007). Mitochondria are implicated in cell signalling both in animals and in plants (Sweetlove *et al.*, 2007), and these organelles are also involved in programmed cell death (PCD) in animal and in plant systems (Vianello *et al.*, 2007).

Mitochondria are not generated *de novo*, but they arise by fission of pre-exiting mitochondria in the cytosol. Mitochondrial fission is an ubiquitous fundamental process in yeasts, animals and plants, important not only for the maintenance of the mitochondrial number during cell cycle, but also for keeping mitochondrial proper morphology (shape and size) within a single cell (Logan, 2003). In addition, mitochondrial fission plays a role in apoptosis in yeasts and animals. In detail, mitochondrial fission and subsequent mitochondrial fragmentation are an early event during apoptosis in yeasts and mammals (Suen *et al.*, 2008). By contrast, a decrease in mitochondrial fission and the subsequent - elongated mitochondrial morphology are protective features in old human endothelial cells cultured *in vitro* (Mai *et al.*, 2010). In plants, similar giant mitochondria during senescence-associated cell death have been reported in *Medicago truncatula* cultured cells (Zottini *et al.*, 2006) and in plants (Chapter 1).

Although these findings indicate that mitochondrial fission is a fundamental cell process, studies in higher plants on mitochondrial division are at the beginning. Molecular mechanisms involved in mitochondrial fission machinery have been studied extensively in yeast *Saccharomyces cerevisiae*. Mitochondrial fission in yeast needs four proteins: Fission1 (Fis1), Dynamin1 (Dnm1), Mitochondrial division1 (Mdv1) and CCR4-associated factor (Caf4). Fis1 is an integral membrane protein, located to the mitochondrial outer membranes. Its N-terminal domain is exposed to the cytosol and forms a tetratricopeptide (TRP)-like bundle helix, involved in protein-protein interaction (Suzuki *et al.*, 2003), while the C-terminal tail contains a single transmembrane domain. For this topology, Fis1 is considered a member of tail-anchored (TA)

(N_{out}-C_{in}) family of membrane proteins (**Borghese *et al.*, 2007**). Dnm1 is a yeast dynamin-related protein (DRP), characterized by an N-terminal GTPase domain and a C-terminal GTPase effector. During mitochondrial division, Fis1 recruits to mitochondrial fission sites the cytosolic molecular adapter Mdv1 (and its paralog Caf4) and Dnm1. Dnm1 and Mdv1 are thought to form higher-order multimer complexes, named fission complexes, that surround and pinch off the mitochondria.

Recently, in *Arabidopsis thaliana*, several genes involved in remodelling of mitochondria have been described: two dynamin-related proteins (DRPs), termed DRP3A (formerly, *Arabidopsis* dynamin-like protein 2A [ADL2a] and ADL2b, respectively; [Zhang and Hu, 2008a]); at least a fission-like protein, homologue of yeast Fis1, termed BIGYIN (formerly, Fission1A [FIS1A]; [Scott and Logan, 2006]; a plant specific protein, named ELM1(named also NETWORK; [Logan, 2010]), that does not present sequence similarity with yeast Mdv1/Caf4 (Arimura *et al.*, 2008). How these proteins specifically interact among them to carry out mitochondrial fission events in plants is unknown. Yeast two-hybrid experiments have demonstrated that ELM1 and DRPs proteins interact among them, but not with BIGYIN (Arimura *et al.*, 2008). Using bimolecular fluorescent complementation (BiFC) assay, the absence of interaction between DRP3A and BIGYIN (Zhang and Hu, 2008a) and the interaction between DRP3A and ELM1 (Arimura *et al.*, 2008) and have been demonstrated.

ELM1 is required for the subcellular transfer of DRP3A from the cytosol to mitochondrial fission sites (Arimura *et al.*, 2008). Yet, since ELM1 protein structure is not predicted to consist of transmembrane domains or other membrane-anchoring domains, it has been supposed that its mitochondrial localization could depend on the interaction with protein(s) located to mitochondrial surfaces. BIGYIN remains one of the proteins proposed to interact with ELM1, although results showing this interaction have not yet reported.

Here, we focus on studying, at subcellular level, BIGYIN and ELM1 proteins in transient expression experiments performed in *Arabidopsis thaliana* leaves protoplasts and *Nicotiana tabacum* mesophyll cells. We report initially a precise subcellular localization of BIGYIN and ELM1. Afterwards, we analyze whether BIGYIN and ELM1 co-localize in the same cells and whether BIGYIN

and ELM1 do interact *in vivo* in our experimental systems. Moreover, we analyze whether *BIGYIN* and *ELM1* are expressed in the same plant tissues in *Arabidopsis*, a prerequisite to make possible their interactions.

RESULTS

Subcellular localization of ELM1::YFP

In order to investigate whether BIGYIN and ELM1 interact *in vivo*, we decided at first to determine the precise subcellular localization pattern of these two proteins, adopting different methods of transient expression, such as the transformation of protoplasts obtained from *Arabidopsis* leaves and the agro-infiltration of *Nicotiana tabacum* leaves, combined with confocal microscope analyses.

To investigate the intracellular localization of ELM1, we fused *ELM1* coding sequence (CDS) to the N-termini of yellow fluorescent protein (*YFP*), downstream the constitutive cauliflower mosaic virus 35S (CaMV 35S) promoter. This fusion construct, termed *ELM1::YFP*, was subcloned into a plant pGreenII binary vector (Hellens *et al*., 2000). The subcellular localization of ELM1::YFP was performed using several organelle markers. To detect mitochondria, two reporters were used: the red fluorescent protein (RFP) fused to *Arabidopsis c*ytochrome c *ox*idase-related (*COX::RFP*; obtained in our laboratory), and the mCherry fluorescent protein fused to yeast cytochrome c oxidase IV pre-sequence (*COX4::mCherry*; Nelson *et al.*, 2007). To visualize peroxisomes, we fused RFP to KSRM sequence tag (*RFP::KSRM*; obtained in our laboratory). To identify chloroplasts, chlorophyll autofluorescence was analyzed in leaf mesophyll cells.

Subcellular localization of ELM1 to mitochondria

To test whether ELM1::YFP fusion protein was localized to mitochondria, the pGreen-*ELM1::YFP* was introduced by polyethylene glycol transformation method (Yoo *et al.*, 2007) into protoplasts isolated from *Arabidopsis* leaves, stably expressing the mitochondrial *COX4::mCherry* marker (Nelson *et al.*, 2007). Protoplasts were analyzed 24h after transfection. ELM1::YFP was present in many discrete structures that mainly overlapped with mitochondrial COX::RFP (Fig. 1A). In detail, ELM1::YFP was located to the periphery of mitochondria, and it surrounded the mitochondrial RFP marker. Moreover, observing mitochondrial distribution in protoplasts transformed with *ELM1::YFP*, we noted

that mitochondria were aggregated in clusters. By contrast, mitochondria were spread throughout the cytoplasm in *ELM1::YFP* un-transformed protoplasts (Fig. 1B).

Mitochondrial localization of ELM1::YFP was also investigated in tobacco mesophyll cells. Tobacco mesophyll cells were agro-infiltrated with a mixture of *Agrobacterium* harbouring the pGreen- *ELM1::YFP* and the mitochondrial marker pBIN-*COX4::mCherry* (Nelson *et al.*, 2007). Confocal laser scanning microscopy analyses were performed 4 days after infiltration procedure. ELM1::YFP overlapped with mitochondrial mCherry marker, indicating that ELM1 was located to mitochondria (Fig. 1C). Moreover, tobacco leaf cells, co-expressing *ELM1::YFP* and mitochondrial marker, were characterized by aggregation of mitochondria in clusters. By contrast, clusters of mitochondria were not observed in tobacco leaf cells not-transformed with *ELM1::YFP* (Fig. 1D).

All together, these data show that ELM1 localizes to the mitochondrial outer membranes, and that the over-expression of ELM1 leads to clusters of mitochondria.

Subcellular localization of ELM1 to peroxisomes

A detailed analyses of previous confocal images indicated that ELM1::YFP was also present in other subcellular compartments, suggesting for ELM1 a multiple targeting fate. To investigate whether ELM1::YFP localized to peroxisomes, protoplasts from *Arabidopsis* leaves, stably expressing the marker of peroxisomal lumen RFP::KSRM, were transiently transfected with pGreen-*ELM1::YFP*. In protoplasts expressing both fusion constructs, ELM1::YFP did not overlap with peroxisomal RFP::KSRM (Fig. 2).

Our data indicate that ELM1 does not localize to peroxisomes..

Subcellular localization of ELM1 to chloroplasts

Next, we have investigated whether ELM1 was localized to chloroplasts. Chlorophyll autofluorescence was detected to identify these organelles in leaf mesophyll cells. Protoplasts from *Arabidopsis* leaves were transiently transfected with pGreen-*ELM1::YFP*. ELM1::YFP was detected surrounding chlorophyll autofluorescence (Fig. 3A), suggesting that ELM1::YFP was localized to

chloroplast outer membranes. Moreover, ELM1::YFP was spread throughout the cytoplasm (Fig. 3B), and, when we observed protoplasts on bright field, we noted that ELM1::YFP was localized to plasma membranes (Fig. 3C).

To further test the subcellular localization of ELM1::YFP to chloroplasts, tobacco mesophyll cells were agro-infiltrated with the pGreen-*ELM1::YFP* and chlorophyll was used to detect these organelles. ELM1::YFP was localized to chloroplasts (Fig. 4A,B), and in detail, the fusion protein enveloped chlorophyll autofluorescence. ELM1::YFP marked the plasma membranes, and it was also spread throughout the cytoplasm (Fig. 4C,D).

All together, our results indicate that ELM1 localizes to chloroplasts outer membranes, cytoplasm and plasma membranes.

Subcellular localization of YFP::BIGYIN

After clearly described the subcellular localization of ELM1, we moved to determine the subcellular localization of BIGYIN. To this aim, we fused *BIGYIN* coding sequence (CDS) to *YFP*, downstream the cauliflower mosaic virus 35S (CaMV 35S) promoter. Since BIGYIN is a (N_{out}-C_{in}) transmembrane protein, it is probably characterized by a C-terminal membrane targeting signal (Borghese *et al.*, 2007). For this reason, *YFP* CDS was fused to the N termini of *BIGYIN* to avoid interference with putative targeting information. This fusion construct, named *YFP::BIGYIN*, was subcloned into the plant pGreenII binary vector (Hellens *et al.*, 2000), to perform transient expression assays in protoplasts of *Arabidopsis* leaves and in tobacco mesophyll cells. The subcellular localization of YFP::BIGYIN was analyzed using several organelle markers.

Subcellular localization of BIGYIN to mitochondria

To investigate whether BIGYIN was localized to mitochondria, *Arabidopsis* protoplasts, stably expressing mitochondrial *COX::RFP* marker, were transiently transfected with the pGreen-*YFP::BIGYIN*. YFP::BIGYIN was detected in many discrete intracellular structures, and part of these structures overlapped with mitochondrial COX::RFP (Fig. 5A). Mitochondrial marker appeared as red spot.

YFP::BIGYIN was, instead, located to the rim of mitochondria, circumscribing the mitochondrial RFP reporter. This particular subcellular localization pattern suggested that BIGYIN was localized to the mitochondrial outer membranes.

Mitochondrial localization of YFP::BIGYIN was also investigated in tobacco mesophyll cells. Tobacco leaves were co-infiltrated with a mixture of *Agrobacterium* harbouring the pGreen-*YFP::BIGYIN* and the mitochondrial marker pBIN-*COX4::mCherry* (Nelson *et al.*, 2007). Also in this experimental system, YFP::BIGYIN was localized to many discrete intracellular structures, and a part of these overlapped and surrounded the mitochondrial COX4::mCherry (Fig. 5B).

Taken together, our results suggest that YFP::BIGYIN localizes to the outer membranes of mitochondria.

Subcellular localization of BIGYIN to peroxisomes

To determine whether YFP::BIGYIN localized to peroxisomes, protoplasts, from *Arabidopsis* leaves stably expressing the peroxisomal lumen RFP::KSRM marker, were transiently transfected with pGreen-*YFP::BIGYIN*. YFP::BIGYIN localized to the periphery of peroxisomes labelled with the peroxisomal lumen marker (Fig. 6A).

To further investigate the subcellular localization of YFP::BIGYIN to peroxisomes, tobacco leaves were infiltrated with a mixture of *Agrobacterium* harbouring the pGreen-*YFP::BIGYIN* and the peroxisomal marker pGreen-*RFP::KSRM*. YFP::BIGYIN displayed partial localization to peroxisomal RFP::KSRM (Fig. 6B).

Our data show that YFP::BIGYIN localizes to peroxisomes.

Subcellular localization of BIGYIN to chloroplasts

Afterwards, we investigated whether BIGYIN was located to chloroplasts. Chlorophyll autofluorescence was used to identify these organelles in leaf mesophyll cells. Protoplasts from *Arabidopsis* leaves were transiently transfected with pGreen-*YFP::BIGYIN*. YFP::BIGYIN mostly was localized to chloroplasts (Fig. 7A). In detail, chlorophyll autofluorescence outlined the distribution of thylakoid membranes. YFP::BIGYIN enveloped the chlorophyll autofluorescence,

suggesting that BIGYIN was localized to the outer membranes of chloroplasts. To test this hypothesis, we performed osmotic lysis of mesophyll protoplasts transiently expressing *YFP::BIGYIN*, in order to release chloroplasts from protoplasts. If BIGYIN was localized to chloroplast outer membranes, BIGYIN should remain present on chloroplast surfaces after osmotic lysis. By contrast, if BIGYIN was not localized to the outer membranes, it should not be present on chloroplasts after osmotic lysis. When we performed osmotic lysis of protoplasts, YFP::BIGYIN was again visible on isolated chloroplasts indicating that YFP::BIGYIN was, indeed, located to the outer membranes of chloroplasts (Fig. 7B). To confirm our results, we analyzed the subcellular localization of the chloroplast outer membrane marker OEP7::GFP (Lee *et al.*, 2001). We introduced in *Arabidopsis* mesophyll protoplasts the pGreen-*OEP7::GFP*. OEP7::GFP was localized to the periphery of chloroplasts, encircling these organelles (Fig. 8). The subcellular localization pattern of this chloroplast outer membrane marker is, therefore, similar to the subcellular localization described by BIGYIN to chloroplast outer membranes.

The localization of YFP::BIGYIN to chloroplasts was investigated in tobacco leaves agro-infiltrated with pGreen-*YFP::BIGYIN*. YFP::BIGYIN was detected in the outer membranes of chloroplasts (Fig. 9C). Moreover, YFP::BIGYIN was also located on thin tubular protrusions extending from the outer membranes of a single chloroplast or of interconnected chloroplasts. No chlorophyll autofluorescence was detected from these tubules, indicating that thylakoid membranes did not extend into them. Similar tubular structures, extending from the chloroplast outer membranes and not detectable with chlorophyll, were termed ‘stromules’ by Köhler and Hanson (2000). Stromules were described in several plants as highly dynamic stroma-filled tubules, enclosed by the outer and inner envelope membranes of all plastids types examined so far, including chloroplasts.

Taken together, our results strongly indicate that YFP::BIGYIN localizes to the outer membranes of chloroplasts and to stromules.

Co-localization analysis of BIGYIN and ELM1

So far, we showed that both BIGYIN and ELM1 localized to mitochondria and chloroplasts in independent experiments. Now, we investigated whether BIGYIN and ELM1 co-localized in the same cells. To do this, we fused ELM1 to the red fluorescent protein DsRed2 (*Discosoma sp*. Red2) in the pSAT6 expression vector (Tzfira *et al.*, 2005), obtaining the pSAT1-*ELM1::DsRed2*. Protoplasts from *Arabidopsis* leaves were transiently co-transfected with pSAT1-*ELM1::DsRed* and pGreen-*YFP::BIGYIN*.

BIGYIN and ELM1 co-localized to several sites, indicated by the overlay signal in yellow in Figure 10. In detail, BIGYIN and ELM1 co-localized to the membranes of different organelles, such as the outer membranes of chloroplasts and other organelles, supposedly mitochondria. The merged signal was not detected on the plasma membranes and cytoplasm, where only ELM1::DsRed2 was present.

These results indicate that BIGYIN and ELM1 co-localize to the membranes of several organelles, i.e. chloroplast outer membranes.

Bimolecular fluorescence complementation assay to test BIGYIN- ELM1 *in vivo* interaction

Our results demonstrated the subcellular localization of ELM1 and BIGYIN to mitochondria and chloroplasts in our experimental system. The next important question was: did BIGYIN and ELM1 physically interact *in vivo* in plant cells? We approached this problem by employing the bimolecular fluorescent complementation (BiFC) technique (Lee *et al.*, 2008). BiFC is based upon tethering split YFP variants to form a functional fluorophore. The association of the split YFP does not occur spontaneously and requires interaction between proteins or peptides that are fused to each of the fluorophore fragments. We fused *ELM1* to the C-terminal of cyan fluorescent protein (CFP^C) and BIGYIN to the N-terminal of Venus ($Venus^N$) fluorescent protein into the pSAT1 expression vectors, to generate pSAT1-*ELM1::*CFP^C and pSAT1-$Venus^N$*::BIGYIN*,

respectively. These constructs were introduced together into *Arabidopsis* mesophyll protoplasts by polyethylene glycol transformation method (Yoo *et al.*, 2007), and confocal laser scanning microscopy analyses were performed 24h after transfection. A recovery of fluorescence was detected in co-transfected protoplasts (Fig. 11A), indicating that ELM1 and BIGYIN did interact *in vivo*.

We wondered whether the the recovery of signal previously detected was due to specific interactions between ELM1 and BIGYIN or whether it was due to a spontaneous association of two split fluorophore molecules. To this aim, the *in vivo* interactions between ELM1 and a not-functional truncated BIGYIN protein were analyzed. Not-functional BIGYIN protein should not be able to interact with ELM1, but it should have the same subcellular localization pattern of the functional BIGYIN protein. In order to define the not-functional BIGYIN protein, we analyzed the BIGYIN protein structure. BIGYIN is characterized by a tetratricopeptide (TPR)-like domain, predicted to play a role in protein-protein interaction, and by a single transmembrane domain located to the C-terminal tail of the protein, predicted to contain the targeting signal for its subcellular localization (Scott *et al.*, 2006). In the light of this *in silico* analysis, we decided that the not-functional BIGYIN protein should be completely deleted of cytosolic N-terminal tail, to lose its putative protein-protein domain, and it should be instead constituted of the C-terminal tail of BIGYIN (last 29 amino acids of BIGYIN, aa 141-170), putatively involved in protein targeting. We produced this truncated protein and we named it BIGYIN^{TMD+CT}. To investigate whether the truncated BIGYIN^{TMD+CT} showed the same subcellular localization pattern of the entire BIGYIN protein, *BIGYIN^{TMD+CT}* CDS was fused to the *YFP* and than subcloned into a pSAT1 expression vector (Lee *et al.*, 2008), to perform transient expression assay in protoplasts. To test whether truncated BIGYIN^{TMD+CT} localized to mitochondria, *Arabidopsis* mesophyll protoplasts, stably expressing mitochondrial COX::RFP marker, were transfected with pSAT1-*YFP::BIGYIN^{TMD+CT}*. YFP::BIGYIN^{TMD+CT} was localized to the rim of mitochondria, circumscribing the mitochondrial RFP reporter (Fig. 12A). Peroxisomal subcellular localization of the truncated BIGYIN^{TMD+CT} was investigated in *Arabidopsis* mesophyll protoplasts, stable expressing peroxisomal RFP::KSRM marker and transiently transfected with the pSAT1-

YFP::BIGYIN^{TMD+CT}. BIGYIN^{TMD+CT} was localized to the periphery of peroxisomes labelled with peroxisomal lumen marker (Fig. 12B). Moreover, the truncated BIGYIN^{TMD+CT} encircled also the chlorophyll autofluorescence (Fig. 12C).

Taken together, these results indicated that the truncated BIGYIN^{TMD+CT} protein was localized to the outer membranes of chloroplasts and mitochondria and to peroxisomes, showing the same subcellular localization pattern of the entire BIGYIN protein (Fig. 5A,6A,7).

Successively, we investigated whether ELM1 and the not-functional BIGYIN^{TMD+CT} did interact *in vivo*. To this aim, we fused the truncated *BIGYIN*$^{TMD+CT}$ to the N-terminal of *Venus* (*Venus*^{N}) fluorescent protein into the pSAT1 expression vector, to generate the pSAT1-*Venus*^{N}*::BIGYIN*$^{TMD+CT}$. In order to perform BiFC assay, *Venus*^{N}*::BIGYIN*$^{TMD+CT}$ and *ELM1::CFP*^{C} were introduced together into *Arabidopsis* mesophyll protoplasts by polyethylene glycol transformation method (Yoo *et al.*, 2007). In the same experiments, we have also investigated the *in vivo* interactions between ELM1 and entire BIGYIN, co-transfecting the *Arabidopsis* protoplasts with *Venus*^{N}*::BIGYIN* and *ELM1::CFP*^{C}. A recovery of fluorescence was detected in protoplasts co-expressing ELM1 both with the entire BIGYIN and with the truncated BIGYIN^{TMD+CT} (Fig. 11A,B). However, the recovery of fluorescence detected on the interaction assay between ELM1 and the truncated BIGYIN^{TMD+CT} was dimmer than that detected on the interaction assay between ELM1 and the entire BIGYIN protein. In fact, when we quantified these signals (Fig. 11C), we obtained that the recovery of fluorescence between ELM1 and the truncated BIGYIN^{TMD+CT} was only fifty percent of that calculated in interaction between ELM1 and the entire BIGYIN protein. These data indicated the *in vivo* interaction detected between ELM1 and BIGYIN was specific and not due to a spontaneous association of two split fluorophore molecules.

To confirm this data obtained in protoplasts, we performed BiFC assay on tobacco mesophyll cells. To this aim, *ELM1::CFP*^{C} and *Venus*^{N}*::BIGYIN* fusion constructs were subcloned from the pSAT1 expression vectors (Lee *et al.*, 2008) into the pGreenII binary vectors (Hellens *et al*., 2000), and pGreen-*ELM1::CFP*^{C} and pGreen-*Venus*^{N}*::BIGYIN* constructs were delivered into *Agrobacterium*.

Then, these constructs were co-expressed in tobacco leaves by agro-infiltration. In co-infiltrated leaf mesophyll cells, there was a recovery of BiFC fluorescence (Figure 12D), suggesting that BIGYIN and ELM1 interacted *in vivo*. As control, the interactions between ELM1 and the truncated BIGYIN^{TMD+CT} protein were investigated. Tobacco mesophyll cells were agro-infiltrated with a mixture of *Agrobacterium* harbouring the pGreen-*ELM1::CFP*^{C} and the pGreen-*Venus*^{N}*::BIGYIN*$^{TMD+CT}$. Agro-infiltrated leaf cells did not show fluorescence or only background fluorescence (Fig. 12E).

All together, these data strongly demonstrate that BIGYIN and ELM1 do interact in vivo.

Subcellular localization of BIGYIN and ELM1-interaction sites

Successively, we investigated the subcellular compartments where BIGYIN and ELM1 physically interacted *in vivo*. *Arabidopsis* mesophyll protoplasts were co-transfected with BiFC constructs (*ELM1::CFP*^{C} and *Venus*^{N}*::BIGYIN*), and they were analysed by means of confocal microscopy 24h later. BiFC fluorescence, chlorophyll autofluorescence and merged images were captured (Fig.13A). In co-transformed protoplasts, the recovery of fluorescence was clearly detected on the chloroplast outer membranes. To test whether BIGYIN and ELM1 interacted also on mitochondria and peroxisomes, the *ELM1::CFP*^{C} and *Venus*^{N}*::BIGYIN* were introduced in *Arabidopsis* mesophyll protoplasts stably expressing the RFP targeted to mitochondria (COX::RFP) and to peroxisomes (RFP::KSRM). BiFC signal was enriched around mitochondria (Fig. 13B), while it was not localized to peroxisomes (Figure 13C).

These data indicate that BIGYIN and ELM1 interact in vivo on outer membranes of chloroplasts and on mitochondria, but not on peroxisomes.

Expression pattern of ELM1 and BIGYIN in seedlings

The next important question was: were ELM1 and BIGYIN co-expressed in same plant tissues? To address this question, we cloned the putative promoter region of *BIGYIN* and *ELM1* genes upstream the reporter gene, coding for the β-glucuronidase enzyme (GUS) (Jefferson *et al.*, 1987), in a pGreeII binary expression vector. Each construct was introduced in *Agrobacterium tumefaciens* and *A. thaliana* plants were transformed by using floral dip method (Clough and Bent, 1998). Several transgenic lines, termed p*ELM1::GUS* and p*BIGYIN::GUS*, were obtained. None of these plants showed any obvious changes in growth or morphology when compared to wild type plants. Histochemical assay, using X-Gluc as substrate for GUS enzyme, was performed on 7-day-old seedlings of these transgenic plants (Fig. 14A). The promoter-driven GUS activity of ELM1 showed that *ELM1* was expressed on leaves and roots. In detail, ELM1 was expressed on leaf tips and throughout the root system, with exception of root epidermis and root hair. The same tissues were also observed in p*BIGYIN::GUS* plants. *BIGYIN* was expressed on leaves and roots, especially on leaf tips and throughout the root system (Fig. 14B).

These results indicate that BIGYIN and ELM1 are co-expressed in the same tissues in Arabidopsis seedlings.

DISCUSSION

ELM1::YFP localizes to mitochondria chloroplasts, cytoplasm and plasma membranes

In this study we have reported a detailed subcellular localization of ELM1, a specific plant protein involved in mitochondrial fission (Arimura *et al.*, 2008). To this aim, we have cloned *ELM1::YFP* fusion construct downstream a constitutive promoter into a plant expression vector, to perform transient expression experiments in *Arabidopsis* leaves protoplasts and tobacco mesophyll cells. To precisely localize ELM1::YFP to mitochondria and peroxisomes, several organelle markers have been used.

We have shown that ELM1 localizes to multiple subcellular sites. In detail, ELM1 localizes mainly to the outer membranes of mitochondria and chloroplasts, while it does not located to peroxisomes. We have shown that ELM1 can be also localizes to plasma membranes and cytoplasm. Mitochondrial localization of ELM1 is in agreement with data reported by Arimura *et al.* (2008) and it is also consistent with the involvement of ELM1 in mitochondrial fission machinery (Arimura *et al.*, 2008). By contrast, the subcellular localization of ELM1 to chloroplasts has never been investigated before. So far, subcellular localization analyses of BIGYIN have been performed only on epidermal leaves (Arimura *et al.*, 2008), where chloroplasts are absent. Subcellular localization of ELM1 to the cytoplasm and to the plasma membrane was not previously reported. However, a cytosolic localization of ELM1 could been expected, because *in silico* analysis of ELM1 protein sequence does not show predicted transmembrane domains or membrane-anchoring domains (Arimura *et al.*, 2008).

Our data show that the over-expression of ELM1 leads to abnormal mitochondrial morphology and distribution inside the cells: mitochondria, in fact, aggregate in clusters. The observed pattern (Fig.1A) suggests that mitochondrial fission occurs, but mitochondria seem not to be able to physically separate from each other and to spread throughout the cytoplasm. There are no published data concerning the consequences of over-expression of ELM1, because ELM1 over-expression has not been investigated so far. Instead, it has been described that the over-expression of DRP3A or DRP3B, two *Arabidopsis* proteins involved in

mitochondrial fission events, caused, in leaf epidermal cells, fragmentation and not aggregation of mitochondria (Fujimoto *et al.*, 2009). ELM1, DRP3A and DRP3B seem therefore to have distinct functions during mitochondrial fission events. Hence, we can speculate that the role of ELM1 could be not sufficient for physical scission of mitochondrial membranes. By contrast, DRP3A and DRP3B could act downstream ELM1 during mitochondrial fission events. DRP3A and DRP3B seem to be actively involved in physical fission of mitochondrial membranes, as suggested also by the homology of DRP3A and DPR3B with the dynamin protein, a class of GTPase mechano-enzymes involved in membrane scission.

YFP::BIGYIN localizes to mitochondria, peroxisomes and chloroplasts

We have shown that ELM1 localizes to different subcellular compartments. Since transmembrane domains or other predicted membrane-anchoring domains are not present in ELM1 structure, we could hypothesize that multiple subcellular localization pattern of ELM1 depends on the interaction with different proteins localized to different organelle compartments. BIGYIN is one of the proteins that have been proposed to interact with ELM1 on mitochondria, because BIGYIN is a transmembrane protein located to mitochondrial outer membranes and it is involved in mitochondrial fission event. However, there are no published data to support this hypothesis. Yet, our results put also another question: how can ELM1 reach the chloroplast outer membranes? To address this question, we have reported a detailed subcellular localization of BIGYIN in the same experimental systems previously adopted for the localizations of ELM1 (transient expression assays in *Arabidopsis* leaves protoplasts and agro-infiltrated tobacco mesophyll cells). To this aim, the *YFP::BIGYIN* was cloned downstream a constitutive promoter into a plant expression vector and co-expressed with several organelle markers. We have shown that BIGYIN localizes to the outer membranes of mitochondria and to the membranes of peroxisomes. These data are in agreement with the subcellular localization of BIGYIN already reported by Zhang and Hu (2008a). These localization patterns are also consistent with the role of BIGYIN as a fission protein involved in mitochondrial and peroxisomal fission events (Zhang and Hu, 2008b).

If we compare the mitochondrial distribution in cells over-expressing BIGYIN and in cells over-expressing ELM1, we observe that mitochondria are not aggregated in clusters in BIGYIN-transformed cells, as we have instead previously reported in ELM1-transformed cells. These findings indicate that BIGYIN and ELM1 play distinct role(s) during mitochondrial fission events.

Interestingly, we show that BIGYIN localizes to chloroplasts outer membrane both in *Arabidopsis* leaf protoplasts and in tobacco mesophyll cells. Moreover, in tobacco mesophyll cells, unlike to *Arabidopsis* protoplasts, we have shown that BIGYIN localizes also to thin protrusions (i.e. stromules), extending from the outer membranes of single chloroplast or of interconnected chloroplasts. Subcellular localization of BIGYIN to chloroplasts has not been previously reported, probably because mesophyll cells, where chloroplasts are present, have not been yet investigated. However, our subcellular localization of BIGYIN to chloroplasts is in agreement with the identification of BIGYIN protein in chloroplast proteome experiments (Zybailov *et al.*, 2008).

Based on these results, BIGYIN is the first transmembrane protein, in detail a tail-anchored (N_{out}-Cin) protein, localized to mitochondrial, chloroplast and peroxisomal membranes.

BIGYIN and ELM1 co-localize to mitochondria and chloroplasts

So far, we have analyzed the subcellular localization of BIGYIN and ELM1 separately in independent experiments. In order to investigate their localization pattern in the same cells, we have performed co-expression experiments in *Arabidopsis* protoplasts. We have shown several sites where co-localization between ELM1 and BIGYIN occurs, i.e. on the outer membranes of chloroplasts and on other organelles, presumably mitochondria. These data are consistent with our previous results of localization of BIGYIN and ELM1. The co-localization of ELM1 and BIGYIN to the chloroplast membranes prompt a new question: do ELM1 and BIGYIN play also a role on chloroplasts?

BIGYIN and ELM1 interact *in vivo*

Having demonstrated that ELM1 and BIGYIN localize in the same organelles, we successively investigated whether they also physically interacted *in vivo*. To this aim, we have employed the bimolecular fluorescent complementation (BiFC) technique for *in vivo* protein-protein interactions in plant cells (Lee *et al.*, 2008). BiFC is based upon tethering split YFP variant to form a functional fluorophore. BiFC assay was performed in *Arabidopsis* mesophyll protoplasts and in tobacco mesophyll cells. We have shown that in both experimental systems there is a recovery of fluorescence indicating that ELM1 and BIGYIN do physically interact *in vivo*.

We have also verified that the recovery of fluorescence between ELM1 and BIGYIN was specific and not due to a spontaneous interactions of two YFP split fluorophore molecules. To this aim, we have analyzed the *in vivo* interactions between ELM1 and a not-functional truncated BIGYIN (i.e. BIGYIN^{TMD+CT}). Truncated BIGYIN^{TMD+CT} is constituted by the C-terminal end of BIGYIN, that is predicted to contain the targeting signal to the subcellular localization of BIGYIN (Scott *et al.*, 2006). We have demonstrated that it shows the same subcellular localization pattern of the entire BIGYIN protein in transiently transformed *Arabidopsis* protoplasts. These data demonstrate that the C-terminal end of BIGYIN protein contains the targeting signal sufficient to the subcellular localization of BIGYIN to mitochondria, peroxisomes and chloroplasts. These data are in agreement with the key role played by the C-terminal hydrophobic anchor in targeting of tail anchored-proteins in other system (Borghese et al.,, 2007). Moreover, we have demonstrated that the N-terminal end of BIGYIN protein is necessary for the protein-protein interactions, because when it has been deleted, the interaction between ELM1 and BIGYIN is not detected.

Successively, we have performed BiFC assay between ELM1 and the truncated BIGYIN^{TMD+CT} protein in *Arabidopsis* leaf protoplasts. Our results clearly demonstrate that interaction between ELM1 and BIGYIN is specific both *in vivo* in *Arabidopsis* leaf protoplasts and in tobacco mesophyll cells.

So far, the interaction between BIGYIN and ELM1 was only hypothesized due to the involvement of these two proteins in the mitochondrial fission machinery, but clear evidences of their physical interaction were still missing.

Yeast-two hybrid experiments were performed to investigate an interaction between ELM1 and BIGYIN, but these experiments didn't detect it (our data not shown, Arimura *et al.*, 2008), probably because BIGYIN expressed in yeast was improperly folded or unstable. Our data, obtained through BiFC technique, have instead demonstrated that BIGYIN and ELM1 do interact *in vivo*.

BIGYIN and ELM1 interact *in vivo* on mitochondria and chloroplasts

In order to identify the subcellular compartments where ELM1 and BIGYIN do interact, BiFC assay have been performed in *Arabidopsis* leaf protoplasts, expressing different organelle markers. We have shown that ELM1 and BIGYIN interact on the outer membranes of mitochondria and on the outer membranes of chloroplasts. The *in vivo* interaction between ELM1 and BIGYIN on mitochondrial outer membranes is in agreement with their involvement in mitochondrial fission machinery. In addition, we have demonstrated that BIGYIN and ELM1 interact also on chloroplast outer membranes. The subcellular localization of both proteins to chloroplasts has not been yet investigated. Their specific interaction on chloroplast membrane is the first indication that ELM1 and BIGYIN could play a role on chloroplasts. Therefore, ELM1 seems to be a protein shared by mitochondrial and chloroplasts, and BIGYIN a tail-anchored protein shared by mitochondria, peroxisomes and chloroplasts.

BIGYIN and ELM1 are expressed in the same plant tissues in *Arabidopsis* seedlings

Afterwards we have analyzed whether the expression pattern of *ELM1* and *BIGYIN* in plant tissues. Our results, obtained through histochemical GUS assay (Jefferson *et al.*, 1987) on 7-day-old seedlings of p*BIGYIN::GUS* and p*ELM1::GUS* transgenic plants, have shown that BIGYIN and ELM1 are expressed in the same organs (leaf and root) and in the same tissues (leaf tips and throughout the root system) in seedlings.

Our subcellular localization analyses and BiFC assays have been performed expressing BIGYIN and ELM1 proteins under the control of a constitutive promoter, and adopting transient expression methods. Expression of BIGYIN and ELM1, under its own promoter, in the same plant tissues at the same

developmental stage is a necessary confirm for our results of specific interaction between ELM1 and BIGYIN on mitochondrial and chloroplast outer membranes.

MATERIAL AND METHODS

Plant materials and growth condition

All the *Arabidopsis thaliana* plants for this study were in the Columbia background. Different *Arabidopsis* transgenic lines were used: plants overexpressing the red fluorescent protein (RFP) targeted to mitochondria by the cytocrome c oxidase-releated (COX) pre-sequence (35S::COX::RFP), and plants overexpressing the RFP targeted to peroxisomes by the sequence tag KSRM fused downstream the *RFP* CDS (35S::RFP::KSMR). These transgenic plants were generated in our laboratory.

The *Arabidopsis thaliana*, Columbia ecotype, and *Nicotiana tabacum* plants were incubated in an environmentally-controlled growth chamber with a long photoperiod (16 hr light and 8 hr dark) at 25 ± 1°C, and a photosynthetic photon flux of 35 μmol m^{-2} s^{-1} Osram cool-white 18 W fluorescent lamps.

Genetic materials

The *Arabidopsis BIGYIN* and *ELM1* coding sequence fragments were first amplified by PCR from *Arabidopsis* cDNA with high-fidelity PCR enzymes (Phusion High Fidelity DNA polymerase [Finnzymes]) and then cloned into the vector of interest. To obtain the $BIGYIN^{TMD+CT}$, only the C-terminal tail (421-510 bp, aa 141-170) of *BIGYIN* coding sequence was amplified, corresponding to the transmembrane domain and the adjacent C-terminal end. All the cloned plasmids were confirmed by sequencing.

Plasmids for the subcellular localization

For the expression of BIGYIN, $BIGYIN^{TMD+CT}$ and ELM1 in plants, the pGreen0179 and pGreen0029 (Hellens *et al*., 2000) binary vectors were used. In the pGreen0179 ($Hygromycin^{R}$) the p*35S::YFP::BIGYIN* and the

p*35S::YFP::BIGYIN*$^{TMD+CT}$ constructs were introduced, while in the pGreen0029 (Kanamycin^{R}) the p*35S::ELM1:YFP* was introduced.

To obtain the p*35S::YFP::BIGYIN* and the p*35S::YFP::BIGYIN*$^{TMD+CT}$ constructs, the *YFP* coding sequence were subcloned from the pAVA554-*35S::YFP* plasmid provided by Prof. Albrecht von Arnim (Von Arnim *et al.*, 1998) to the pSAT1-*35S::Venus*^{N} vector (stock number E3228, Lee *et al.*, 2008) by replacing into the *NcoI/BglII* sites the *Venus*^{N} cDNA sequence digesting with *NCoI/BglII* enzymes. The BIGYIN and the BIGYINT^{TMD+CT} PCR products were amplified using primers where the *SacI/KpnI* sites were introduced (For: 5'-CATGGAGCTCAAGGTGTTATAGGGATAGGGATCACG-3';
Rev: 5'-CATGGGTACCTCATTTCTTGCGAGACATCG-3'). The amplicons were digested with *SacI/KpnI* and they were cloned into the pSAT1-p*35S::YFP* vector. The pSAT1-p*35S::YFP::BIGYIN* and the pSAT1-p*35S::YFP::BIGYIN*$^{TMD+CT}$ fusion constructs were subcloned with *EcoRV/NotI* restriction sites into the pGreen0179 vector digested with *SmaI/NotI* to obtain the pGreen0179-p*35S::YFP::BIGYIN* and pGreen0179-p*35S::YFP::BIGYIN*$^{TMD+CT}$ binary vectors.

The pGreen0029-p*35S::ELM1::YFP* binary vector was constructed introducing first the p*35S::YFP* from the pAVA554-*35S::YFP* plasmid (von Arnim *et al.*, 1998) into the pGreen0029 vector between the *KpnI/SacI* sites and then cloning the ELM1 PCR product into the *NCoI* site (Primer For: 5'-CATGCCATGGCCATGAGGCCAATCCT-3'; Rev: 5'-CATGCCATGGCTGCAGACCGTAAACTCCATCC-3').

For the transiently co-expression of *BIGYIN* and *ELM1* in *Arabidopsis* protoplasts, the pSAT1-p*35S::BIGYIN* previously described and the pSAT6 p*35S::ELM1::DsRed2* were used. The pSAT6-p*35S::ELM1::DsRed2* was obtained cloning with the *KpnI* restriction enzyme the ELM1 PCR product (For:5'-CATGGGTACCGGATGAGGCCAATCCTATTGCCGG-3';Rev: 5'-CATGGGTACCCTGCAGACCGTAAACTCCATCCACGTGC-3') into the pSAT6-*DsRed*2 vector provided by Citovsky (Tzifira *et al.*, 2005).

Plasmids for the BiFC assay

The pSAT1-p*35S::Venus*^{N} (stock number E3228) and the pSAT1-p*35S::CFP*^{C} (stock number E3449) vectors were provided by Prof. Gelvin (Lee *et al.*, 2008). The *BIGYIN*$^{TMD+CT}$ cDNA were amplified by PCR (5'-CATGGAGCTCAAATGGATGCTAAGATCGGAC-3'; Rev: 5'-CATGGGTACCTCATTTCTTGCGAGACATCG-3';). The products were digested with *SacI/KpnI* and cloned into the pSAT1-p*35S::Venus*^{N}, to obtain the pSAT1-p*35S::Venus*^{N}*::BIGYIN::* and p*35S::Venus*^{N}*::BIGYIN*$^{TMD+CT}$. The *ELM*1 coding sequence was amplified by PCR using specific 5' and 3' primers where the *KpnI/Kpn*I sites were introduced (5'-CATGGGTACCGGATGAGGCCAATCCTATTGCCGG-3'; Rev: 5'-CATGGGTACCCTGCAGACCGTAAACTCCATCCACGTGC-3'). The amplicon was digested with *KpnI* enzyme and cloned into the pSAT1-p*35S::CFP*^{C}, to obtain the pSAT1-p*35S::35S:ELM1::CFP*^{C}.

pBIGYIN:GUS and pELM1::GUS constructs and generation of transgenic lines

Transgenic *Arabidopsis* lines used for histochemical studies carried the following promoter-reporter gene fusions: *pBIGYIN*::*GUS* and *pELM1*::*GUS*.

The *GUS* (*β-glucuronidase*)-coding sequence was fused to the *BIGYIN* promoter (base pair -862 to -1). The 862 bp promoter fragment was amplified by PCR using genomic DNA extracted from *Arabidopsis* leaves as template. The pair of primers, both carrying an *EcoRI* restriction site, were as follows: forward primers 5'-CATGGAATTCCTTTCGAGGCTCACCTCAAC-3 and reverse primer 5'-CATGGAATTCTGAAGGCGATTTTGAGCTTTGA-3'). After digestion, the promoter was cloned upstream of the *GUS* coding region, into a modified pGreen0029 binary vector (Kamaycin^{R}; Hellens *et al.*, 2000), where the GUS coding sequence, fused with the *nos* terminator, was previously inserted in the polylinker between *KpnI-SacI* restriction sites.

To obtain the *pELM1*::*GUS* fusion construct, a similar working strategy was adopted. The ELM1 promoter consist of a 960 bp genomic fragment (base pair -960 to -1) and it was amplified by PCR with specific primer containing the *EcoRI* restriction site (Primer For: 5'-

CATGCTCGAGCCTAACTGTTTACAACCTGCACA -3'; Rev: 5'-CATGCTCGAGGCCGGTTAGATTATCGATTCC-3').

The pGreen-pBIGYIN::GUS and pGreen-p*ELM1::GUS* constructs were transferred into GV3101-pSoup *Agrobacterium* strain (Hellens *et al*., 2000) and *Arabidopsis* plants were transformed by floral dip method (Clough and Bent, 1998) and screened on half-strength MS agar medium containing 50 mgL^{-1} kanamycin. The GUS-staining analyses were performed on T_2 plants.

Organelle marker used in transient expression experiments

For the localization of the mitochondria in transient expression transformation, the red fluorescent protein (RFP) targeted was fused to the *Arabidopsis* cytocrome c oxidase-releated (COX) pre-sequence (p*35S::COX::RFP*; obtained in our laboratory). For the localization of the peroxisomes, the *RFP* was fused to sequence tag KSRM (p*35S::RFP::KSRM;* obtained in our laboratory). To detect the chloroplast outer membrane, we used the OEP7::GFP (Lee *et al.*, 2001).

Accession Numbers

Sequence data from this article can be found in the GenBank/EMBL data libraries under accession numbers At5g22350 for ELM1, named also NETWORK, and At3g57090 for BIGYIN, previously termed FIS1A.

Protoplasts isolation

Protoplasts were isolated following the protocol of Yoo *et al.* (2007) with some modifications. Leaves of 3-4 weeks old *Arabidopsis* plants were cut into approximately 0.5-1mm strips, placed in a Petri dish containing the enzymatic solution (1.25% cellulase R10 [Yakult Pharmaceutical, Japan], 0.3% macerozyme R10 [Yakult Pharmaceutical, Japan], 0.4M mannitol, 20mM KCl, 20mM MES pH 5.7, 10mM $CaCl_2$, 0.1% BSA; filter sterilized) and vacuum-infiltrated for 30min. The digestion was continued for 3h without shaking in the dark at 22°C. After incubation the solution containing protoplasts was filtered with 50 μm nylon mesh sieve and centrifuged in 10ml polystyrene tubes at 100xg

for 5min to pellet the protoplasts. The protoplasts were washed twice with W5 solution (154mM NaCl, 125mM $CaCl_2$, 5mM KCl, 2mM MES, pH 5.8; filter sterilized) and kept on ice for 30min. Then protoplasts were collected by centrifuging at 100xg for 1min and the pellet was resuspended in an appropriate volume of MMg solution (0.4M mannitol, 15mM $MgCl_2$) in order to obtain approximately $2x10^4$ protoplasts in 0.1 mL of MMg.

Protoplasts transfection assay

Protoplasts were transfected according to the procedure of Yoo *et al.* (2007) with some modifications.

In a 2ml eppendorf tube 10μg of plasmid DNA was added to $2x10^4$ protoplasts and mixed with an equal volume of a freshly prepared polyethylene-glycol (PEG) solution (40% w/v PEG4000 [Fluka], 0.1M $CaCl_2$, 0.2M mannitol). The solution was gently mixed and incubated for 20min in the dark at room temperature. After incubation, 2 volumes of W5 solution (154mM NaCl, 125mM $CaCl_2$, 5mM KCl, 2mM MES, pH 5.8; filter sterilized) were added to the tube to dilute and washed out the PEG. The protoplasts were collected by 1min centrifugation at 100xg and then resuspended in 1 ml of W5 solution. The protoplasts were incubated at 20°C in the dark for at least 16 hr before the microscopy analysis.

***Agrobacterium tumefaciens* strain**

For the use of pGreenII–derived binary vectors, the *A. tumefaciens* GV3101 strain was co-transformed with the pSoup vector (Hellens *et al.*, 2000). Competent cells of *A. tumefaciens* GV3101 strain were prepared according to Main *et al.* (1995) and the binary vectors were introduced by 'freeze-thaw' method. 1μg of plasmid DNA was added to the competent cells, frozen in liquid nitrogen for 5min and heated at 37°C for 5min. The bacterial culture was incubated at 28°C for 3hr with gentle shaking in 1ml YEP medium (10g/L bacto-trypton, 10g/L yeast extract, 5g/L NaCl; pH 7.0) and then spread on a YEP agar plate containing the appropriate antibiotic selection (gentamycin 50 mgL^{-1}, rifampicin 50 mgL^{-1}, kanamycin 50 mgL^{-1} and tetracyclin 5 mgL^{-1}).

Tobacco leaf agroinfiltration

Agrobacterium-mediated transient expression was performed essentially as described in Zottini *et al.* (2008). Single colonies of *A. tumefaciens* growing on agar plate were inoculated in 3mL of YEP liquid medium supplemented with specific antibiotics. The bacteria were incubated for 2 days at 28°C at 200rpm on an orbital shaker. 25μL of confluent bacterial culture was re-inoculated in 5mL (1/200 ratio, v/v) of fresh YEP medium (10g/L bacto-trypton, 10g/L yeast extract, 5g/L NaCl; pH 7.0) containing the appropriate antibiotics, and this new culture was grown under the same condition for an additional day. 2mL of bacterial suspension was pellet by centrifugation at 1.500xg for 4min at room temperature. The pellet was washed twice with 2mL of infiltration buffer [50mM MES pH 5.6, 2mM Na_3PO_4, 0.5% w/v glucose, and 100μM acetosyringone (Aldrich, Italy)] and then diluted with infiltration buffer to a final OD_{600} of 0.2. Approximately 300μL of this *Agrobacterium* mixture was infiltrated into a young leaf of *N. tabacum* through the stomata of the lower epidermis by using 1-ml syringe without a needle. For experiments requiring co-infection of more than one construct, bacteria strains containing the constructs were mixed before performing the leaf infection, with the inoculum of each construct adjusted to a final OD_{600} of 0.2. After infiltration the plants were maintained in the environmentally-controlled chamber under standard growth condition. The transient expression was assayed four days after infection.

Confocal analyses

Confocal microscopies were performed by using a Nikon PCM2000 (Bio-Rad, Germany) and an inverted SP/2 (Leica, http://www.leica.com). laser scanning confocal imaging systems. For GFP/YFP and RFP detection, excitation was at 488nm and 543nm respectively, and emission between 515/530nm for YFP and 550/650nm for RFP, respectively. For the mCherry detection, excitation was at 543 nm and detection 550/650nm. For the chlorophyll detection, excitation was at 488nm and detection over 600nm. The images acquired from the confocal microscope were processed using the software ImageJ bundle software (http://rsb.info.nih.gov/ik/).

BiFC fluorescence quantification

The confocal acquisitions were made in the same experimental condition and 10 protoplasts were analyzed in three replicates. BiFC signal fluorescence quantification was obtained normalizing the signal intensity of the interaction to chlorophyll autofluorescence one. The data were plotted comparing the mean of the BiFC signal intensity between ELM1 and BIGYIN^{TMD+CT} with the mean of the BiFC signal between ELM1 and BIGYIN. The error standard was calculated.

***β-glucuronidase* (*GUS*) histochemical analyses**

GUS histochemical staining was performed at four developmental stages: germinating seeds (32 h after imbibition), 5-day-old seedlings (cotyledons open), 7-day-old seedlings (first leaves developing), and flowering mature plants.

Samples were analysed for GUS activity following the protocol described by Jefferson et al. (1987). The samples were vacuum infiltrated for 30 min in the following solutions: 2 mM X-gluc, 0.5% Triton X-100, 0.1% Tween 20, 0.5 mM $K_3Fe(CN)6$, 0.5 mM $K_4Fe(CN)_6\_3H_2O$, 10 mM Na_2EDTA and 50 mM sodium phosphate buffer, pH 7.0, and then incubated at 37°C for 16 h. After staining, samples were cleared by several washes with methanol/acetic acid (3:1 v/v) solution and kept at 4°C in 70% ethanol.

Statistic

All experiments were conducted al least in triplicate, and pictures represented typical example.

REFERENCE

- **Arimura SI**, Fujimoto M, Doniwa Y, Kadoya N, Nakazono M, Sakamoto W, Tsutsumi N (2008). *Arabidopsis* ELONGATED MITOCHONDRIA1 is required for the localization of DYNAMIN-RELATED PROTEIN3A to mitochondrial fission sites. The Plant Cell, 20(6):1555-1566
- **Bauwe H**, Hagemann M, Ferine AR (2010). Photorespiration: players, partners and origin. Trends in Plant Science, 15 (6):330-336
- **Borghese N**, Brambilasca S, Colombo S (2007). How tails guide tail-anchored proteins to their destinations. Current Opinion in Cell Biology, 19:368–375
- **Clough S**J, Bent AF (1998). Floral dip: a simplified method for *Agrobacterium*-mediated transformation of *Arabidopsis thaliana*. The Plant Journal, 16 (6):735–743
- **Fujimoto M**, Arimura S, Mano S, Kondo M, Saito C, Ueda T, Nakazono M, Nakano A, Nishimura M, Tsutsumi N (2009). *Arabidopsis* dynamin-related proteins DRP3A and DRP3B are functionally redundant in mitochondrial fission, but have distinct roles in peroxisomal fission. Plant Journal, 58 (3):388-400
- **Hellens RP**, Edwards EA, Leyland NR, Bean S, Mullineaux PM (2000). pGreen: a versatile and flexible binary Ti vector for Agrobacterium-mediated plant transformation. Plant Molecular Biology, 42:819–832
- **Köhler RH**, Hanson MR (2000). Plastid tubules of higher plants are tissue-specific and developmentally regulated. Journal of Cell Science, 113 (1):81-89
- **Jefferson RA**, Kavanagh TA, Bevan MW (1987). GUS fusions: beta-glucuronidase as a sensitive and versatile gene fusion marker in higher plants. EMBO Journal, 6(13):3901-3907.
- **Lee LY**, Fang MJ, Kuang LY, Gelvin SB (2008). Vectors for multi-color bimolecular fluorescence complementation to investigate protein-protein interactions in living plant cells. Plant Methods, 4:24
- **Lee YJ**, Kim DH, Kim YW, Hwang I (2001). Identification of a signal that distinguishes between the chloroplasts outer envelope membrane and the endomembrane system in vivo. The Plant Cell, 13:2175-2190

- **Logan DC** (2010). The dynamic plant chondriome. Seminars in Cell & Developmental Biology, 21 (6):550-557
- **Logan DC** (2003). Mitochondrial dynamics. New Phytologist, 160 (3): 463–478
- **Mai S**, Klinkenberg M, Auburger G, Bereiter-Hahn J, Jendrach M (2010). Decreased expression of Drp1 and Fis1 mediates mitochondrial elongation in senescent cells and enhances resistance to oxidative stress through PINK1. Journal of Cell Science, 123: 917-926
- **Main GD**, Reynolds S, Gartland JS (1995) Electroporation protocols in *Agrobacterium*. In: Gartland KMA, Davey MR (eds) Methods in molecular biology, vol 44: Agrobacterium protocols. Humana Press, Totowa, pp 405–412
- **Nelson BK**, Cai X, Nebenführ A (2007). A multicolored set of *in vivo* organelle markers for co-localization studies in *Arabidopsis* and other plants. The Plant Journal, 51 (6):1126-36
- **Noctor G**, De Paepe R, Foyer CH (2007). Mitochondrial redox biology and homeostasis in plants. TRENDS in Plant Science, 12 (3):125-134
- **Scott I**, Tobin AK, Logan DC (2006). BIGYIN, an orthologue of human and yeast FIS1 genes functions in the control of mitochondrial size and number in *Arabidopsis thaliana*. Journal of Experimental Botany, 57 (6):1275-1280
- **Suen DF**, Norris KL, Youle RJ (2008). Mitochondrial dynamics and apoptosis, Genes and Development, 22: 1577-1590
- **Suzuki M**, Jeong SY, Karbowski M, Youle RJ, Tjandra N (2003). The solution structure of human mitochondria fission protein Fis1 reveals a novel TPR-like helix bundle. Journal of Molecular Biology, 334 (3):445-58
- **Sweetlove L**, Fait A, Nunes-Nesi A, Williams T, Fernie AR (2007). The mitochondrion: an integration point of cellular metabolism and signalling. Critical Reviews in Plant Sciences, 26:17-43
- **Tzfira T**, Tian GW, Lacroix B, Vyas S, Li J, Leitner-Dagan Y, Krichevsky A, Taylor T, Vainstein A, Citovsky V (2005). pSAT vectors: a modular series of plasmids for autofluorescent tagging and expression of multiple genes in plants. Plant Molecular Biology, 57:503-516

- **Vianello A**, Zancani M, Peresson C, Petrussa E, Casolo V, Krajňáková J, Patui S, Braidot E, Macrì F (2007). Plant mitochondrial pathway leading to programmed cell death. Physiologia Plantarum, 129 (1):242-252
- **Von Arnim AG**, Deng XW, Stacey MG (1998). Cloning vectors for the expression of green fluorescent protein fusion proteins in transgenic plants. Gene, 221:35–43
- **Yoo SD**, Cho YH, Sheen J (2007). *Arabidopsis* mesophyll protoplasts: a versatile cell system for transient gene expression analysis. Nature Protocols, 2(7):1565-1572
- **Zhang XC**, Hu JP (2008a).Two small protein families, DYNAMIN-RELATED PROTEIN3 and FISSION1, are required for peroxisomal fission in *Arabidopsis*. The Plant Journal, 57(1):146-59
- **Zhang XC**, Hu JP (2008b). FISSION1A and FISSION1B proteins mediate the fission of peroxisomes and mitochondria in Arabidopsis. Molecular Plant, 1(6):1036-1047
- **Zottini M**, Barizza E, Costa A, Formentin E, Ruberti C, Carimi F, Lo Schiavo F (2008). Agroinfiltration of grapevine leaves for fast transient assays of gene expression and for long-term production of stable transformed cells. Plant Cell Reports, 27(5):845-853
- **Zybailov B**, Rutschow H, Friso G, Rudella A, Emanuelsson O, Sun Q, Van Wijk KJ (2008). Sorting signals, N-terminal modification and abundance of the chloroplast proteome. PLoS One, 3(4):e1994

Chapter 3

The subcellular localization of BIGYIN, an *Arabidopsis* protein involved in mitochondrial and peroxisomal division, unveils a dynamic network of tubules and organelles

INTRODUCTION

Mitochondria, peroxisomes and plastids are essential and ubiquitous subcellular organelles in plants. Each of these organelles plays specific roles in the metabolism of plant cells, for example mitochondria in oxidative phosphorylation, peroxisomes in β-oxidation of fatty acids, and chloroplasts in photosynthesis. However, in higher plants, extensive metabolic interactions between mitochondria, peroxisomes and chloroplasts have been described during several processes, such as photorespiration, where individual reactions are distributed over chloroplast, peroxisome, mitochondrion and cytosol (Bauwe *et al.*, 2010). This metabolically link requires an intimate physical contact among these organelles. However, this inter-organellar physical continuity has not yet been demonstrated. Although several ultrastructural studies of plant cells described chloroplasts, mitochondria and peroxisomes often very close located each other, only very few electron micrographs documented interactions among them. These few electron micrographs showed that inter-organellar interactions could occur both trough direct continuity between membranes of different organelles, or trough membranous tubular protrusions extending from organellar membranes (Crotty and Ledbetter, 1973). Nowadays, new tools are available in addition of electron microscopy opening the possibility to further investigate the inter-organellar interactions in plant cells. In detail, confocal microscopy studies have documented the close vicinity between organelles and the presence of tubular structures extending from organellar membranes in living cells. These tubular structures were termed ‘stromules’, when extending from plastidial outer membranes (Natesan *et al.*, 2005); ‘matrixules’ if extending from mitochondrial outer membranes (Scott *et al.*, 2007); and ‘peroxules’ if extending from peroxisomal membranes (Jedd and Chua, 2002). The precise role(s) of these tubular structures is so far unknown. It has been reported that stromules allow the exchange of molecules between interconnected plastids (Kwok and Hanson, 2004a), and in a more general context, it has been proposed that peroxules might exchange molecules between peroxisomes (Mano *et al.*, 2002), and matrixules between mitochondria (Scott *et al.*, 2007). Yet, in the light of metabolic interactions that occurred among organelles, it has been proposed that these

tubular structures might increase the transfer efficiency of inter-organelle metabolites, through transient physical interactions between the tubules of different organelles (Scott *et al.*, 2007). However no data have been reported so far to confirm this hypothesis.

Interestingly, mitochondria and peroxisomes share certain morphological similarity. Both organelles are highly dynamic, capable of changing their shape, of moving rapidly throughout the cell and of dividing (from one to at least two peroxisomes or two mitochondria) as shown in yeasts, mammals and higher plants. Yet, mitochondria and peroxisomes share also several components of their division machinery, like the dynamin-related proteins (DRPs) and the Fission1-like (FIS1) protein. These proteins have been extensively studied in yeast *Saccharomyces cerevisiae* and mammals. These studies have indicated that DRPs are members of the dynamin superfamily of membrane-remodeling GTPases. DRPs are cytosolic proteins that are direct involved in mitochondrial and peroxisomal membrane scission (Thomas and Erdmann, 2005). FIS1 protein is, instead, integral membrane protein targeted to both peroxisomes and mitochondria. This transmembrane protein is considered a member of tail-anchored (N_{out}-C_{in}) family of membrane proteins, because it possesses a single membrane-spanning domain located near the C-terminal tail and an N-terminal region predicted to be exposed to cytosol (Borghese *et al.*, 2007). During division of mitochondria and peroxisomes in yeasts and mammals, FIS1 protein act as adaptor for DRP proteins, recruiting cytosolic DRPs to organelles in order to perform membrane fission (Kobayashi *et al.*, 2007). The *Arabidopsis* genome has two closely related DRPs, functional orthologs of yeast and mammalian DRPs (Fujimoto *et al.*, 2009), and two FIS1 orthologs termed BIGYIN (previously named FIS1A, At3g57090) and FIS1B (At5g12390), both involved in peroxisomal and mitochondrial fission (Zhang and Hu, 2008b). It has been reported that, when BIGYIN is ectopically overexpressed by the cauliflower mosaic virus 35S (CaMV 35S) promoter, it localizes to mitochondrial outer membranes and peroxisomal membranes (Zhang and Hu, 2008a). We have shown (Chapter 2), that BIGYIN displays also a subcellular localization to chloroplasts in leaf mesophyll cells, when BIGYIN is overexpressed by CaMV 35S promoter in *Arabidopsis* leaf mesophyll protoplasts transiently transfected or in tobacco

leaves agro-infiltrated. So far, the role(s) of BIGYIN on chloroplasts has not yet been investigated, and above all it is not clear whether these multiple localization patterns occur in native *Arabidopsis* plants.

The similarity between mitochondria and peroxisomes in their fission machinery could be explained analyzing these organelles at an evolutionary level. It is widely accepted that mitochondria originated from common ancestral free-living α-proteobacteria, that colonised pro-eukaryotic cells around two billion years ago (Gray *et al.*, 1999). Concerning peroxisomal origin, recent studies suggest that the original peroxisome was possibly derived from a cellular membrane system, such as endoplasmic reticulum, as an invention of eukaryotic cell (Michels *et al.*, 2005). It is possible that peroxisomes were already present when pro-mitochondria colonised the early eukaryotic cell. As mitochondria appear to have lost components of their bacterial origin, mitochondria may have also co-opted the main components of their outer membrane fission machinery from peroxisomes (Schrader, 2006). As result, peroxisomes and mitochondria share several components of their division machinery.

Similarly to mitochondria, plastids arose from prokaryotic endosymbionts during eukaryotic evolution: it is widely accepted that plastid ancestor was a cyanobacterium engulfed and enslaved by a non-photosynthetic protist (Gray, 1999). As mitochondria and peroxisomes, also plastids arise by division of pre-existing organelles through binary fission. The plastid division process can be separated into four distinct stages: (1) slight plastid elongation; (2) plastid constriction that causes the formation of the typical plastidial ‘dumbbell-shape’; (3) further constriction, isthmus formation, and thylakoid membrane separation; (4) isthmus breakage, plastid separation and envelope releasing (Aldridge *et al.*, 2005). In most organisms, the plastid division apparatus consist of a double ring structure, with one ring on the cytosolic face of the outer membrane (outer ring), and one on the stromal face of the inner envelope (inner ring) (Maple and Møller, 2007). Recent studies have revealed that the plastid division is controlled by a combination of prokaryote-derived and host eukaryote-derived proteins. The division of plastids is, in fact, dependent on two machineries, one analogous to bacterial cell division machinery located on stromal face of the inner ring, and one unique to plants, located on cytosolic face of the outer ring (Maple and Møller,

2007). Similarly to mitochondria and peroxisomes, also in plastids orthologs of dynamin superfamily GTPases are involved in plastid division. In particular in *Arabidopsis*, one of these orthologs is DRPB5 (previously namely ARC5, At3g19720) and very recent data have demonstrated that this chloroplast division protein plays a role also in peroxisomal division (Zhang and Hu, 2010).

All together, these findings indicate that, in *Arabidopsis*, peroxisomes and chloroplasts share at least one component of their division machinery, and that peroxisomes and mitochondria share several components of their division machinery. The use of shared components could be a mechanism to promote coordinated division among these organelles that are at least metabolically linked (Schrader, 2006).

Here, we focus on the study of BIGYIN, an *Arabidopsis* Fission1-like protein involved in mitochondrial and peroxisomal fission. We report, in *Arabidopsis* plants, a detailed subcellular localization of BIGYIN, expressed under control of its own promoter. We are in fact initially interested in elucidating whether the multiple subcellular localization patterns of BIGYIN to mitochondria, peroxisomes and chloroplasts, observed in our previously analyses (Chapter 2) using the constitutive CaMV promoter, are maintained when *BIGYIN* expression is driven by the native promoter. Then, we analyze the subcellular localization of mutated BIGYIN protein showing on chloroplasts surfaces a very interesting pattern that provides the first indication that this protein could be involved in chloroplast fission. Yet, we dissect BIGYIN to define domains crucial for its multiple targeting. In addition, we report the localization of BIGYIN to the tubular protrusions extending from mitochondrial, peroxisomal and chloroplast membranes, and we investigated whether inter-organellar interactions occurred through these tubular structures in plants.

RESULTS

Structure of *Arabidopsis FIS1*-type proteins

Fission1(FIS1)-type proteins are evolutionarily conserved transmembrane proteins implicated in maintaining the proper morphology of mitochondria and peroxisomes. Yeasts and humans contain a single copy of *FIS1*-type gene termed *FIS1* and *hFIS1*, respectively. The *Arabidopsis* genome contains, instead, two *FIS1*-type genes, which are referred to as *FIS1A* or *BIGYIN*, and *FIS1B*. *BIGYIN* encodes a protein of 170 amino acid residues, and *FIS1B* encodes a protein containing 167 residues. Overall amino acid identity between BIGYIN and FIS1B is 57.1% (Fig. 1A). Analysis of their protein sequences using ClustalW2 Multiple Sequences Alignment (http://www.ebi.ac.uk/Tools/msa/clustalw2/, Fig. 1B) showed that BIGYIN shared the highest similarity with the human hFis1 (30.1% identity, 57% similarity). Conversely FIS1B shared the highest similarity with the yeast Fis1p (33.7% identity, 54% similarity).

FIS1-type proteins are characterized by a tetratricopeptide repeat (TPR)-like helix bundle (Suzuki *et al.*, 2003), involved in protein-protein interaction and located within the N-terminal tail of the protein. The C-terminal structure contains a single-pass transmembrane domain and the N-terminal tail is predicted to be exposed to the cytoplasm. In *silico* analysis of the protein structures of BIGYIN and FIS1B, using InterProScan (http://www.ebi.ac.uk/Tools/InterProScan/), revealed a conserved TPR-like helix domain (residues 16-141 in BIGYIN and 23-143 in FIS1B) located within the N-terminal tail of the protein and a single C-terminal putative transmembrane domain (residues 143-163 in BIGYIN and 144-164 in FIS1B, Fig. 2) with a topology predicted to leave the N-terminal region exposed to the cytoplasm. For this particular topology BIGYIN and FIS1B, and more in general all the FIS1-type proteins, belong to the class of the tail anchored (TA) (N_{out}-C_{in})-proteins. TA proteins are a class of single-pass transmembrane proteins characterized by a hydrophobic membrane-anchoring region close to the COOH terminus and by a NH_2-terminal active cytosolic domain (Kutay *et al.*, 2005; for a review see Pedrazzini, 2009).

Published microarray data (http://bbc.botany.utoronto.ca/) revealed that the expression level of *BIGYIN* is higher than that of *FISB* in most of tissues, while *FIS1B* is expressed mainly in mature pollen (Fig.3). For this reason, we focused in detail on studying of BIGYIN, analyzing its gene expression pattern and its protein localization pattern in the whole plant.

BIGYIN expression pattern in germinating seeds, young seedlings, adult rosettes and mature flowering plants

To investigate in detail the expression pattern of *BIGYIN*, we generated transgenic *Arabidopsis* plants carrying an 862 bp promoter fragment of *BIGYIN* (-862 to -1 from the ATG start codon) fused to the *β-glucuronidase* (*GUS*) reporter gene (p*BIGYIN*::*GUS*) (Jefferson *et al.*, 1987). Several transgenic p*BIGYIN*::*GUS* lines were obtained as independent transformants. None of these plants showed any obvious changes in growth or morphology when compared to wild type plants. Histochemical observations in four independent second generation (T_2) p*BIGYIN*::*GUS* lines were performed, using X-Gluc as substrate for GUS enzyme. These lines showed a similar *BIGYIN* expression pattern of *BIGYIN*, yet characterized by varying intensity levels of visible blue coloration among the four transgenic lines. In detail, *BIGYIN* expression was higher in a transgenic line (number 3) than in the other tree transgenic lines. Representative stereo-microscope images of leaf tissues of 7-day-old seedlings were reported in Figure 4. RT-PCR analyses of *β-glucuronidase* and *BIGYIN* transcript abundance levels were performed to individualize a transgenic p*BIGYIN*::*GUS* line, where p*BIGYIN* promoter activity was comparable with the activity of endogenous p*BIGYIN* promoter. Leaf tissues were used as starting material for RNA extraction, because in leaves we clearly detected, in all transgenic lines, a p*BIGYIN* promoter activity, shown by histochemical GUS staining assay. The results showed that transcript levels of *GUS* (Fig. 4B) and *BIGYIN* (Fig. 4C) were similar in one transgenic line (number 3). This transgenic line was used to analyze in detail the *BIGYIN* expression pattern in different organs and developmental stages, through histochemical GUS assay.

An ubiquitous *BIGYIN* expression was detected in all developmental stages, from germinating seeds to mature plants. In germinating seeds at 32 hour after imbibition (Fig. 5), a strong p*BIGYIN* promoter activity was detected in several tissues (i.e. shoots, hypocotyls and radicles). In 5-day-old seedlings (Fig. 6), *BIGYIN* expression was most intense at the tips (termed also 'leaf teeth') and veins of cotyledons and leaf primordia, in the central cylinder of hypocotyls and roots, and in root tips. A close inspection of p*BIGYIN* promoter activity at the level of root tips showed that *BIGYIN* expression was observed in root tips but not in root caps. A similar expression pattern was observed in 7-day-old seedlings (Fig.7). In detail, *BIGYIN* expression was intense in leaf teeth of cotyledons and leaf primordia, and in petioles. GUS blue staining observed in petioles continued along the veins of cotyledons and leaf primordia. Cell-specific *BIGYIN* expression was found in trichomes. p*BIGYIN* promoter activity was detected throughout most of the root system, including root hairs, with the strongest *BIGYIN* expression observed in root tips and root caps, in lateral root primordia, and in steles both in primary and lateral roots. Similar to our observations in earlier developmental stages, in mature plants (Fig. 8), *BIGYIN* expression was typically detected in the leaf teeth both in young leaves and in old leaves, in mid veins, in vascular tissues of blades and in rosette petioles. In cauline leaves, p*BIGYIN* promoter activity showed the same pattern. However, in general, expanding leaves had higher *BIGYIN* expression than old leaves. A strong p*BIGYIN* promoter activity was observed in node, in developing stem, and in lateral bud. In 6-week-old plants, *BIGYIN* expression was shown also in floral tissues (Fig. 9), with the highest levels observed in veins of sepals, and in carpels typically in stigma and in germinated pollen. *BIGYIN* expression was also detected in floral buds of secondary branches. In developing siliques, *BIGYIN* expression was present in replum, funiculi, abscission zone and pedicel, but absent in seeds.

These results show an ubiquitous BIGYIN expression in germinating seeds, in seedlings and in mature plants, indicating that BIGYIN is expressed in all developmental stages. In detail, BIGYIN expression is observed in meristematic zones, where plant growth takes place, including leaf teeth, leaf primordia, developing stems, nodes, lateral root primordia, root tips and flower buds.

Localization pattern of BIGYIN protein in germinating seeds, young seedlings, adult rosettes and mature flowering plants

In order to analyze the localization pattern of BIGYIN protein in physiological conditions, we produced *Arabidopsis* transgenic plants expressing the *YFP::BIGYIN*) under the control of p*BIGYIN* promoter (p*BIGYIN::YFP::BIGYIN*). Since BIGYIN is a (N_{out}-C_{in}) transmembrane protein, it is probably characterized by a C-terminal membrane targeting signal (Borghese *et al.*, 2007). For this reason, *YFP* coding sequence (CDS) was fused to the N-termini of *BIGYIN* CDS to avoid the interference with putative targeting information. This fusion construct was subcloned into the plant pGreenII binary expression vector (Hellens *et al.*, 2000), it was introduced in *Agrobacterium tumefaciens* and *A. thaliana* plants were transformed by using floral dip method (Clough and Bent, 1998). Several transgenic *Arabidopsis* independent lines were obtained. Second generation (T_2) transgenic seedlings were used to analyze in detail the localization pattern of BIGYIN protein in different organs and developmental stages, by means YFP fluorescence.

BIGYIN was detected in all developmental stages, from germinating seeds to mature plants. In germinating seeds (32 hour after imbibition; Fig. 10), BIGYIN was observed in all tissues (i.e. shoots, hypocotyls, and radicles). In 5-day old seedlings (Fig. 11), BIGYIN was most detected in leaf teeth and veins of cotyledons, in the apical zones, in hypocotyl, in shoot-root junctions, in roots, in root hair and root tips. In detail, in stems and roots, BIGYIN was observed at the level of epidermal cells and steles. A similar pattern was observed in 7-day-old seedlings (Fig.12). BIGYIN was detected in leaf teeth of cotyledons and leaf primordia, and in petioles. YFP::BIGYIN fluorescence in the leaf teeth continued in trichomes, along the veins of cotyledons and leaf primordia, in stems and in shoot-root junctions. BIGYIN was detected throughout most of the root system, including root hair, with the strongest YFP::BIGYIN fluorescence observed in root steles, in developing lateral roots, in root tips and root caps. Analysis of root stele showed that BIGYIN was typically present in the upper root zones (termed also zones of cell maturation and differentiation) than in the lower root zones (named zones of cell division and elongation). A close inspection of BIGYIN

localization in roots was obtained using propidium iodide to counterstain the root cells. In the differentiation zone (Fig. 13A-B), BIGYIN was typically detected in cells of stele and epidermis. In root tip (Fig. 13C-D), BIGYIN was present in the root caps and in cells of epidermis.

Similar to our previous observations in earlier developmental stages, in mature plants, BIGYIN was ubiquitously present. In detail, BIGYIN was typically present on leaf teeth of cauline leaves and of all developmental stages of rosette leaves (expanding, adult, old leaf). YFP::BIGYIN fluorescence extended in mid veins, in vascular tissues of blades, in trichomes, in stems and in nodes (Fig. 14). In mature 6-week-old plants (Fig. 15), BIGYIN was detected on floral tissues, typically on veins of sepals and petals, on filaments, on pistils typically on stigma and germinated pollen, and on receptacle. In developing siliques, BIGYIN was present in replum, funiculi and pedicel, but absent in seeds.

All together, these results show that BIGYIN is ubiquitously present in all plant developmental stages (germinating seeds, seedlings and mature plants). In particular BIGYIN protein is typically present in meristematic zones, where plant growth takes place, including leaf teeth, leaf primordia, developing stems, nodes, lateral root primordia, root tips and flower buds.

Subcellular localization of YFP::BIGYIN in *Arabidopsis* plants

So far, YFP::BIGYIN fusion protein driven by constitutive CaMV 35S promoter was localized to peroxisomes and mitochondria in *Arabidopsis* epidermal leaves (Zhang and Hu, 2008b), and we showed that BIGYIN was localized also to chloroplasts in transient expression experiments, performed in *Arabidopsis* leaves protoplasts and in tobacco mesophyll cells (Chapter 2). We investigated if this multiple subcellular localization pattern was maintained also when BIGYIN expression was driven by its native promoter. To do this, we crossed p*BIGYIN::YFP::BIGYIN Arabidopsis* plants with several transgenic plants containing specific organelle markers. To detect mitochondria, plants carrying the mitochondrial COX::RFP (*Arabidopsis* cytocrome c oxidase-releated fused to red fluorescence protein) marker were used. To visualize peroxisomes,

plants expressing peroxisomal RFP::KSRM (RFP fused to KSRM sequence tag) marker were used. COX::RFP and RFP::KSRM *Arabidopsis* transgenic lines were generated in our laboratory. To detect chloroplasts, the autofluorescence of chlorophyll was analyzed in p*BIGYIN::YFP::BIGYIN* plants.

Subcellular localization of BIGYIN to mitochondria

To investigate whether BIGYIN was localized to mitochondria, transgenic *Arabidopsis* plants stably co-expressing *YFP::BIGYIN* and mitochondrial *COX::RFP* marker were obtained and analyzed in several tissues of 7-day-old seedlings. BIGYIN and mitochondria were detected by means YFP and RFP fluorescence using confocal laser scanning microscopy (CLSM).

BIGYIN was mostly localized to mitochondria in cells of leaf epidermis (Fig. 16A), in hypocotyls (Fig. 16B), and in roots (Fig. 16C). Mitochondria appeared as red spots. BIGYIN was, instead, located to the rim of mitochondria, and in detail BIGYIN surrounded these organelles. This particular pattern suggested that BIGYIN was localized to mitochondrial outer membranes. Interesting, BIGYIN was also localized to protrusions extending from mitochondrial membranes. As result, YFP::BIGYIN marked mitochondria and a network of tubules among the mitochondria. Similar mitochondrial protrusions were previously observed and termed 'matrixules' ('matrix-filled tubules') by Logan *et al.* (2004).

Even if matrixules have been described as 'commonly found in wild type plants', their role(s) is not yet known (Scott *et al.*, 2007). In order to investigate the behaviour and dynamics of mitochondria and especially of matrixules labelled with BIGYIN, time-lapse analyses were performed in leaves of seedlings of these transgenic *Arabidopsis* co-transformed plants. BIGYIN and mitochondria were analyzed by means YFP and RFP fluorescence using CLSM. Mitochondria appeared as very dynamic organelles. BIGYIN and mitochondria moved together inside the cytoplasm clearly indicating that BIGYIN localized to these organelles. BIGYIN was also located to matrixules that appeared as mitochondrial protrusions freely moving throughout the cytoplasm. In detail, matrixules, labelled with BIGYIN, could extend or retract within the cytoplasm (Fig. 17). A close association between matrixules and direction of mitochondrial movements was

also detected. Linear streaming of mitochondria was, in fact, observed along matrixules marked with BIGYIN (Fig. 17).

Taken together, our results indicate that BIGYIN localizes to the mitochondrial outer membranes and matrixules. Mitochondria and matrixules show highly dynamics throughout the cytoplasm.

Subcellular localization of BIGYIN to peroxisomes

To determine whether BIGYIN localized to peroxisomes, transgenic *Arabidopsis* plants stably co-expressing the YFP::BIGYIN and the peroxisomal RFP::KSRM marker were obtained and analyzed in several tissues. BIGYIN and peroxisomes were detected by means YFP and RFP fluorescence using confocal laser scanning microscopy (CLSM). Representative confocal images of leaf epidermis, stems and roots of 7-day-old seedlings were reported in Figure 18. In epidermal cells (Fig. 18A), BIGYIN was localized to peroxisomes and to thin tubular projections, extending from peroxisomal surfaces. A similar subcellular localization pattern was observed in cells of stems (Fig. 18B) and roots (Fig. 18C). High resolution images allowed to discern between BIGYIN localized to the periphery of peroxisomes and RFP marker inside the lumen of peroxisomes, indicating that BIGYIN was located at the level of peroxisomal membranes (arrows in Fig. 18B). Peroxisomal tubular protrusions were observed by Cutler *et al.* (2000) in *Arabidopsis* plants and termed 'peroxules' (i.e. 'peroxisomal-filled tubules').

Dynamics of peroxisomes and especially of peroxules, labelled with YFP::BIGYIN, were examined by time-lapse analyses in leaves of *Arabidopsis* seedlings, stable co-transformed with *YFP::BIGYIN* and peroxisomal *RFP::KSRM*. BIGYIN and peroxisomes were detected by means YFP and RFP fluorescence using CLSM. Peroxisomes were motile organelles. BIGYIN and peroxisomes moved together inside the cytoplasm, suggesting that BIGYIN was localized to peroxisomes (Fig. 19A). As the peroxisomes, also peroxules moved freely throughout the cytoplasm. Based on the direction of movement of peroxisomes, peroxules could be considered leading or trailing peroxisomal movements (Fig. 19B). Moreover, peroxules could create among them an interconnected network of tubular protrusions, and peroxisomes seemed to move along this network.

All together, these results suggest that BIGYIN localizes to peroxisomal membranes and to peroxules. A dynamic network of peroxules is detected and peroxisomes movements are linked to peroxules dynamics.

Subcellular localization of BIGYIN to chloroplasts

Successively, we investigated whether BIGYIN, driven by its native promoter, was localized to chloroplasts. To identify these organelles, chlorophyll autofluorescence was detected in transgenic *Arabidopsis* plants stably expressing *YFP::BIGYIN*. In Figure 20A, representative confocal images of mesophyll cells of 7-day-old seedlings were reported. BIGYIN was mostly localized to chloroplasts. In detail, chlorophyll autofluorescence outlined the distribution of thylakoid membranes. BIGYIN, instead, enveloped the chlorophyll autofluorescence, indicating that BIGYIN was localized to the outer membranes of chloroplasts. Moreover, BIGYIN was also detected on thin tubular protrusions extending from chloroplast outer membranes. No chlorophyll autofluorescence was detected in these tubules, indicating that the thylakoid membranes did not extend into them. A similar subcellular localization pattern of BIGYIN was observed also in cells of hypocotyl (Fig. 20B). Also in these cells, in fact, BIGYIN was detected to the outer membranes of chloroplasts and to thin tubular protrusions extending from outer membranes of a single chloroplast or interconnected chloroplasts. Similar tubular projections, extending from chloroplasts and containing no chlorophyll, were termed by Köhler and Hanson (2000) 'stroma-filled tubules' or 'stromules'. Movements of stromules were observed in time-lapse analyses performed in hypocotyl of *Arabidopsis* 7-day-old seedlings stable transformed with *YFP::BIGYIN*. Stromules were highly motile: they might undulate within the cytoplasm, extend or retract from plastids, that might be moving or completely stationary. Based on the direction of movement of chloroplasts, stromules could be considered leading or trailing chloroplast movements (Fig. 20C).

BIGYIN has been described to be involved in mitochondrial and peroxisomal division (Zhang *et al.*, 2008a). By contrast, its role on chloroplast membranes has not been yet investigated. In light of the fission role of BIGYIN in mitochondria and in peroxisomes, we investigated the subcellular localization of

BIGYIN during chloroplast division. We analyzed therefore, in *Arabidopsis YFP::BIGYIN* plants, chloroplasts in developing tissues, where chloroplast divisions highly occurred. In detail, we observed the cells of stigma of flower buds and of young hypocotyls. Representative confocal images were reported in Fig. 21. BIGYIN was detected by means YFP fluorescence, while chlorophyll autofluorescence was used to identify chloroplasts. All morphological changes, that characterized chloroplast division event, were observed: the initial constriction, the further constriction with the isthmus formation, the thylakoid separation with the consequent isthmus narrowing and the final separation with the envelope resealing. When chloroplast was in the initial constriction phase, YFP::BIGYIN protein was localized to the chloroplast outer membranes, while it was localized to the isthmus, when isthmus was in formation (asterisks in Fig.21). Moreover, during the final stage of chloroplast fission, BIGYIN was clearly localized to the ring structures encircling the division sites between two chloroplasts (arrows, in Fig. 21).

Our data indicate that BIGYIN localizes to chloroplasts and stromules. The outgrowth of stromules is characterized by transient extension and retraction in a movement completely no synchronous in the cell. Moreover, these results show that the subcellular localization of BIGYIN during chloroplast division is strictly associated with chloroplast outer membranes and especially with the ring structures encircling the chloroplast division sites.

Subcellular localization of BIGYIN to chloroplasts, mitochondria and peroxisomes of leaf mesophyll cells

We have previously demonstrated that BIGYIN was a transmembrane protein belonging to the group of the tail anchored protein, localized to peroxisomes and mitochondria of leaf epidermal, hypocotyl and root cells. Moreover, we described as BIGYIN was localized to chloroplasts of hypocotyl and mesophyll cells. Interesting, another *A. thaliana* tail anchored protein, named cytochrome b5 isoform (cyt b5), was described to be localized to different organelles (mitochondria and chloroplasts), but its subcellular localization was dependent on both cell type and cell function (Maggio *et al.*, 2007). The authors reported, in fact, that in mesophyll cells, where chloroplasts were detectable, cyt b5 isoform

was never localized to mitochondria and it was always associated with chloroplasts. By contrast, cyt b5 was localized to mitochondria in epidermal cells, where chloroplasts were not detected. In light of these findings, we investigated whether BIGYIN showed a different subcellular localization pattern in leaf mesophyll and epidermal cells. To detect BIGYIN proteins, mitochondria and chloroplasts, *Arabidopsis* transgenic plants, stably co-expressing *YFP::BIGYIN* and mitochondrial *COX::RFP* marker, were used. YFP signal (in green) and RFP fluorescence (in pink) were detected together with the autofluorescence of chlorophyll (in red) (Fig.22). In epidermal cells, BIGYIN was localized to the mitochondrial marker, while BIGYIN was localized both to mitochondria and chloroplasts in mesophyll cells. Similarly, we observed that YFP::BIGYIN localized to peroxisomes in leaf epidermal cells and to peroxisomes and chloroplasts in leaf mesophyll cells of transgenic *Arabidopsis* plants stably co-expressing the *YFP::BIGYIN* and peroxisomal *RFP::KSRM* marker.

Our results indicate e that the subcellular localization of BIGYIN does not change in different cell types. In all analyzed cells, in fact, BIGYIN localizes to mitochondria, peroxisomes and, when chloroplasts were present, also to chloroplasts.

Network of 'bigyinules'

Our data demonstrated that BIGYIN showed a multiple subcellular localization pattern, i.e. to mitochondria, peroxisomes, chloroplasts and membranous protrusions extending from these organelles. These tubular structures were termed 'matrixules' for mitochondria, 'peroxules' for peroxisomes and 'stromules' for chloroplasts. However, the terms 'matrixules', 'peroxules' and 'stromules' were originally coined to indicate the 'matrix-filled tubules', the 'peroxisomal-filled tubules', and the 'stroma-filled tubules'. To clearly distinguish BIGYIN that marked the tubular membranes but not the inner space enclosed by the membranes, we termed 'bigyinules' the tubular membrane protrusions, labelled with the YFP::BIGYIN, extending from mitochondria, peroxisomes and chloroplasts. Below we have examined in detail the behaviour and dynamics of

bigyinules in order to investigate the possible role(s) of these membranous tubules.

Network of bigyinules among mitochondria and chloroplasts

In order to observe in detail bigyinules from mitochondria and chloroplasts simultaneously, we analyzed *Arabidopsis* seedlings co-expressing the *YFP::BIGYIN* and the mitochondrial *COX::RFP* marker. We observed in particular hypocotyl cells, where chloroplasts were present. BIGYIN was localized, as expected, to chloroplasts, mitochondria and several tubules (Fig. 23). Mitochondria and chloroplasts could be found in close vicinity or spread throughout the cytoplasm. Multiple bigyinules that protruded from chloroplasts and mitochondria could form a complex and interconnected network among these organelles. A single bigyinule could form a bridge between a chloroplast and a mitochondrion, it could interconnect through a unique tubular structure several chloroplasts and mitochondria, and it could also be linked with other bigyinules creating a very intricate network of tubules.

The behaviour and dynamics of chloroplasts, mitochondria and especially of bigyinules were examined through time-lapse analyses. Mitochondria, chloroplasts and the tubules labelled with BIGYIN created together a complex and interconnected network of dynamic structures (Fig. 23C-D). They could move when connected to stationary chloroplasts (Fig. 24A), they could lead mitochondrial movement (Fig. 24B) or be trailed by moving mitochondria (Fig. 30C). Bigyinules could also break up into small tubules or in distinct vesicle-structures that moved independently within the cytoplasm (Fig. 23C,D).

Our data indicate that there is not a truly stereotypical form of bigyinule movement.

Network of bigyinules among peroxisomes and chloroplasts

Successively, we described in detail bigyinules coming from peroxisomes and chloroplasts simultaneously, analyzing *Arabidopsis* seedlings co-expressing *YFP::BIGYIN* and peroxisomal *RFP::KSRM* marker. We observed cells of hypocotyl and leaf mesophyll, where chloroplasts were present. Representative confocal images were reported in Fig. 25. YFP::BIGYIN was shown in green

colour; peroxisomes in red; while chloroplasts were easily distinguish by their dimension. BIGYIN was localized, as expected, to chloroplasts, peroxisomes and several tubules. As previously observed in the case of mitochondria and chloroplasts, also peroxisomes and chloroplasts could be close localized or dispersed within the cytoplasm. Several bigyinules protruded from chloroplasts and peroxisomes forming a complex network interconnecting these different organelles.

The behaviour and dynamics of chloroplasts, peroxisomes and especially of bigyinules were examined by time-lapse analyses (Fig. 26). Peroxisomes, chloroplasts and tubules, labelled with BIGYIN, described together a complex and interconnected network of dynamic structures. Bigyinules could extend or retract freely from organelles. Bigyinules could also protrude from peroxisomes to chloroplasts or *vice versa*. Based on the direction of movements of peroxisomes, bigyinules could be considered leading or trailing the peroxisomal movements: bigyinules could, in fact, be trailed by moving peroxisomes or, on the contrary, bigyinules could lead peroxisomes. Bigyinules could break up into small tubules or in distinct vesicle-structures that moved independently within the cytoplasm (Fig. 26C).

These results confirmed that there are not truly stereotypical forms of bigyinule movement.

Analysis of the anti-BIGYIN antibody specificity

A specific polyclonal antibody was generated against a peptide of 15aa located to the N-terminal tail of BIGYIN (aa 33-47), in order to confirm the multiple subcellular localization of BIGYIN by means biochemical techniques (i.e. immunogold electron microscopy assay and immunoblot assay of protein extracts enriched in specific subcellular compartments). So far, we tested the anti-BIGYIN-antibody in western blot assay using crude extracts from transgenic plants stably expressing *YFP::BIGYIN* and from wild type plants. As result, we obtained that the anti-BIGYIN antibody was specific, given that it specifically recognized in wild type plants the BIGYIN protein (18,7 kDa) (Fig. 27), and in

p*BIGYIN::YFP::BIGYIN* transgenic plants both the BIGYIN protein (18,7 kDa) and the YFP::BIGYIN fusion protein (46,3 kDa). Moreover, we observed that the YFP::BIGYIN fusion protein was more intense that BIGYIN in the crude extracts obtained from the transgenic p*BIGYIN::YFP::BIGYIN* plants.

All together, these results indicate that the anti-BIGYIN-antibody is specific for BIGYIN. Moreover, our data indicate that in* p*BIGYIN::YFP::BIGYIN* plants, *although the YFP::BIGYIN is driven by the* p*BIGYIN promoter, the YFP::BIGYIN fusion protein is more abundant than the endogenous BIGYIN protein.

Characterization of pBIGYIN::YFP::BIGYIN transgenic plants

It was been reported that in BIGYIN overexpressing plants the number of peroxisomes increased to about three fold compared with the wild type, and that the total peroxisomal area in BIGYIN overexpressing plants increased of five to six times from that of wild type plants (Zhang and Hu, 2008b). In order to investigate if in our p*BIGYIN::YFP::BIGYIN* plants a similar aberrant morphology of peroxisomes occurred, we used ImageJ software to measure the peroxisomal area and the peroxisomal number in plant co-expressing the p*BIGYIN::YFP::BIGYIN* and the peroxisomal (RFP::KSRM) marker and in plant expressing the peroxisomal RFP::KSRM, used as control of peroxisomal morphology (Fig. 28). We obtained that the number of peroxisomes was increased to about two fold compared with the control, and that the area of peroxisomes per cell was decreased to about two fold compared with the control. The total peroxisomal area did not show any difference between the transgenic and wild type plants.

All together, our results demonstrate that in pBIGYIN::YFP::BIGYIN plants the number of peroxisomes increase to about two fold compared with the control, while the total peroxisomal area per cell remain invariable.

Effects of an actin inhibitor on movement of organelles labelled with YFP::BIGYIN and bigyinules

In plants the intracellular movements of mitochondria, peroxisomes and chloroplasts are modulated by a microfilament-based cytoskeleton. We wondered whether the actin cytoskeleton played a role in the movements of organelles marked with YFP::BIGYIN and of bigyinules. To this aim, we treated YFP::BIGYIN seedlings with Lantruculin B (LatB), an inhibitor of actin polymerization. The treatment with Lat B inhibited the movement of the subcellular structures marked by YFP::BIGYIN. As result, the distribution of organelles and of tubules labelled with YFP::BIGYIN in the hypocotyl cells did not change over 40 seconds (Fig. 29B,C). To verify the inhibitor action, transgenic reporter plants were included in the analyses. Seedlings expressing mitochondrial COX::RFP or peroxisomal RFP::KSRM marker were treated with Lat B and we observed that mitochondria and peroxisomes were almost stationary (Fig. 30B,D). These data confirmed the treatment efficacy.

Taken together these results demonstrated that the actin-based cytoskeleton plays a role in the movement of bigyinules and of organelles marked with YFP::BIGYIN.

Effects of an actin inhibitor on movement of YFP::BIGYIN within organelle membranes

We wondered whether the YFP::BIGYIN fusion protein could also move within the organelle membranes that it marked. Fluorescence recovery after photobleaching (FRAP) was used to monitor the movement of YFP::BIGYIN between membranes of two connected chloroplasts in p*BIGYIN::YFP::BIGYIN* seedlings (Fig. 31). FRAP assay was performed on chloroplasts because their big dimension and their low dynamics guaranteed a perfect experimental condition. When chloroplast membranes, marked with YFP::BIGYIN, were bleached, fluorescence gradually recovered, at the expense of YFP fluorescence in the connected plastid (Fig. 31B). Recovery was complete within 50 seconds. As

control, an unbleached and unconnected plastid in the same observation area did not show loss fluorescence over time, indicating that no photobleaching was occurred. These data indicated that there was a trafficking of YFP::BIGYIN proteins among the outer membranes of connected chloroplasts.

Successively, we investigated whether the YFP::BIGYIN could move among membranes of chloroplasts, mitochondria and peroxisomes. To this aim, a single chloroplast not connected with other chloroplasts was bleached and then monitored over 150 seconds (Fig. 32). Interestingly, during the observation period many organelles labelled with YFP::BIGYIN were observed to go to the bleached chloroplast. As result, the bleached chloroplast regained completely the fluorescence within 94 seconds. As control, an unbleached and unconnected plastid in the same observation area showed a minimal loss of fluorescence after the 90 seconds as result of photobleaching. Since the bleached chloroplast was not connected with other chloroplasts, and many YFP::BIGYIN-marked organelles were observed approaching the bleached chloroplast during its fluorescence recovery, it could be possible that trafficking of YFP::BIGYIN proteins occurred among membranes of these different organelles.

To determine whether the movement of YFP::BIGYIN through the organelle membranes was dependent on actin microfilaments, photobleaching experiments were conducted after treatment with Lantruculin B (LatB) in p*BIGYIN::YFP::BIGYIN* seedlings. To monitor YFP::BIGYIN trafficking, FRAP experiment was performed on a chloroplast connected via bigyinules with another chloroplast (Fig.33). When chloroplast membranes, marked with YFP::BIGYIN, were bleached, no significant recovery of fluorescence was detected over time. In addition, no organelles labelled with YFP::BIYIN were observed to go to the bleached chloroplast. As control, an unbleached plastid in the same observation area did not show a significant loss of fluorescence indicating that no photobleaching was occurred during analysis. These results indicated that the trafficking of the YFP::BIGYIN proteins among the organelle membranes is dependent on actin-based cytoskeleton.

All together, our data demonstrate that a YFP::BIGYIN trafficking actin-dependent occurs among membranes of different organelles labelled with YFP::BIGYIN.

Effects of an ER-Golgi vesicle trafficking inhibitor on movement of YFP::BIGYIN

Next, we investigated whether the ER-Golgi vesicle trafficking was involved in YFP::BIGYIN-membrane trafficking. To this end, FRAP analyses were performed in *Arabidopsis* seedlings treated with BFA. This drug blocks the early stages of endocytosis, leading to the accumulation of recently endocytosed membranes and of the trans Golgi network (TGN) into the so-called BFA-compartments (Samaj et al., 2005). A single chloroplast, not connected with other chloroplasts, was bleached and then monitored over 65 seconds. During the observation period many dynamic organelle bodies labelled with YFP::BIGYIN were observed to go to the bleached chloroplast. As result, the bleached chloroplast regained completely the fluorescence within 27 seconds (Fig. 34). As control, an unbleached and unconnected plastid, in the same observation area, showed no loss of fluorescence over time indicating that no photobleaching was occurred.

Successively, the subcellular localization of BIGYIN with the Golgi apparatus was investigated through transient transfection of tobacco mesophyll cells mediated by agroinfiltration. As Golgi marker, the truncated form of soybean α1-2 mannosidase fused to the mCherry fluorescent protein (Nelson *et al.*, 2007) was used. The Golgi stacks appeared as perfectly round discs (in red in Fig. 35) and the YFP::BIGYIN (in green) was localized close but not to the Golgi membranes.

All together, these data indicate that YFP::BIGYIN movement is independent by ER-Golgi vesicle trafficking.

Characterization of T-DNA insertional mutant for *BIGYIN*

The role of BIGYIN in the fission of peroxisomes and mitochondria has been described by Zhang *et al.* (2008a), while its role on chloroplasts and on membranous tubules has not been yet investigated. We analyzed a T-DNA insertion mutant of *BIGYIN* (SALK_086794; Kanamycin^R; NASC stock centre),

previously used by Scott *et al.* (2006) and by Zhang and Hu (2008a). This mutant was reported as a T-DNA insertional line in the last exon and previous papers were shown that it had a *BIGYIN* expression virtually nil.

The seeds obtained from NASC stock centre was germinated on kanamycin selection media, and the presence of the T-DNA insertion within BIGYIN was confirmed by PCR analyses on genomic DNA. Since it was expected that the T-DNA insertion would lead to generation of a nonsense transcript, the effect of the insertion on *BIGYIN* transcript abundance was determined by analysis of the abundance of the mature *BIGYIN* mRNA in an homozygous T-DNA line. In detail, using RT-PCR analysis (Fig. 36), we did not detect an RT-PCR product extending from the start codon of *BIGYIN* to a fragment of its 3'-UTR, but we detected the *BIGYIN* mRNA extending from *BIGYIN* start codon to its codon stop.

We observed that the transcript levels of *BIGYIN* in the *bigyin* transgenic line was lower in the wild type plants, suggesting that the analyzed transgenic line was a knockdown mutant. To define the precise site of the T-DNA insertion, we sequenced the RT-PCR product previously obtained. Results of sequencing analysis demonstrated that the T-DNA was inserted 11 bp after the stop codon in the 3'-UTR, and not in the last exon as reported.

Since this *bigyin* mutant was reported to display an abnormal mitochondrial morphology, characterized by a large increase in the size of individual mitochondria per cell (Logan *et al.*, 2006), we investigated the mitochondrial morphology in the homozygous *bigyin* line and in wild type plants. Mitochondria were stained using the tetramethyl rhodamine methyl ester (TMRM) dye. As result, the mitochondria of *bigyin* plants did not show any difference in size when compared with mitochondria in wild type both in leaf epidermal cells (Fig. 36C,D) and in root leaves (Fig. 36 E,F).

Our results indicate that the bigyin mutant line is a knock-down mutant with the T-DNA insertion in the 3'-UTR. Moreover, in our analyses this bigyin mutant do not show any difference in mitochondrial morphology when compared with the wild type.

Analyses in BIGYIN protein structure of domains involved in multiple targeting

The C-terminal tail of BIGYIN protein has been reported to be important to target BIGYIN both to mitochondria and peroxisomes (Zhang *et al.*, 2008a). In our analyses, we demonstrated that BIGYIN was also localized to chloroplasts. In light of these findings, we dissected BIGYIN to define the domains crucial for the multiple targeting of BIGYIN protein. Initially, we wondered whether a short region located to the C-terminal end of BIGYIN was sufficient to target BIGYIN to mitochondria, peroxisomes and chloroplasts. In hFIS1 protein, an orthologue of BIGYIN in human, the transmembrane domain (TMD) along with a short basic segment at the C-terminal end is essential for mitochondrial and peroxisomal targeting (Koch *et al.*, 2005). An alignment with BIGYIN and hFIS1 proteins revealed strong conservation in their C-terminus, especially in the TMD (Fig. 1B). Basic residues (an arginine and two lysines) were also found to flank TMD at the 3' end of BIGYIN. Based on these findings, we analyzed if this short C-terminal tail, including the TMD and its 3' flanking sequence (the last 29 amino acids of BIGYIN, aa 141-170) and named BIGYIN^{TMD+CT}, was sufficient to multiple targeting (i.e. to mitochondria, peroxisomes and chloroplasts), when expressed under the control of p*BIGYIN* promoter.

Localization analysis of the C-terminal end of BIGYIN protein

To investigate the intracellular destiny of the truncated BIGYIN^{TMD+CT} , its CDS was fused to the C-termini of a *YFP* CDS and the resulting construct was cloned downstream the p*BIGYIN* promoter obtaining the p*BIGYIN::YFP::BIGYIN*$^{TMD+CT}$ construct. Then, this fusion construct was subcloned into the pGreenII binary vector (Hellens *et al*., 2000) for transient expression assays in *Arabidopsis* and tobacco leaf mesophyll cells mediated by agro-infiltration.

To analyze whether the C-terminal tail of BIGYIN was sufficient for targeting it to chloroplasts and mitochondria, we transiently co-transformed in *Arabidopsis* leaves the *YFP::BIGYIN*$^{TMD+CT}$ with the *COX4::mCherry* marker (yeast pre-sequence of the cytochrome c oxidase IV fused to the mCherry fluorescent marker; Nelson *et al.*, 2007). The chloroplasts, instead, were easily

distinguished by their dimension and by chlorophyll autofluorescence. As control, in the same analysis, *Arabidopsis* leaves were co-infiltrated also with *Agrobacterium* harbouring the pGreen-p*BIGYIN::YFP::BIGYIN* and the pBIN-*COX4::mCherry*. YFP::BIGYIN^{TMD+CT} was clearly localized to mitochondria and chloroplasts (Fig. 37A). These organelles were dispersed within the cytoplasm and no tubular protrusions labelled with YFP::BIGYIN^{TMD+CT} extending from the organelle membranes were detected. By contrast, *Arabidopsis* mesophyll cells co-transformed with the entire YFP::BIGYIN showed several bigyinules that connected chloroplasts and mitochondria marked with YFP::BIGYIN (Fig. 37B). These data indicated that the truncated BIGYIN^{TMD+CT} was sufficient for the mitochondrial and chloroplast targeting, but that it was not localized to the tubular protrusions extending from the organelle membranes. Comparing the chloroplast morphology in cells agro-infiltrated with the truncated BIGYIN^{TMD+CT} and with the BIGYIN protein, we observed that chloroplasts labelled with YFP:: BIGYIN^{TMD+CT} were round or in an 'attached' form (Fig.37A), as if two half semicircular chloroplasts were attached. On the contrary, the chloroplasts labelled with YFP::BIGYIN appeared in their typical oval form (Fig. 37B).

To further investigate the chloroplast morphology in chloroplasts labelled with YFP::BIGYIN^{TMD+CT}, we transient transformed also tobacco mesophyll cells. As shown in Fig. 38A, YFP::BIGYIN^{TMD+CT} was localized to chloroplasts and to other organelles, that could be mitochondria and peroxisomes. On chloroplast membranes, the truncated form of BIGYIN produced striated features that appeared as single ring structures located to the larger diameter of single round chloroplasts or as multiple rings. No bigyinules were observed. As control, in the same analysis, tobacco mesophyll cells were also infiltrated with the pGreen-p*BIGYIN::YFP::BIGYIN*. The YFP::BIGYIN fusion protein localized, as expected, to chloroplasts and small organelles presumably mitochondria and peroxisomes (Fig. 38B). Moreover YFP::BIGYIN did not produce on chloroplast membranes any striated features previously described in the experiments performed with the truncated BIGYIN form, and bigyinules were detected. These results confirmed that the expression of the truncated BIGYIN^{TMD+CT} leaded to aberrant morphology of chloroplasts and that the truncated BIGYIN^{TMD+CT} was not localized to the tubular protrusions extending from organelle membranes.

Successively, we investigated if the truncated BIGYIN^{TMD+CT} was sufficient for targeting to peroxisomes. We transiently expressed *YFP::BIGYIN^{TMD+CT}* in *Arabidopsis* RFP::KSRM mesophyll cells by agro-infiltration assay. As control, in the same analysis *Arabidopsis* leaves were infiltrated also with *Agrobacterium* harbouring the pGreen-p*BIGYIN::YFP::BIGYIN*. As result, YFP::BIGYIN^{TMD+CT} was localized to peroxisomes (Fig. 39A). These organelles were dispersed within the cytoplasm and no tubular protrusions labelled with YFP::BIGYIN^{TMD+CT} extending from peroxisomal membranes were detected. By contrast, mesophyll cells, co-transformed with YFP::BIGYIN and peroxisomal marker, showed thin tubules labelled with BIGYIN that linked two peroxisomes (arrow in Fig. 39B). Time-lapse analyses were performed in *Arabidopsis* mesophyll cell co-expressing *YFP::BIGYIN* and *RFP::KSRM*. Dynamic tubular protrusions extending from peroxisomes were detected by means peroxisomal marker, but they were not labelled with the truncated YFP::BIGYIN^{TMD+CT} (Fig. 39C), that indeed was only localized to peroxisomes.

We demonstrated that the last 29 amino acid of the BIGYIN protein were not sufficient for targeting it to tubular protrusions and we also described that the presence of the truncated BIGYIN was associated with an aberrant chloroplast morphology. To further analyze these findings, we stable introduced in the *Arabidopsis bigyin* knockdown mutant background the YFP::BIGYIN^{TMD+CT} under the control of the p*BIGYIN* promoter (p*BIGYIN::YFP::BIGYIN^{TMD+CT}*). As control, we obtained also *bigyin* knockdown mutant plants carrying the p*BIGYIN::YFP::BIGYIN* construct.

To investigate the subcellular localization of the truncated BIGYIN^{TMD+CT} and of BIGYIN to chloroplasts, we performed confocal microscope analyses in leaf mesophyll cells of seedlings. Chlorophyll autofluorescence was used to detect chloroplasts (Fig. 40). YFP::BIGYIN^{TMD+CT} fusion protein was clearly localized to the outer membranes of chloroplasts and to small organelles, likely mitochondria and peroxisomes, while no tubular protrusions, marked with the truncated BIGYIN^{TMD+CT}, were detected. The chloroplasts were round or in an 'attached' form, as if semicircular chloroplasts were attached. In both cases, the YFP::BIGYIN^{TMD+CT} fluorescent signal produced, on the chloroplasts surfaces,

striated features that appeared as ring structures localized to the larger diameter of the round chloroplasts (arrow in Fig. 40A) or to the membranes between the attached semicircular chloroplasts (asterisk in Fig. 40A). The particular localization pattern of these ring structures to the larger diameter and between the attached semicircular chloroplasts suggested that YFP::BIGYIN^{TMD+CT} marked the ring structures encircling the division sites of chloroplasts (Miyagishima *et al.*, 2006). By contrast, the entire YFP::BIGYIN showed the same pattern previously detailed described: BIGYIN was localized to chloroplasts and to small organelles (Fig 40B). Chloroplasts were round or oval, and the attached semicircular chloroplasts were not often observed. YFP::BIGYIN did not show any ring features on chloroplast outer membranes. In addition, several protrusions labelled with BIGYIN were observed extending from chloroplasts and connecting several organelles among them.

These results indicate that the last 29 amino acids of BIGYIN are sufficient to target BIGYIN to mitochondria, chloroplasts and peroxisomes, but this C-terminal tail is not sufficient to target BIGYIN to the tubular protrusions extending from organelle membranes. Moreover, the expression of this truncated form of BIGYIN protein provokes an aberrant chloroplasts morphology.

Localization analysis of the N-terminal tail of BIGYIN protein

Successively, we analyzed the subcellular localization of the N-terminal tail of BIGYIN protein to verify if in this tail any targeting sequence to specific organelles was present. We considered the first 1-139 amino acids including the TPR-like domain and we termed this fragment BIGYIN^{NT+TPR}. We fused the *BIGYIN^{NT+TPR}* CDS to the *YFP* downstream the p*BIGYIN* promoter. We subcloned the p*BIGYIN::YFP:: BIGYIN^{NT+TPR}* construct into a pGreenII binary vector (Hellens *et al*., 2000), and we used it for transient expression assays mediated by *Agrobacterium* in tobacco mesophyll cells. YFP:: BIGYIN^{NT+TPR} was localized to the cytosol and nuclei, identified by the presence of the nucleolus (Fig. 41A). As control, in the same analysis, tobacco mesophyll cells were agro-infiltrated also with the YFP::BIGYIN protein (Fig. 41B). YFP::BIGYIN was localized to chloroplasts and to other small organelles (presumably mitochondria

and peroxisomes). Moreover, we detected YFP::BIGYIN fluorescence also on subcellular structures very similar to the nucleus. To further investigate the subcellular localization of BIGYIN to the nucleus, we co-infiltrated tobacco leaves with YFP::BIGYIN and with a cytosolic RFP (Campbell *et al.*, 2002) able to diffuse spontaneously inside the nucleus. The YFP::BIGYIN was localized mainly to chloroplasts and to tubular protrusions, that were often arranged in a circular network around and not inside the nucleus (Fig. 41C).

To further investigate the subcellular localization of the BIGYIN^{NT+TPR}, we stable introduced, into the *Arabidopsis bigyin* knockdown mutant background, the YFP::BIGYIN^{NT+TPR} under the control of the p*BIGYIN* promoter (p*BIGYIN::*YFP:: BIGYIN^{NT+TPR}) and we performed confocal microscope analyses in leaf mesophyll cells of seedlings (**Fig. 42A**). The BIGYIN^{NT+TPR} fusion protein was localized to the cytosol, to the nucleus and it seemed to mark also the plasma membranes. To verify if this subcellular localization patter was characteristic of a cytosolic protein, we performed confocal microscope analyses in leaves of transgenic plants expressing a cytosolic YFP (Von Arnim *et al.*, 1998) (Fig. 42B). The cytosolic YFP marked the cytosol, the nucleus and also the plasma membranes, showing the same subcellular localization pattern of the YFP::BIGYIN^{TMD+CT} (Fig. 49B)

All together, our results indicated that the N-terminal tail of the BIGYIN protein did not show any targeting sequence to specific organelles.

DISCUSSION

BIGYIN is a tail anchored protein belonging to the FIS1-type proteins

The FISSION1 (FIS1)-type proteins are evolutionarily conserved integral membrane proteins involved in maintaining the morphology of mitochondria and peroxisomes in mammals (James *et al.*, 2003), yeast (Zhang, 2007), and plants (Zhang and Hu, 2008b). The *Arabidopsis thaliana* genome contains two closely related FIS1-type proteins, orthologs of yeast FIS1 and human hFis1: BIGYIN (previously named FIS1A, At3g57090) and FIS1B (At5g12390).

Analyzing published microarray data (http://bbc.botany.utoronto.ca/), we observe that that both *BIGYIN* and *FIS1B* are constitutively expressed in *Arabidopsis*. However, *FIS1B* is especially expressed only in mature pollen, while the expression level of *BIGYIN* is higher than that of *FISB* in most of tissues.

In silico analyses show that BIGYIN and FIS1B, as all FIS1-type proteins, are characterized by a tetratricopeptide (TPR)-like domain, predicted to be exposed to cytosol, and by a single transmembrane domain located to the C-terminal end of the protein. Based on this topology, we can considered these proteins as members of tail-anchored (TA; N_{out}-C_{in}) family of membrane proteins (Borghese *et al.*, 2007).

Expression and localization pattern of BIGYIN in *Arabidopsis*

In this study, we have shown that p*BIGYIN* promoter is constitutively active in all plant developmental stages from germinating seeds to mature plants and in all tissues (leaves, stems and roots). Our data are in agreement with microarray data already published (http://bbc.botany.utoronto.ca/). Yet, we have reported that BIGYIN protein is constitutively present in all developmental stages and in all tissues. In addition, we have shown that tissues where plant growth takes place (i.e. leaf teeth, leaf primordia, developing stems, nodes, flower buds, lateral root primordia and root tips) are characterized by the highest p*BIGYIN* promoter activity and by the highest presence of BIGYIN protein. By contrast, p*BIGYIN* promoter activity and BIGYIN protein are low detected in fully expanded leaves or in mature stems.

Since BIGYIN is involved in mitochondrial and peroxisomal fission events, it is expected that BIGYIN is more abundant in dividing cell, where the mitochondrial and peroxisomal division processes are highly request to maintain the organelle number during cells cycle. However, mitochondrial and peroxisomal fission events take place ubiquitously within a single cell, because they are important for keeping the organelle morphology (shape and size). The cell, therefore, presumptively necessitate ubiquitously of proteins, like BIGYIN, involved in organelle fission machinery, and this fits with the constitutively presence of BIGYIN in all tissues in all developmental stages.

BIGYIN localizes to mitochondria, peroxisomes, chloroplasts and to membranous protrusions extending from these organelles

Interestingly, we have reported that, when BIGYIN is ectopically overexpressed by the cauliflower mosaic virus 35S (CaMV 35S) promoter, it localizes to mitochondria, peroxisomes and also to chloroplasts (Chapter 2). In the light of these findings, we have investigated whether these multiple subcellular localization patterns are maintained also when *BIGYIN* is expressed under the control of its own promoter. To this aim, we have generated and selected several *Arabidopsis* transgenic lines, stable co-transformed with the p*BIGYIN::YFP::BIGYIN* (i.e. the *YFP::BIGYIN* fused downstream the p*BIGYIN* promoter) and different organelle markers. In these transgenic plants, we have confirmed that BIGYIN localizes to the outer membranes of mitochondria and chloroplasts and to the membranes of peroxisomes. The subcellular localization of BIGYIN to mitochondria and peroxisomes is consistent with the role of BIGYIN as a fission protein involved in mitochondrial and peroxisomal fission events (Zhang and Hu, 2008b). By contrast, there are no published data concerning the subcellular localization of BIGYIN to chloroplasts, probably because mesophyll cells, where chloroplasts are present, have not been yet investigated. However, our subcellular localization of BIGYIN to chloroplasts is in agreement with the identification of BIGYIN protein in chloroplast proteome experiments (Zybailov *et al.*, 2008).

We have also reported that BIGYIN localizes to tubular protrusions extending from the outer membranes of mitochondria and chloroplasts and from

the membranes of peroxisomes (termed matrixules, stromules and peroxules, respectively). The subcellular localization of BIGYIN to matrixules and peroxules has not be previously reported, while we have already shown the subcellular localization of BIGYIN to stromules in our previous results (Chapter 2).

These multiple subcellular localization pattern have been described in all analyzed tissues (leaves mesophyll cells, leaves epidermal cells, hypocotyls and roots), demonstrating that the localization of BIGYIN is not dependent on cell type or on cell function. Instead, Maggio *et al.* (2007) reported that another tail anchored protein, termed cyt b5 isoform, localized promiscuously to mitochondria and chloroplasts, with a preference for the chloroplasts, demonstrating competition between the two organelles in capturing this protein. Our data have demonstrated that BIGYIN is a tail anchored protein targeted at the same time to peroxisomes, mitochondria and chloroplasts too, indicating that this protein has multiple targeting signals to be localized to different organelles in the same cell at the same time.

C-terminal of BIGYIN is necessary and sufficient for BIGYIN targeting

In order to determine what specific signals in BIGYIN protein are recognized by the different targeting machinery of mitochondria, peroxisomes and chloroplasts, we dissected BIGYIN in truncated forms and analyzed their subcellular localization. We have shown that the N-terminal end of BIGYIN (139 amino acids, i.e. *YFP::BIGYIN*$^{NT+TPR}$) localized the protein to the cytosol and the nucleus, indicating that this part is not involved in targeting BIGYIN to mitochondria, peroxisomes and chloroplasts. These findings are in agreement with the lacking of N-terminal signal peptide in TA-proteins in other organisms (Borghese *et al.*, 2003).

Similarly, we have investigated whether the targeting sequence was located to the C-terminal end of BIGYIN, by analyzing the subcellular localization of the last 29 amino acids (a region that includes the hydrophobic transmembrane domain and its 3' flanking sequence, i.e. *YFP::BIGYIN*$^{TMD+CT}$). Our results demonstrate that the C-terminal end is necessary and sufficient to target BIGYIN to mitochondria, peroxisomes and chloroplasts, accordingly with the key role played by the hydrophobic anchor in targeting of TA-proteins in other

system (Borghese *et al.*, 2003). By contrast, Zhang and Hu (2008b) have described that the C-terminal end is targeted to the nucleus and to the plasma membranes in tobacco leaf agro-infiltrated. We think that the mistargeting of their truncated BIGYIN could depend on its over expression due to a fusion protein driven by the constitutive promoter CaMV 35S. In our system, instead, where p*BIGYIN* promoter was used, the C-terminal end of BIGYIN clearly and specifically localized to mitochondria, peroxisomes and chloroplasts.

On the other hand, we have shown that the C-terminal end of BIGYIN is not sufficient for targeting the protein to the tubular protrusions extending from the membranes of mitochondria, chloroplasts and peroxisomes. The entire protein is therefore necessary for subcellular localization of BIGYIN to tubular structures.

The mode of insertion of BIGYIN and, more in general, of TA-proteins into different organelle membranes is mandatory post transitional, given that their hydrophobic domains emerge from the ribosome only after their translation is entirely accomplished. However, the molecular machinery involved in interpreting the targeting information has not yet been identified. So far, we have demonstrated, using brefeldin A inhibitor, that BIGYIN is located to the membranes of organelles that are not part of the secretory system. BIGYIN is therefore a TA-protein that can reach the membranes of mitochondria, chloroplasts and peroxisomes directly from the cytosol, without passing through the ER. Proteins belonging to the TA-family with a similar post transcriptional control have been described by **Borghese *et al.* (2003**) and Pedrazzini (2009) in animal and plant cells.

Anti-BIGYIN-antibody is specific for BIGYIN

So far, we have shown that the anti-BIGYIN-antibody is specific for BIGYIN, opening the possibility to validate our subcellular localization results by means of immunogold electron microscopy assay and immunoblot assay of protein extracts enriched in specific subcellular compartments. Yet, we have demonstrated, through immunoblot assay, that in transgenic plants, stable transformed with p*BIGYIN::YFP::BIGYIN*, the YFP::BIGYIN fusion protein is more abundant than the endogenous BIGYIN protein, although the fusion protein is driven by the BIGYIN promoter.

We have demonstrated that in these transgenic plants, the number of peroxisomes per cells increases to about two fold compared with the wild type, suggesting that an increase in peroxisomal division may occurs. This data are in agreement with previously published data by Zhang and Hu (2008b) that reported that in BIGYIN overexpressing plants (i.e. 35S::BIGYIN) the number of peroxisomes increases to about three fold compared with the wild type. Indeed, in our plants the phenotype was definitely mild compared with the one reported in BIGYIN overexpressing plants (Zhang and Hu (2008b). Moreover, we have shown that total peroxisomal area per cell do not show any difference between the transgenic and wild type plants, indicating that the BIGYIN is not necessary for the maintenance of total peroxisomal volume.

BIGYIN unveils a dynamic network of organelles and tubular protrusions

On our knowledge, BIGYIN is the unique known protein that shows a multiple subcellular localization pattern on the membranes of these different organelles (mitochondria, chloroplast and peroxisomes), and, BIGYIN is therefore the first transmembrane protein that localizes the same time to the different tubular structures extending from these organelle membranes. Since the terms ‘matrixules’, ‘peroxules’ and ‘stromules’ were originally coined to indicate the ‘matrix-filled tubules’, the ‘peroxisomal-filled tubules’, and the ‘stroma-filled tubules’, we have termed ‘bigyinules’ the tubular membranous structures labelled with YFP::BIGYIN and extending from mitochondria, peroxisomes and chloroplasts. The term ‘bigyinules’, therefore, includes all organelle tubules (i.e. matrixules, peroxules and stromules). The new term is necessary to clearly indicate that BIGYIN marked the membranes and not the inner space enclosed by the membranes.

Although several ultrastructural studies in plant cells have described that chloroplasts, mitochondria and peroxisomes are often very close located, only very few electron micrographs document physical continuity between their membranes both trough direct membrane-membrane contact or through membranous tubular protrusions (Crotty and Ledbetter, 1973). The paucity of electron micrograph of these tubules is due by the difficulty to preserve these

protrusions during the standard fixation required by electron microscopy (Köhler and Hanson, 2000). Our transgenic plants expressing BIGYIN are significant because allow to analyze at the same time different organelles and especially the tubular protrusions that extend from different organelle membranes, observing the dynamics and behaviour of these interesting interconnected tubules.

Mitochondria, chloroplasts and peroxisomes could be close located or spread randomly throughout the cytoplasm. Interestingly, even when mitochondria, chloroplasts or peroxisomes are spread within the cell, the presence of bigyinules could allow interconnections among them: several bigyinules could protrude from chloroplasts, mitochondria and peroxisomes forming a complex and highly dynamic network of tubules. A similar motility have been described for stromules (Gunning, 2005) and peroxules (Sincalir *et al.*, 2009), but not for matrixules. How is it this motility achieved? We have demonstrated that the actin-based cytoskeleton plays a role in movement of bigyinules and of mitochondria, chloroplasts and peroxisomes marked with YFP::BIGYIN. This is in agreement with previous studies on effect of actin-polymerization inhibitors on movements of mitochondria, of peroxisomes, chloroplasts and stromules (Gestel *et al.*, 2002; Jedd and Chua, 2002; Kandesamy and Meagher, 1999).

Moreover, we have also shown a trafficking of BIGYIN through the membranes of connected organelles (for example two chloroplasts, Fig. 31) or through the membranes un-connected organelles (Fig. 32). These data support the existence of physical inter-organellar connections and of a trafficking of proteins among physical un-connected organelles. There are few published data concerning physical inter-organellar interactions, although their existence has been often proposed in the light of several metabolic and functional interactions among organelles (i.e. chloroplast, mitochondria and peroxisomes, for example during respiration). The existence of a trafficking of molecules for example between mitochondria and chloroplasts has been proposed in the literature by Kwok and Hanson (2004a-b) and supported by Jouhet *et al.* (2004), when they demonstrated the transfer of digalactosyldiacylglycerol glycolipids between plastids and mitochondria. Moreover, the authors suggested that this transfer depended upon contacts between plastids and mitochondria or upon vesicles without the involvement of the endomembrane system. Similarly, we have

demonstrated that endomembrane system is not involved in the trafficking of structures labelled with BIGYIN, and we have also shown that free vesicle-like structures labelled with BIGYIN can separate from bigyinules or organelles (Fig. 22, 26C). Vesicle-structures originated from stromules and detached from by stromules have been also described by Pyke and Howells (2002). Authors suggested that these vesicle-structures could be an export mechanism for the secretion of plastid products. In the light of these findings, we can suggest that the vesicle-structures labelled with BIGYIN could be an export mechanism for the secretion of organelle product.

Moreover, we have shown that chloroplasts and bigyinules could be close located to the surface of nuclei suggesting that this close vicinity may facilitate the exchange of molecules and signal between chloroplasts and nuclei. This data are in agreement with Kwok and Hanson (2004b), that proposed a similar role for stromules located near nuclei.

BIGYIN may play a role also in chloroplast division

BIGYIN has been demonstrated to be involved in mitochondrial and peroxisomal division (Zhang and Hu, 2008a). By contrast its role(s) on chloroplasts and on membranous tubules has not yet been analyzed. In order to further investigate the function(s) played by BIGYIN on chloroplasts and on tubular protrusions, we have analyzed an *Arabidopsis* T-DNA insertional line for BIGYIN, reported to be a knock-out mutant and having a T-DNA insertion in the last exon (Scott *et al.*, 2006; Zhang *et al.*, 2008a). We have demonstrated this line as a knock down mutant with the T-DNA insertion in the 3'-UTR. In addition, we have not observed any difference in mitochondrial morphology between *bigyin* mutant and wild type plants, as instead reported by previous paper (Scott and Logan, 2006; Zhang and Hu, 2008a). Based on these findings, we could not use this mutant for our analyses.

In the light of the fission role of BIGYIN in mitochondria and in peroxisomes, we have investigated the subcellular localization of BIGYIN during chloroplast division in developing tissues (flower buds and young hypocotyls), where chloroplast fission highly occurs (Miyagishima *et al.*, 2006). We have shown that BIGYIN localizes to the outer membranes of chloroplasts and around

the isthmus in formation. Interestingly, BIGYIN localizes also to the constriction sites between two chloroplasts in division, when organelles are in the typical 'dumbbell'-form, step preceding the last phase of chloroplast fission (Aldridge *et al.*, 2005). Moreover, we have reported that transgenic plants stably expressing a truncated form of BIGYIN (i.e. YFP::BIGYIN^{TMD+CT}, completely deleted in the cytosolic tail involved in protein-protein interactions, as demonstrated in Chapter 2), shows a particular chloroplast morphology and a very interesting subcellular localization pattern on chloroplast membranes. In these transgenic plants, we have shown that chloroplasts could be round or constricted in the 'dumbbell'-form, usually observed when chloroplast fission takes place (Aldridge *et al.*, 2005), although we performed these analyses on fully expanded leaves, where chloroplast division does not usually occur. Moreover, the truncated BIGYIN creates, on the chloroplast surfaces, striated features that appear to mark the ring structures encircling the division sites of chloroplasts. By contrast, transgenic plants expressing the entire BIGYIN shows a normal chloroplast morphology (typically oval or round in fully expanded leaves), and BIGYIN is located to the chloroplast surfaces without create any striated features. These findings suggested that the particular chloroplast morphology, observed in plants expressing the truncated *BIGYIN*, might be the result of a dominant-negative effect of the deleted and un-functional protein. Similar constricted 'dumbbell'-form chloroplasts have been reported in *Arabidopsis* mutant with defects in chloroplast division (Miyagishima *et al.*, 2006). In the light of these findings, we suggest a possible role of BIGYIN in chloroplast division. BIGYIN proteins, therefore, is an *Arabidopsis* Fission1-type protein that is involved in mitochondrial and peroxisomal fission, as reported by Zhang and Hu (2008b), and that could also play a role in chloroplasts division.

MATERIAL AND METHODS

Plant materials and growth condition

All the *Arabidopsis thaliana* plants for this study were in Columbia (Col-0) background. Different *Arabidopsis* transgenic lines were used: plants overexpressing red fluorescent protein (RFP) targeted to mitochondria by *Arabidopsis* cytocrome c oxidase-releated (COX) pre-sequence (35S::COX::RFP), plants overexpressing RFP targeted to peroxisomes by sequence tag KSRM fused downstream *RFP* coding sequence (35S::RFP::KSMR), and plants transformed with the cytosolic YFP (35S::YFP) or cytosolic RFP (35S::RFP). These transgenic lines were generated in our laboratory.

Arabidopsis thaliana, Columbia ecotype, and *Nicotiana tabacum* plants were incubated in an environmentally-controlled growth chamber with a long photoperiod (16 hr light and 8 hr dark) at 25 ± 1°C, and a photosynthetic photon flux of 35 μmol m^{-2} s^{-1} Osram cool-white 18 W fluorescent lamps. When *in vitro* growth of *Arabidopsis* plants was required, *Arabidopsis* seeds were sterilized using the vapour-phase surface-sterilization. Seeds and a beaker containing 100 ml bleach were placed in a dessicator jar. 3 ml concentrate HCl was added to the bleach and then immediately the jar was sealed to allow sterilization by chlorine fumes to proceed for 5-6 hours. Then the seed were sown on half-strength Murashige and Skoog (MS) medium (Sigma).

DNA constructs

All the cloned plasmids were confirmed by sequencing.

pBIGYIN::GUS constructs and generation of transgenic lines

The *GUS* (*β-glucuronidase*)-coding sequence was fused to the *BIGYIN* promoter (base pair -862 to -1). The 862 bp promoter fragment was amplified by PCR using genomic DNA extracted from *Arabidopsis* leaves as template. The pair of primers, both carrying an *EcoRI* restriction site, were as follows: forward primer

5’-CATGGAATTCCTTTCGAGGCTCACCTCAAC-3 and reverse primer 5’-CATGGAATTCTGAAGGCGATTTTGAGCTTTGA-3’). After digestion, the promoter was cloned upstream of the *GUS* coding region, into a modified pGreen0029 binary vector (Kamaycin^{R}; Hellens *et al*., 2000), where the GUS coding sequence, fused with the *nos* terminator, was previously inserted in the polylinker between *KpnI-SacI* restriction sites. The pGreen-p*BIGYIN::GUS* construct was transferred into GV3101-p*Soup* Agrobacterium strain (Hellens *et al*., 2000) and *Arabidopsis* plants were transformed by floral dip method (Clough and Bent, 1998) and screened on half-strength MS agar medium containing 50 mgL^{-1} kanamycin. The GUS-staining analyses were performed on T_2 plants. No one of the transgenic lines selected, with the different constructs, showed phenotypic differences or abnormalities in our standard growth conditions.

pBIGYIN::YFP::BIGYIN, pBIGYIN::YFP::BIGYIN^{TMD+CT} and p*BIGYIN::YFP::BIGYIN^{NT+TPR} constructs and generation of the Arabidopsis transgenic lines*

The *Arabidopsis BIGYIN* coding sequence was first amplified by PCR from *Arabidopsis* cDNA with proofreading PCR enzymes (Phusion High Fidelity DNA polymerase [Finnzymes]) and then cloned into the vector of interest.

To obtain the *BIGYIN^{TMD+CT}*, the C-terminal tail of *BIGYIN* coding sequence was amplified (Primer For: 5’-CATGGAGCTCAAGGTGTTATAGGGATAGGGATCACG-3’; Rev: 5’-CATGGGTACCTCATTTCTTGCGAGACATCG-3’), corresponding to the transmembrane domain and the adjacent C-terminal tail (421-510 bp, corresponding to the last 29 amino acids of BIGYIN, aa 141-170).

To obtain the *BIGYIN^{NT+TPR}*, the N-terminal tail of BIGYIN coding sequence was amplified (Primer For: 5’-catgGAGCTCAAATGGATGCTAAGATCGGAC-3’; Rev: 5’-CATGggtaccTCACTTTGTGATTTTGTCTTCGATGGTC-3’), corresponding to the N-terminal end and of TPR-like domain(417 bp, corresponding to the first 139 amino acids of BIGYIN, aa 1-139). For the expression of BIGYIN, BIGYIN^{TMD+CT} BIGYIN^{NT+TPR} in plants, the pGreen0179 (hygromycin^{R}; Hellens *et al.*, 2000) binary vector was used.

p*BIGYIN::YFP::BIGYIN* construct contained the promoter region of *BIGYIN* (862 bp upstream region, base pair -862 to -1) fused to *YFP::BIGYIN* coding sequence, and the cauliflower mosaic virus 35S terminator. The promoter region was amplified by PCR using specific 5' and 3' primers (forward primers 5'-CATGGAATTCCTTTCGAGGCTCACCTCAAC-3 and reverse primer 5'-CATGGAATTCTGAAGGCGATTTTGAGCTTTGA-3') where the *EcoRI/EcoRI* sites were introduced. The p*BIGYIN* amplicon was then digested with *EcoRI* and cloned into the pGreen0179, obtaining the pGreen0179-p*BIGYIN* vector. At the same time the *YFP* coding sequence was subcloned from the pAVA554-35S::YFP plasmid provided by Prof. Albrecht von Arnim (von Arnim et al., 1998) to the pSAT1-35S::nVenus vector (stock number E3228, Lee *et al.*, 2008) by replacing the *nVenus* cDNA sequence digesting with *NCoI/Bgl*I enzymes. The BIGYIN PCR product was amplified using primers where the *SacI/KpnI* sites were introduced (Primer For: 5'-catgGAGCTCAAATGGATGCTAAGATCGGAC-3'; Rev: 5'- CATGggtaccTCATTTCTTGCGAGACATCG-3'). Amplicons were then digested with SacI/KpnI and cloned into the pSAT1-35S::YFP vector. The pSAT1-35S::YFP::BIGYIN fusion construct was then subcloned with EcoRV/NotI restriction sites into the pGreen0179-p*BIGYIN* digested with SmaI/NotI to obtain the pGreen0179-p*BIGYIN::YFP::BIGYIN* binary vector. A similar strategy was used to obtain the Green0179-p*BIGYIN:YFP::BIGYIN*$^{TMD+CT}$ and Green0179-p*BIGYIN:YFP::BIGYIN*$^{NT+TPR}$ binary vectors. These binary vectors were introduced into *Agrobacterium. tumefaciens* strain GV3101 (Labereke *et al.*, 1974) and transferred to *A. thaliana* wild type and *bigyin* mutant plants by floral dip method (Clough and Bent, 1998), in order to obtained plants stable transformed with the *pBIGYIN::YFP::BIGYIN*, p*BIGYIN:YFP::BIGYIN*$^{TMD+CT}$ or p*BIGYIN:YFP::BIGYIN*$^{NT+TPR}$. Homozygous T_2-indipendent lines were then selected by segregation analysis on MS agar plates containing 15 mgL^{-1} hygromycin. No one of the transgenic lines selected, with the different constructs, showed phenotypic differences or abnormalities in our standard growth conditions.

Generation of the Arabidopsis transgenic lines co-transformed with pBIGYIN::YFP::BIGYIN and p35S::COX::RFP, or pBIGYIN::YFP::BIGYIN and p35S::RFP::KSRM

The transgenic *Arabidopsis* plants stable co-transformed with *pBIGYIN::YFP::BIGYIN* and p*35S::COX::RFP*, or p*BIGYIN::YFP::BIGYIN* and p*35S::RFP::KSRM* were obtained crossing their mature flowers: a recipient flower was prepared removing all the flower parts with exception of the ovary and then this prepared ovary was brushed by the pollen of stamens of fully mature flowers of the plant of interest. Siliques obtained were sown and seedlings were selected by fluorescent signals.

Organelle marker used in tansient expression experiments

For the localization of the Golgi apparatus, the cytoplasmatic tail and transmembrane domain (first 49 amino acids) of soybean α-1,2-mannosidase-I fused to the mCherry marker (Nelson *et al.*, 2007) were used. For the localization of mitochondria, the first 29 amino acids of yeast (Saccharomyces *cerevisiae*) cytochrome c oxidase IV fused to the mCherry marker (Nelson *et al.*, 2007) were used.

Semi-quantitative RT-PCR analysis in p*BIGYIN::GUS* plants

Total RNA was extracted from leaves of 3-week-old plants as described by Formentin *et al.* (2004.)

After DNAse I treatment (Ambion Ltd, UK), first strand synthesis and PCR were carried out starting from 1 μg of total RNA, according to the manufacturer's instructions (M-MLV Reverse Transcriptase, Promega). After first strand cDNA synthesis, samples were diluted 5 times and used as templates for semi-quantitative RT-PCR.

RT-PCR analyses were performed to compare the transcript levels between β-*glucuronidase* and *BIGYIN* in each of the four transgenic p*BIGYIN::GUS* lines. Specific primers were design to amplified a fragment of 575 bp into the *GUS* and of 511 bp into *BIGYIN*.

RT-PCR reactions were performed using GoTaq® DNA Polymerase (Promega), in a total reaction volume of 50μL according to manufacturer's recommendations

containing 5μL of cDNA. PCR amplification cycle was performed with an initial denaturation step at 94°C for 2min, followed by 34 cycles (94°C for 30s; 61°C for 20s; 72°C for 40s), and finally with an elongation step at 72°C for 5min. The number of cycles was determined as described in the QuantumRNA protocol. PCR products were observed in 1% agarose gel electrophoresis, stained with ethidium bromide. Ultra-pure water was used as the negative template control.

β -*glucuronidase* (GUS) histochemical analysis

GUS histochemical staining was performed at four developmental stages: germinating seeds (32 h after imbibition), 5-day-old seedlings (cotyledons open), 7-day-old seedlings (first leaves developing), and flowering mature plants.

Samples were analysed for GUS activity following the protocol described by Jefferson et al. (1987). The samples were vacuum infiltrated for 30 min in the following solutions: 2 mM X-gluc, 0.5% Triton X-100, 0.1% Tween 20, 0.5 mM $K_3Fe(CN)6$, 0.5 mM $K_4Fe(CN)_6\_3H_2O$, 10 mM Na_2EDTA and 50 mM sodium phosphate buffer, pH 7.0, and then incubated at 37°C for 16 h. After staining, samples were cleared by several washes with methanol/acetic acid (3:1 v/v) solution and kept at 4°C in 70% ethanol.

Inhibitor treatment

For Brefeldin A treatment, we used a 50 mM stock solution (made in dimethyl sulfoxide) further diluted in distilled water to achieve an effective working solution of 50 μM before submerge the seedlings of 7-day old for 2 h (Geldner *et al*., 2001). Lantruculin B was used at 500 nM for 0.5 h.

Antibody

Polyclonal antibodies against BIGYIN were designed in our laboratory and produced by BioGenes GmbH (Berlin, Germany). In detail, polyclonal antibody was raised in rabbits against an antigenic peptide corresponding to amino acids 33-47 of the BIGYIN protein.

Protein extraction and Western blot analysis

0,1 g of fresh leaves were grinded with a mortar and pestle and 2 ml Elution Buffer (320 mM Sucrose, 50 mM Tris-HCl pH 7.4, 1 mM EDTA, 10 mM DTT, 1,17 μM Leupeptin, 1,75 μM Pepstatin, 1 μM PMSF), centrifugate for 15 min at 500 xg at 4 degrees Celsius. Supernatant was kept and centrifuged again for 20 min at xg at 4 degrees Celsius. The surnatant contained the total protein extracts. Proteins (25 mg) were separated on 10% polyacrylamide gels (Laemmli, 1970) and transferred to nitrocellulose membranes (Sartorius, Germany). Membranes were blocked and incubated with the affinity-purified anti-BIGYIN antibody diluted 1:500, followed by incubation with an anti-rabbit antibody conjugated to alkaline phosphatase (SantaCruz, USA) diluted 1:10.000. After washing, blots were visualised using the BCIP/NBT (Sigma-Aldrich, Italy) reagent system.

BIGYIN insertion mutant

Arabidopsis thaliana T-DNA insertion line (SALK_086794, Kan^R) of the BIGYIN gene (At4g25000) was obtained from the Salk Institute Genomic Analyses Laboratory. To identify individuals homozygous for the T-DNA insertion, genomic DNA was obtained from kanamycin-resistant seedlings and subjected to PCR-based genotyping using the specific primers designed according to the related data from Signal (http://signal.salk.edu/isectprimers.html). PCR reactions were performed using the GoTaq® DNA Polymerase (Promega), in a total reaction volume of 50μL according to manufacturer's recommendations containing 2μL of genomic DNA. PCR amplification cycle was performed with an initial denaturation step at 94°C for 3min, followed by 35 cycles (94°C for 45s; 56°C for 45s; 72°C for 60s), and finally with an elongation step at 72°C for 5min. PCR products were observed in 1% agarose gel electrophoresis, stained with ethidium bromide. Ultra-pure water was used as the negative template control. Other primers were designed to identify the precise site of the T-DNA insertion and to sequence the PCR product obtained. The sequencing was performed by the BMR genomics (Padova).

Analysis of mitochondria

The tetramethylrhodamine methyl ester dye (TMRM, Molecular Probes, Leiden, the Netherlands), a mitochondrial membrane potential sensor, was used for visualizing mitochondria in seedlings of *bigyin* mutants and wild type plants. 7-day-old seedlings of were incubated in an eppendorf tube with 1 mL MSR2 medium containing 0.5 M TMRM for 15 minutes. Then the seedlings were washed three times with MSR2 medium and visualized under a confocal microscope (excitation 548 nm, emission 573 nm).

Transient expression experiments

Agrobacterium tumefaciens strain

For the use of pGreen–derived binary vectors, the *A. tumefaciens* GV3101 strain was co-transformed with the pSoup vector (Hellens *et al.*, 2000). Competent cells of *A. tumefaciens* GV3101 strain were prepared according to Main *et al.* (1995) and the binary vectors were introduced by 'freeze-thaw' method. 1μg of plasmid DNA was added to the competent cells, frozen in liquid nitrogen for 5min and heated at 37°C for 5min. The bacterial culture was incubated at 28°C for 3hr with gentle shaking in 1ml YEP medium (10g/L bacto-trypton, 10g/L yeast extract, 5g/L NaCl; pH 7.0) and then spread on a YEP agar plate containing the appropriate antibiotic selection (gentamycin 50 mgL^{-1}, rifampicin 50 mgL^{-1}, kanamycin 50 mgL^{-1} and tetracyclin 5 mgL^{-1}).

Arabidopsis leaf agroinfiltration

Single colonies of *A. tumefaciens* growing on agar plate were inoculated in 5mL of YEP liquid medium supplemented with specific antibiotics. The bacteria were incubated overnight at 28°C at 150 rpm on an orbital shaker. 2mL of overnight bacterial culture was collected in 15-mL sterile tubes by centrifugation (3000xg for g minutes), and resuspended in 4 mL induction medium supplemented with 100 μM Acetosyringone (4'-Hydroxy-3',5'-dimethoxyacetophenone; 3',5'-Dimethoxy-4'-hydroxyacetophenone) and appropriate antibiotics. The agroacterial suspension was incubated for 5 hours at 28°C and than collected by centrifugation

(3000xg for 5min). The bacterial cells were resuspended in the infiltration medium (containing 200 μM acetosyringone) to a final OD_{600} of 0.4. Approximately 300μL of *Agrobacterium* suspension was infiltrated into a young fingernail-sized leaf of 4-week-old Arabidopsis plants through the stomata of the lower epidermis by using 1-ml syringe without a needle. For experiments requiring co-infection of more than one construct, bacteria strains containing the constructs were mixed before performing the leaf infection, with the inoculum of each construct adjusted to a final OD_{600} of 0.4. Competence for transient transformation was enhanced by placing plants under complete darkness for 16 h before infiltration. After infiltration the plants were maintained in the environmentally-controlled chamber under standard growth condition. The transient expression was assayed four days after infection.

Tobacco leaf agroinfiltration

Agrobacterium-mediated transient expression was performed essentially as described in Zottini *et al.* (2008). Single colonies of *A. tumefaciens* growing on agar plate were inoculated in 3mL of YEP liquid medium supplemented with specific antibiotics. The bacteria were incubated for 2 days at 28°C at 200rpm on an orbital shaker. 25□L of confluent bacterial culture was re-inoculated in 5mL (1/200 ratio, v/v) of fresh YEP medium containing the appropriate antibiotics, and this new culture was grown under the same condition for an additional day. 2mL of bacterial suspension was pellet by centrifugation at 1.500xg for 4min at room temperature. The pellet was washed twice with 2mL of infiltration buffer [50mM MES pH 5.6, 2mM Na_3PO_4, 0.5% w/v glucose, and 100μM acetosyringone (Aldrich, Italy)] and then diluted with infiltration buffer to a final OD_{600} of 0.2. Approximately 300μL of this *Agrobacterium* mixture was infiltrated into a young leaf of *N. tabacum* through the stomata of the lower epidermis by using 1-ml syringae without a needle. For experiments requiring co-infection of more than one construct, bacteria strains containing the constructs were mixed before performing the leaf infection, with the inoculum of each construct adjusted to a final OD_{600} of 0.2. After infiltration the plants were maintained in the environmentally-controlled chamber under standard growth condition. The transient expression was assayed four days after infection.

Confocal analyses

Four developmental stages were examined: germinating seeds (32 h after imbibition), 5-day-old seedlings (cotyledons open), 7-day-old seedlings (first leaves developing), and flowering mature plants.

Confocal microscopies were performed by using a Nikon PCM2000 (Bio-Rad, Germany) and an inverted SP/2 (Leica, http://www.leica.com). laser scanning confocal imaging systems. For YFP and RFP detection, excitation was at 488nm and 543nm respectively, and emission between 515/530nm for YFP and 550/650nm for RFP, respectively. For the mCherry detection, excitation was at 543 nm and detection 550/650nm. For the chlorophyll detection, excitation was at 488nm and detection over 600nm. The images acquired from the confocal microscope were processed using the software ImageJ bundle software (http://rsb.info.nih.gov/ik/).

Fluorescence recovery after photobleaching

Fluorescence recovery after photobleaching (FRAP) experiments were performed by using the Leica TCS-SP2 FRAP wizard application in the "FlyMode" configuaration. For each experiment, a suitable plastid was selected and a pre-bleached image was acquired. YFP photo-bleaching was accomplished with three scans by using 100% 488 nm laser power. Recovery images were collected at 1.6 second intervals for the time indicated in each analysis. Images were analysed using ImageJ software. Total fluorescence was measured in the regions of interest (ROI) around the analysed plastids during the entire images acquisition and the data were plotted on X(time)/Y(pixel intensity) graph. Total fluorescence was expressed as relative fluorescence normalizing the fluorescence by each ROI with the fluorescence of the same ROI in the in the pre-bleach image.

Accession Numbers

Sequence data from this article can be found in the GenBank/EMBL data libraries under accession numbers At3g57090 for BIGYIN previously named FIS1A, and At5g12390 for FIS1B.

Statistic

All experiments were conducted al least in triplicate, and pictures represented typical example.

REFERENCE

- **Aldridge** C, Maple J, Møller SG (2005).The molecular biology and plastid division in higher plant. Journal of Experimental Botany, 56 (414):1016-1077
- **Bauwe** H, Hagemann M, Ferine AR (2010). Photorespiration: players, partners and origin. Trends in Plant Science, 15 (6):330-336
- **Borghese N**, Colombo S, Pedrazzini e (2003). The tale anchored proteins: coming from the cytosol and looking for a membrane. Journal of Cell Biology, 161 (6): 1013-1019
- **Campbell RE**, Tour O, Palmer AE, Steinbach PA, Baird GS, Zacharias DA, Tsien RT (2002). A monomeric red fluorescein protein. PNAS, 99: 7877-7882
- **Clough SJ**, Bent AF (1998). Floral dip: a simplified method for *Agrobacterium*-mediated transformation of *Arabidopsis thaliana*. The Plant Journal, 16 (6):735–743
- **Crotty WD**, Ledbetter MC (1973). Membrane continuities involving chloroplasts and other organelles in plant cells. Science, 182: 839-841
- **Cutler SR**, Ehrhardt DW, Griffitts JS, Sommerville CR (2000). Random GFP::cDNA fusions enable visualization of subcellular structures in cells of *Arabidopsis* at high frequency. PNAS, 97 (7):3718-3723
- **Formentin E**, Varotto S, Costa A, Downey P, Bregante M, Naso A, Picco C, Gambale F, Lo Schiavo F (2004). DKT1, a novel K+ channel from carrot, forms functional heteromeric channel with KDC1. FEBS Letters, 573(1-3):61-7
- **Fujimoto M**, Arimura S, Mano S, Kondo M, Saito C, Ueda T, Nakazono M, Nakano A, Nishimura M, Tsutsumi N (2009). *Arabidopsis* dynamin-related proteins DRP3A and DRP3B are functionally redundant in mitochondrial fission, but have distinct roles in peroxisomal fission. Plant Journal, 58 (3):388-400
- **Geldner N**, Friml J, Stierhof YD, Jürgens G, Palme K (2001). Auxin transport inhibitors block PIN1 cycling and vesicle trafficking. Nature, 413 (6854):425-8.

- **Gestel KV**, Kohler RH, Verbelen JP (2002). Plant mitochondria move on F-actin, but their positioning in the cortical cytoplasm depends on both F-actin and microtubules. Journal of Experimental Botany, 5 (369):659-667
- **Gray MW**, Burger G, Lang BF (1999). Mitochondrial evolution. Science, 283 (5407):1476-1481
- **Gray MV** (1999). Evolution of organellar genomes. Current Opinion in Genetics and Development, 9 (6):678-687
- **Gunning BES** (2005). Plastid stromules: video microscopy of their outgrowth, retraction, tensioning, anchoring, branching, bridging, and tip-shedding. Protoplasma, 225: 33-42
- **Hellens RP**, Edwards EA, Leyland NR, Bean S, Mullineaux PM (2000). pGreen: a versatile and flexible binary Ti vector for *Agrobacterium*-mediated plant transformation. Plant Molecular Biology, 42:819–832
- **James DJ**, Parone PA, Mattenberger Y, Martinou JC (2003). hFIS1, a novel component of the mammalian mitochondrial fission machinery. The Journal of Biological Chemistry, 278 (38):36373-36379
- **Jedd G**, Chua NH (2002). Visualization of peroxisomes in living plant cells reveals acto-myosin dependent cytoplasmic streaming and peroxisome budding. Plant Cell Physiology, 43 (4):384-392
- **Jefferson RA**, Kavanagh TA, Bevan MW (1987). GUS fusions: beta-glucuronidase as a sensitive and versatile gene fusion marker in higher plants. EMBO Journal, 6(13):3901-3907.
- **Jouhet J**, Maréchal E, Baldan B, Bligny R, Joyard J, Block MA (2004). Phosphate deprivation induces transfer of DGDG galactolipid from chloroplast to mitochondria. The Journal of Cell Biology, 167 (5):863-874
- **Kandasamy MK**, Meagher RB (1999). Actin-organelle interaction: association with chloroplast in arabidopsis leaf mesophyll cells. Cell motily and the cytoskeleton, 44 (2):110-118
- **Kobayashi S**, Tanaka A, Fujiji Y (2007 o 2006). Fis1, DLP1, and Pex11p coordinately regulate peroxisome morphogenesis. Experimental Cell Research, 313 (8):1675-1686

- **Koch A**, Yoon Y, Bonekamp NA, McNiven MA, Schrader M (2005). A role for Fis1 in both mitochondrial and peroxisomal fission in mammalian cells. Molecular Biology of the Cell, 16 (11):5077–5086,
- **Köhler RH**, Hanson MR (2000). Plastid tubules of higher plants are tissue-specific and developmentally regulated. Journal of Cell Science, 113 (1):81-89
- **Kutay U**, Ahnert-Hilgerl G, Hartmann E, Wiedenmann B, Rapoport TA (1995). Transport route for synaptobrevin via a novel pathway of insertion into the endoplasmatic reticulum membrane. The EMBO Journal, 14 (2):217-23
- **Kwok EY**, Hanson MR (2004a). GFP-labelled Rubisco and aspartate aminotransferase are present in plastid stromules and traffic between plastids. Journal of Experimental Botany, 55(397):595-604
- **Kwok EY**, Hanson MR (2004b). Stromules and dynamic nature of plastid morphology. Journal of Microscopy, 214 (2):124-137
- **Labereke NV**, Engler G, Holster J, Elsacker SV, Zaenen J, Schilperoort RA, Schell J (1974). Large plasmid in *Agrobacterium tumefaciens* essential for crown gall-inducing ability. Nature, 252: 169–170
- **Laemmli U K** (1970). Cleavage of structural proteins during the assembly of the head of bacteriophage T4. Nature 227, 680-685
- **Logan DC**, Scott I, Tobin AK (2004).AL2a, like ADL2b, is involved in the control of higher plant mitochondrial morphology. Journal of Experimental Botany, 55(397):783-785
- **Maggio C**, Barbante A, Ferro F, Frigerio L, Pedrazzini E (2007). Intracellular sorting of the tail-anchored protein cytochrome b5 in plants: a comparative study using different isoforms from rabbit and *Arabidopsis*. Journal of Experimental Botany, 58 (6):1365-1379
- **Main GD**, Reynolds S, Gartland JS (1995) Electroporation protocols in *Agrobacterium*. In: Gartland KMA, Davey MR (eds) Methods in molecular biology, vol 44: A*grobacterium* protocols. Humana Press, Totowa, pp 405–412
- **Mano S**, Nakamori C, Hayashi M, Kato A, Kondo M, Nishimura M (2002). Distribution and characterization of peroxisomes in *Arabidopsis*

by visualization with GFP: dynamic morphology and actin-dependent movement. Plant Cell Physiology, 43 (3):331-341

- **Maple J** and Møller SG (2007). Plastid division coordination across a double-membraned structure. FEBS Letter, 581 (11):2162-2167.
- **Michels PA**, Moyersoen J, Krazy H, Galland N, Herman M, Hannaert V (2005). Peroxisomes, glyoxysomes and glycosomes. Molecular membrane biology, 22(1-2):133-145
- **Miyagishima SY**, Froehlich JE, Osteryoung KW (2006). PDV1 and PDV2 mediate recruitment of the dynamin-related protein ARC5 to the plastid division site. The Plant Cell, 18 (10):2517-2530
- **Natesan SK**, Sullivan JA, Gray JC (2005). Stromules: a characteristic cell-specific feature of plastid morphology. Journal of Experimental Botany, 56 (413):787-797
- **Nelson BK**, Cai X, Nebenführ A (2007). A multicolored set of in vivo organelle markers for co-localization studies in *Arabidopsis* and other plants. The Plant Journal, 51 (6):1126-36
- **Pedrazzini E** (2009). Tail-anchored proteins in plants. Journal of Plant Biology, 52 (2):88-101
- **Pyke KA**, Howells CA (2002). Plastid and stromule morphogenesis in tomato. Annals of Botany, 90 (5):559-566
- **Samaj J**, Read ND, Volkmann D, Menzel D, Baluska F (2005). The endocytic network in plants. Trends in Cell Biology ,15 (8):425-33.
- **Scott I**, Tobin AK, Logan DC (2006). BIGYIN, an orthologue of human and yeast FIS1 genes functions in the control of mitochondrial size and number in *Arabidopsis thaliana*. Journal of Experimental Botany, 57 (6):1275-1280
- **Schrader M** (2006). Shared components of mitochondrial and peroxisomal division. Biochimica et Biophysica Acta, 1763(5-6):531-541
- **Scott I**, Sparkes IA, Logan DC (2007). The missing link: inter-organellar connection in mitochondria and peroxisomes? TRENDS in Plant Science, 12 (9):380-381

- **Sinclair AM**, Trobacher CP, Mathur N, Greenwood JS, Mathur J (2009). Peroxule extension over ER-defined paths constitutes a rapid subcellular response to hydroxyl stress. The Plant Journal, 59:231-247
- **Suzuki M**, Jeong SY, Karbowski M, Youle RJ, Tjandra N (2003). The solution structure of human mitochondria fission protein Fis1 reveals a novel TPR-like helix bundle. Journal of Molecular Biology, 334 (3):445-58
- **Thomas S**, Erdmann R (2005). Dynamin-related proteins and Pex11 proteins in peroxisome division and proliferation. FEBS Journal, 272: (20)5169-5181
- **Von Arnim AG**, Deng XW, Stacey MG (1998). Cloning vectors for the expression of green fluorescence protein fusion proteins in transgenic plants. Gene, 221 (1):35:43
- **Zhang Y**, Chan DC (2007). Structural basis for recruitment of mitochondrial fission complexes by Fis1. Proceedings of the National Academy of Sciences of the United States of America, 104 (47):18526-30
- **Zhang XC**, Hu JP (2008a).Two small protein families, DYNAMIN-RELATED PROTEIN3 and FISSION1, are required for peroxisome fission in *Arabidopsis*. The Plant Journal, 57(1):146-59
- **Zhang XC**, Hu JP (2008b). FISSION1A and FISSION1B proteins mediate the fission of peroxisomes and mitochondria in *Arabidopsis*. Molecular Plant, 1 (6): 1036-1047
- **Zhang XC**, Hu JP (2010). The *Arabidopsis* chloroplast division protein DYNAMIN-RELATED PROTEIN5B also mediates peroxisomes division. The Plant Cell, 22 (2):431-42.
- **Zottini M**, Barizza E, Costa A, Formentin E, Ruberti C, Carimi F, Lo Schiavo F (2008). Agroinfiltration of grapevine leaves for fast transient assays of gene expression and for long-term production of stable transformed cells. Plant Cell Reports, 27(5):845-853
- **Zybailov B**, Rutschow H, Friso G, Rudella A, Emanuelsson O, Sun Q, Van Wijk KJ (2008). Sorting signals, N-terminal modification and abundance of the chloroplast proteome. PLoS One, 3(4):e1994

CONCLUSIONS

Analyses of morphological mitochondrial changes during growth and senescence was observed in grapevine cultured cells and leaves allowing us to show a link between characteristic mitochondrial morphology and ageing cells. In particular, in senescent cultured cells and leaf tissues, a decrease in mitochondria number and an increase in their volume was detected.

These results clearly indicate that similar events take place in both experimental systems, suggesting that analyses performed in a not complex experimental system, as cultured cells, may contribute positively to understand cellular mechanisms of important physiological processes, that occurred in complex systems, such as plant organ and tissues.

The observed morphological variations prompt questions of why and how different mitochondrial shapes are associated with different stages of cell ageing, and how these mitochondrial changes are regulated.

To start to answer these open questions, the molecular mechanisms responsible for mitochondrial fission in *Arabidopsis* plants, a model organism in plant biology was analysed. Initially, the subcellular localization of two proteins involved in mitochondrial fission events (ELM1 and BIGYIN) was analysed. Our results have shown that ELM1 and BIGYIN localized and interacted *in vivo* on mitochondrial outer membranes. These results allow us to elucidate and to better define the interaction pattern of proteins involved in mitochondrial fission events. In our analyses, the subcellular localization of BIGYIN on peroxisomes was observed. In addition, we have shown that ELM1 and BIGYIN localized and interacted *in vivo* on chloroplast outer membranes. This is the first indication that these two proteins may play a role on chloroplasts.

Yet, our data suggest that ELM1 is a protein shared by mitochondria and chloroplasts and that BIGYIN is a protein, properly a transmembrane protein, belonging to the tail anchored (N_{out}-C_{in}) proteins, localized to mitochondria, peroxisomes and chloroplasts. On my knowledge, BIGYIN is the first transmembrane proteins characterized to have these multiple targeting. Our results also demonstrated that BIGYIN reached the organelle membranes directly from cytosol, without passing through the ER. The BIGYIN protein was also dissected,

and the C-terminal tail was identified to be sufficient to target BIGYIN to mitochondria, peroxisomes and chloroplasts. Moreover, our data unveiled an association between BIGYIN and chloroplast morphology. In fact,we observed that BIGYIN localized to the chloroplast outer membranes and to the ring structures encircling the chloroplast division sites during chloroplast division. But, a mutated BIGYIN protein provoked chloroplast morphology changes. Our data are the first indication of the involvement of BIGYIN with chloroplast division.
Recently, an anti-BIGYIN-antibody has been designed, and tested for its specificity. This antibody will allow us in a near future to validate our subcellular localization results, by means of immunogold electron microscopy assay and immunoblot assay of protein extracts, enriched in subcellular compartments.

Last, the molecular aspects of physical organellar interactions among mitochondria, peroxisomes and chloroplasts in plants were investigated by imaging analyses of a protein (i.e. BIGYIN) localized to these different organelles. BIGYIN unveiled a dynamic network of tubular protrusions extending from the membranes of chloroplasts (i.e. stromules), mitochondria (i.e. matrixules), and peroxisomes (peroxules). These tubules connected different organelles among them, and we demonstrated that the actin-based cytoskeleton played a role in the movement of tubules and organelles. Interestingly, we demonstrated that a BIGYIN trafficking occurred among membranes of different organelles, demonstrating, in this way, physical inter-organellar interactions.